MINNESOTA GEOLOGICAL SURVEY
Harvey Thorleifson, Director

SME Twin Cities Annual Conference

INDUSTRIAL MINERALS OF THE UPPER MIDWEST

Proceedings of the

51ST FORUM ON THE GEOLOGY OF INDUSTRIAL MINERALS

Presented in cooperation with the Annual Conference of the Twin Cities Subsection of the Society for Mining, Metallurgy & Exploration (SME)

August 17 – 20, 2015

Editor: Harvey Thorleifson, Minnesota Geological Survey

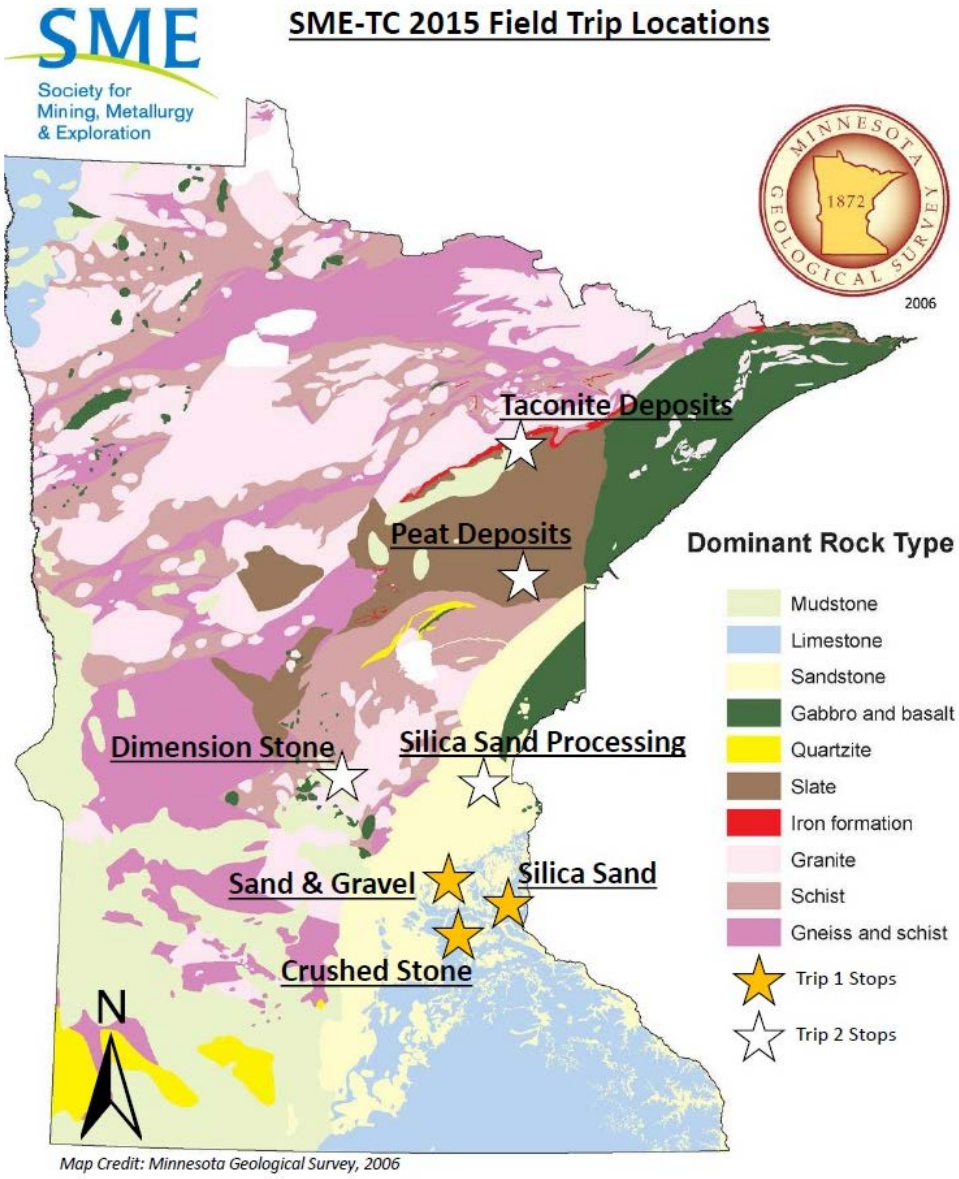

Map Credit: Minnesota Geological Survey, 2006

Minnesota Geological Survey Open File Report 16-2
University of Minnesota
Saint Paul – 2016

This open file is accessible from the web site of the Minnesota Geological Survey (http://www.mngs.umn.edu/) as a PDF file readable with Acrobat Reader.

Date of release: 8 February 2016

Recommended citation

Thorleifson, L. H., editor, 2016, Industrial minerals of the Upper Midwest; Proceedings of the 51st Forum on the Geology of Industrial Minerals, presented in cooperation with the Annual Conference of the Twin Cities Subsection of the Society for Mining, Metallurgy & Exploration (SME), August 17 – 20, 2015, Minnesota Geological Survey Open File Report 16-2, 76 p.

Minnesota Geological Survey
2609 West Territorial Road
St Paul MN 55114-1009
Telephone: 612-626-2969
Email address: mgs@umn.edu
Web site: http://www.mngs.umn.edu/

Contents

Preface

On August 17 – 20, 2015, the Twin Cities Subsection of the Society for Mining, Metallurgy & Exploration (SME) hosted the 51st Forum on the Geology of Industrial Minerals. The theme of the meeting, whose conference sessions and field trips were enjoyed by about 100 people, was ‘Industrial minerals of the Upper Midwest’.

SME, headquartered in Denver, is a professional society whose more than 15,000 membership represents all professionals serving the minerals industry in more than 100 countries. SME advances the worldwide mining and underground construction community through information exchange and professional development.

In Minnesota, the SME Minnesota Section maintains a broad program of activities that focuses on the annual spring conference in Duluth. The SME Twin Cities Subsection organizes an annual autumn conference, monthly luncheons, student activities, and social functions.

Following a hiatus, the SME Twin Cities Subsection annual conference was restarted in 2011. For 2012 and subsequent years, the subsection has worked with a different partner each year, to present a conference program aligned with broad mining-related topics, while focusing on the sort of mining that takes place in the Twin Cities region, such as crushed stone, sand and gravel, and silica sand.

For 2015, the SME Twin Cities Subsection was pleased to work in cooperation with organizers of the Forum on the Geology of Industrial Minerals.

The Forum meets regularly, and it has been customary for a proceedings volume to be produced. Among the 17 presenters who gave presentations at the 2015 Forum, seven chose to contribute a paper.

The Minnesota Geological Survey is pleased to have an opportunity to support the activities of SME and the Forum by facilitating availability of the 2015 Proceedings of the 51st Forum on the Geology of Industrial Minerals.

L. H. Thorleifson, Editor, February 2016

IDENTIFYING NEW RESOURCE PROSPECTS AND RESOURCE ASSESSMENT WITH GEOSPATIAL MODELING TECHNIQUES: THE CENTRAL TEXAS FRAC SAND DISTRICT

Elliott, B.A.[1], Verma, R.[1,2]

[1] The Bureau of Economic Geology, The University of Texas at Austin, University Station, Box X Austin, Texas 78713-8924, brent.elliott@beg.utexas.edu

[2] Department of Geological Sciences, The University of Texas at Austin, Austin, Texas 78712

1. ABSTRACT

The Cambrian depositional setting in central Texas has been a source of specialty sand for hydraulic fracturing in the past and has potential to play a bigger role in proppant supply to markets in and around Texas. Sandstone in the Hickory Formation is suitable in compressive strength, grain size and shape to be used as proppant. The Hickory sandstone forms a basal sequence nonconformity deposited on Precambrian basement and is a complex succession of terrestrial and transgressive marine sands and silts similar to settings through the upper Midwest that produce the northern white sands proppant material. The geologic setting that led to the formation's deposition is transitional between shallow transgressive marine and terrestrial eolian environments. The quantity and location of sand resources in the Central Texas Frac Sand district is illustrated through Fuzzy logic geospatial volumetric techniques and estimated at 5 billion tons of proppant material. The modelling of favorable characteristics in existing resource locations is used to predict new sites for resource development, and quantify the abundance of prospective natural sand resource in the Central Texas Frac Sand district.

2. INTRODUCTION

Naturally occurring sand is one of the most commonly used proppants in hydraulic fracturing, with the petroleum industry being the biggest consumer of industrial sand. It has been estimated that by 2018, 23% of petroleum and 57% of natural gas wells may be using hydraulic fracturing for production (Elliott 2012). In 2012, the world produced 139 Mt of industrial sand; more than 50 Mt was produced in the U.S. and more than 61% was used in hydraulic fracturing (USGS 2014). Texas produces about 9 Mt of industrial sand, but uses more than 17 Mt each year. Wells in the Permian, Barnett and Eagle Ford oil and gas basins are employing hydraulic fracturing using sand from a variety of sources, including Wisconsin, Illinois and Minnesota. These sources are located in the Great Lakes area, approximately 1300 miles from the oil and gas fields located in and around Texas, and require rail transport to be economical. This creates a logistic challenge and additional cost for consumers. The Central Texas Frac Sand district provides a closer and relatively economical alternative for many of the new wells being developed in Texas.

The Hickory Sandstone of the Riley Formation is centrally located within 200 miles of all major oil and gas reservoirs in Texas. Sands rich in silica with grains of high compressive strength, roundness and sphericity qualify for use in hydraulic fracturing, as specified by ISO 13503-2. Further characteristics (size-fraction distribution, resistance to proppant embedment and scaling, and geochemical composition, for example) are desired based on the reservoir where the sand is used (Terracina et al. 2010) The geologic setting of the central Texas region and depositional setting of the sand makes it ideal for use in hydraulic fracturing. While there are a few producers presently taking advantage of this logistic opportunity with extraction facilities in central Texas, a much larger resource exists in this area yet to be developed.

3. GEOLOGIC SETTING

The Llano Uplift and Precambrian basement rocks

The Llano Uplift is currently a broad regional eroded depression, with the Precambrian basement rocks forming the central exposure of the regional landform (Figure 1). Paleozoic sedimentary strata non-conformably overly metamorphic rocks and granitic intrusions as a thin marginal apron. Middle to Late Cambrian and Ordovician units are covered locally by a veneer of Cretaceous carbonates extending away from the Llano Uplift as the Edwards Plateau.

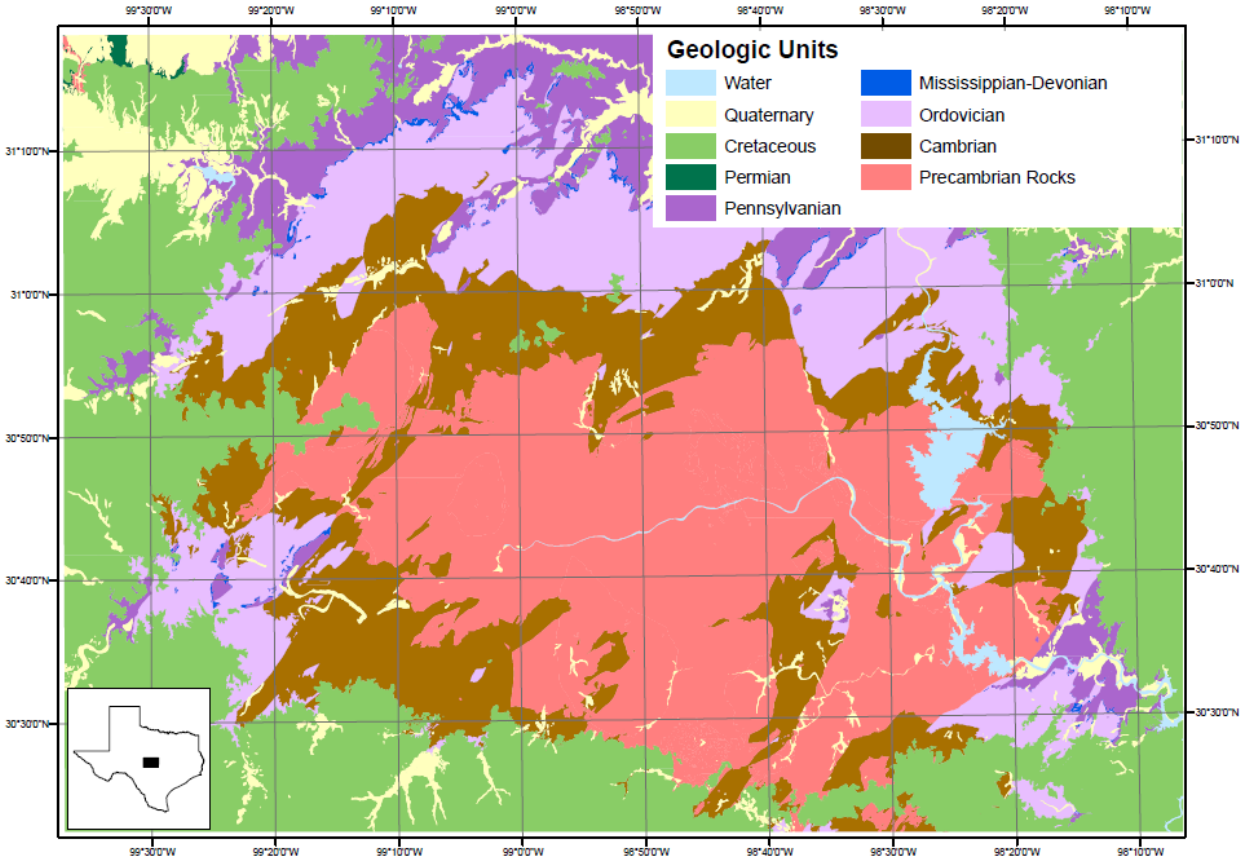

Figure 1. General geologic map of the Llano uplift area.

The Proterozoic core of the Llano Uplift consists of a complex series of mostly metavolcanic and metasedimentary rocks dated at ~1.36 to 1.26 Ga (Helper 2000; Mosher et al. 2008). Sediments originating from older rhyolitic volcanic rocks and tuffaceous sediments accumulated as a coastal plain and continental shelf to form the Valley Spring sedimentary wedge. These were covered with dark, fine-grained muddy sediments of the Packsaddle Formation. These rocks were trapped in a tectonic collision zone and are polydeformed, contemporaneous with an intermediate- to high-pressure, upper amphibolite to lower granulite facies regional metamorphism (Walker 1992; Mosher 1993; Reese 1995; Roback 1996; Carlson 1998; Mosher 1998; Reese et al. 2000), and have been subdivided into lithotectonic domains based on lithology, field relations, geochemistry, and U/Pb ages. Late Mesoproterozoic granitic magmatism in Texas occurred between 1119 and 1070 Ma (Garrison et al. 1979; Walker 1992) on both sides of the Grenville Front (Smith et al. 1997). In the Llano Uplift, 1119–1070 Ma, syn- to post-tectonic granites intruded the Grenville ~1360–1232 Ma metaigneous and metasedimentary rocks (Mosher 1993; Mosher 1995; Mosher 1996; Mosher 1998).

Following the development of Proterozoic metamorphic and igneous rocks, uplift and exhumation during an extensive period of erosion created the surface on which the Late Cambrian sediments were deposited. Estimated depths of granite emplacement require that 8 to 10 km of Precambrian cover were removed to bring the metamorphic and igneous rocks to sea level prior to the deposition of the late Middle Cambrian sediments (~515 Ma). Crustal thickening did occur during the late Precambrian as evidenced by a positive Bouger Gravity anomaly centered on the current Llano Uplift. However, thicknesses of sedimentary rocks deposited on the eroded igneous and metamorphic rocks during the Paleozoic (Barnes and Bell 1977) show a variety of patterns that do not provide clear evidence of the uplift having always been a positive topographic feature, even relative to surrounding areas. The units deposited in the uplift region throughout time have been shallow water facies. At no time since the Precambrian have the rocks of the Llano Uplift ever been at more than 1-2km of water depth. One consistent feature of the rocks deposited throughout the lower Paleozoic is that, where it is possible to interpret a depositional setting, the rocks are shallow marine (ocean) to terrestrial (land) in origin. Paleotopography appears to have been dictated by weathering of underlying bedrock in an arid environment, with finer grained granite, quartzofeldspathic gneiss, and marble supporting areas of higher relief, and schists, amphibolite and other less resistant rocks underlying lower relief regions (Barnes and Bell 1977). The thickness and facies of the lowermost Cambrian strata were strongly controlled

by the paleotopography, which had as much as 200m of relief. A few topographic highs persisted as islands until they were buried by Late Cambrian sedimentation.

The Riley Formation and Hickory Sandstone

The lowermost Paleozoic sediments of the Llano Uplift comprise the three members of the Middle to Late Cambrian Riley Formation (as part of the lower member of the Moore Hollow Group; Barnes and Bell 1977). The Hickory Formation forms the base of the sequence and is a complex succession of terrestrial and transgressive marine arkosic to quartz arenitic sandstone/siltstone, and can incorporate mudstone and ironstone that is as much as 150m thick. The Hickory Formation grades into Cap Mountain Limestone, consisting of progradational intertidal, subtidal, and shallow-shelf sandstones/siltstones and transgressive shallow-shelf and shoal carbonate packstones and fossiliferous grainstones, with a total local thickness of 150m. The Cap Mountain Limestone grades into the Lion Mountain Sandstone, composed of tidally dominated, progradational, argillaceous, green glauconitic sand with trilobite coquina lenses and beds, ranging from 6–23m in thickness (Barnes and Bell 1977; Krause 1996). The Hickory and the Cap Mountain strata are locally absent where the Lion Mountain rests directly on Precambrian basement. The thickness and facies of the Hickory Sandstone varies in response to the paleotopography of the underlying Precambrian rocks. The Hickory reaches a thickness of 180m along the western margin of the Llano Uplift, but generally is less than 110m thick. The basal Hickory facies is the most variable, ranging from alluvial conglomerates and cross-bedded fluvial sandstones in paleo-lows to marine-influenced fine-grained siliciclastic sediments resting directly on granite highs (Kyle and McBride 2012; Krause 1996). Sequence stratigraphic and lithofacies analysis (Krause 1996) suggests that the Riley Formation is an unconformity-bounded, depositional sequence representing perhaps as little as 4 million years (ca. 514 – 510 Ma) of deposition.

The Wilberns Formation and Post-Cambrian strata

The Riley Formation is overlain by transgressive and progradational shallow-water marine sandstone, siltstone, limestone, and dolomite of the Wilberns Formation. The Wilberns Formation consists of medium-grained marine sandstones of the Welge Sandstone (3–9m thick) grading upward into Morgan Creek Limestone. Morgan Creek Limestone (38–44m thick) consists of intertidal and shallow shelf oolitic, glauconitic and stromatolitic limestone(s). Overlying Morgan Creek Limestone is Point Peak Member (averages 52m thick) comprised of terrigenous siltstone, silty and stromatolitic limestones, and intraformational conglomerates. Point Peak Member grades into San Saba Member (85–137m thick), which is a laterally variable unit consisting largely of limestone and, locally stromatolitic and glauconitic, dolostone (Barnes and Bell 1977). The San Saba Member is calcareous sandstone and sandy dolomite in the western Llano Uplift and is time transgressive, containing an early Ordovician trilobite fauna (Barnes and Bell 1977).

The boundary with the overlying Ordovician Ellenburger Group carbonates is commonly gradational. Post-Lower Ordovician, pre-Pennsylvanian strata are poorly represented in the Llano Uplift, as the region appears to have been largely emergent during this time, perhaps with short-lived, periodic marine incursions separated by longer erosional events. Adams (1954) suggested that in the Ordovician there existed a continental peninsula running north-northwest to south-southeast in central Texas. Deeper water and thicker sediments occurred offshore from the peninsular topography. However, it was suggested that the peninsula was not centered on an area in central Texas defined by a gravity anomaly and that the current Llano Uplift was on the east flank of the peninsular structure. Erosion of the Ordovician Ellenburger Formation suggests tilting of the Llano area at this time. Pennsylvanian strata (Marble Falls Limestone and Smithwick Formation) record a return to marine conditions, with the establishment of deeper water depositional systems for terrigeneous sediment derived from an easterly source. Kier (1980) describes the Pennsylvanian Marble Falls Formation as being a carbonate bank centered on the current area of the Llano Uplift. Sedimentation was in part synchronous with the development of the northeast-trending fault system of the Llano Uplift and overlaps in time with the development of the Ouachita fold-thrust belt, the subsurface extension of which lies to the south and east. During the Ouachita Orogeny, which was most intense east and south of the Llano Uplift, the uplift was cut by a series of northeast-trending faults with normal to oblique slip. The large grabens of Paleozoic rocks which strongly influence the current topography were formed during this time. Barnes et al. (1972) estimated that some of these faults have displacements of as much as 900m.

Rifting to initiate the formation of the Gulf of Mexico during the early Mesozoic (Salvador 1991) resulted in regional subsidence that created a broad shelf during the early Cretaceous on which the extensive limestones of the Edwards Plateau were deposited. The absence of Permian, Triassic, and Jurassic strata beneath the Cretaceous strata records another extensive period of subaerial exposure and erosion. Erosion on the uplifted northwest side of the Llano Uplift resulted in the removal of the thin veneer of Cretaceous to Eocene strata (Corrigan et al. 1998), producing the present Llano Uplift character. A reconstructed burial history indicates that the Hickory strata were never buried more than 1km around the flanks of the Llano Uplift (McBride et al. 2002).

It is imperative to understand the geologic setting and depositional history of the central Texas stratigraphy in order to better identify areas with the appropriate geology for sand resource development. This provides a crucial framework for efficient and economical exploration, by precluding unfavorable areas. Since most of the frac sand resource formations are non-conformably overlying Precambrian basement rock, and overlain by younger Ordovician, understanding the regional and local geology is a critical first-step to identifying and predicting new resource locations with geospatial techniques.

3. METHODOLOGY

This section discusses the methodology of prospectivity mapping, and examines the relative favorability of establishing sand extraction facilities in the central Texas region. The Hickory Sandstone is spread over an area of over 41,000km^2 in the central Texas region. Although the whole is of interest to the proppant mining industry, certain areas are more favorable than others. For example, mining companies would have high favorability for regions with greater volume of resource, low cost of extraction and a convenient transportation network for distributing resources. On the other hand, even if some regions are favorable, they might be restricted from surface mining. We attempt to combine these characteristics to form a map of favorability rated on a scale of 0 to 1, with 0 being the least favorable and 1 being the most favorable. The first step discusses the method of sand and overburden volume calculation, the second step integrates favorability variables to rate the identified sand volumes on a relative favorability scale, and finally the third step discusses restricted areas and calculates available sand resources.

Volume calculation

For volume calculations, we use water well log data made publically available by Texas Water Development Board (TWDB). The water well log data holds stratigraphic information of the rock layers in the area shown in Figure 1. For this study, we have analyzed the subsurface stratigraphy of approximately 2,000 water wells.

To create a model for sandstone layers, first we create a data base of sandstone layers' upper and lower bounds at water well locations and then interpolate boundary surfaces using geospatial methods to create a block model for sandstone layers. The relative elevation of the upper and lower bound is simply obtained by subtracting sandstone layer's respective boundary depth from well top's surface elevation. Equations 1 and 2 illustrate this relation.

$$z_{itop} = z_{isurface} - D_{SS} \quad [1]$$

$$z_{ibottom} = z_{isurface} - D_{SS} - T_{SS} \quad [2]$$

Where z_{itop} is the upper bound of sandstone layer at the ith well location, $z_{ibottom}$ is the lower bound, $z_{isurface}$ is the surface elevation of the well top, D_{SS} and T_{SS} are the depth of sandstone layers and thickness of sandstone layers, respectively, as determined from water well log data. The location of all the water wells analyzed in this study are shown in Figure 2.

To predict the value for z_{itop} and $z_{ibottom}$ at points where we do not have well data we use natural neighborhood method for spatial interpolation. Natural neighbor interpolation, explained in Figure 3, uses elevation values of known locations and predicts the elevation of a sandstone layer's upper and lower bounds and constructs continuous rasters for sandstone layers' upper and lower elevation level. Rock layers above the identified sandstone layers form the overburden, or waste rock, layers. In a few regions we observed up to three layers of sandstone separated by few feet of overburden. To calculate sandstone and overburden volume in such locations, we constructed separate rasters for the second and third layers. With addition of each sandstone layer, the waste rock between the layers are added to the total overburden volume. The analysis helps us determine whether it is preferable to dig deeper or expand laterally, in order to extracting higher volumes of sand and avoid the cost of removing additional overburden and waste rock.

After calculating elevation rasters for sandstone layers, we divide the entire area into a fishnet with grid spaces approximately 100m^2 in area. For each of these grids, we then calculate sandstone thickness as the difference between a sandstone layer's upper elevation value and lower elevation value (see Equation 3),

$$Sandstone\ Thickness = Z_{top} - Z_{bottom} \quad [3]$$

where Z_{top} and Z_{bottom} are elevation levels of a sandstone layer's top and bottom, respectively. Due to particularly adverse impacts of surface mining below the groundwater level, as noted by Sengupta (1993), we took the precaution

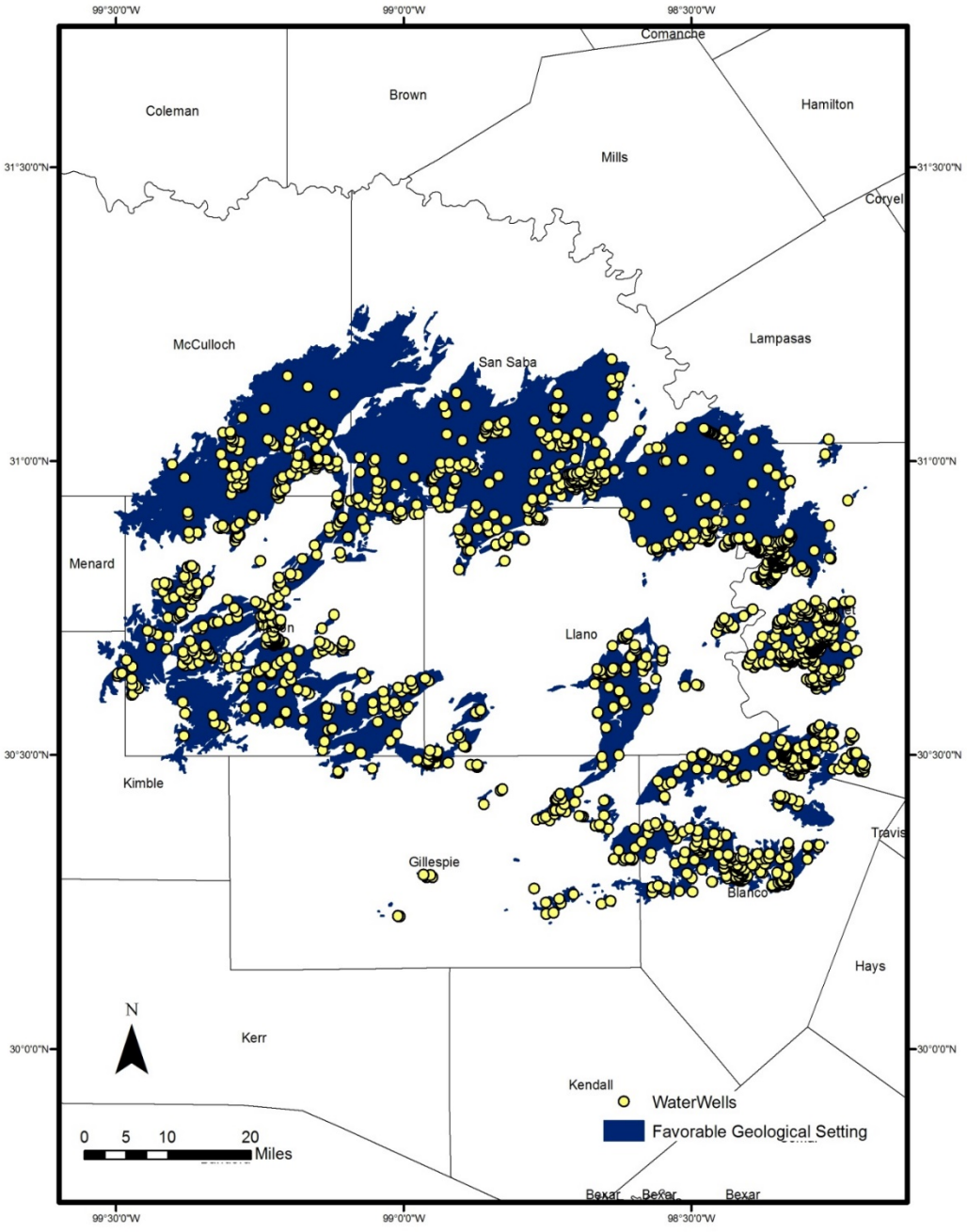

Figure 2. Water well location used for sandstone layer interpolation

of conservatively estimating the sand resources to include only those resources which lie above the groundwater level. For this, we first constructed an elevation raster of groundwater level based on groundwater data from the TWDB, and then limited the lower bound of extractable sand to be the groundwater table elevation. Therefore we create a new variable, ZAW_{bottom} (i.e. the lower bound of sandstone layer above groundwater table; Equation 4),

$$ZAW_{bottom} = \max\left(Z_{groundWater}, Z_{bottom}\right) \quad [4]$$

where $Z_{groundWater}$ is the elevation of groundwater level relative to surface elevation. Therefore, the sandstone thickness, T_{aw}, above the groundwater level can be defined by Equation 5.

$$T_{aw} = \begin{cases} Z_{top} - ZAW_{bottom} & , Z_{top} > Z_{groundWater} \\ 0 & , Z_{top} \leq Z_{groundWater} \end{cases} \quad [5]$$

Natural neighbor interpolation

The method developed by Sibson (1981) is based on Voronoi Tessellation and works equally well in regularly and irregularly distributed data as noted by Watson (1992). Voronoi Tessellation, or Voronoi partition, for a set of selected points can be constructed by drawing perpendicular bisectors of lines joining adjacent points in space to create polygons, called Voronoi cells, around every point, such that no two polygons overlap. A simple example of such a partition with a set of 5 points is shown in Figure 3a. For a corollary to our study, assume that the five points shown in Figure 3a are five water well locations, where z variables for sandstone layers' upper and lower boundaries are known. If we now have to predict the same variables at another point, for example point 6 which lies somewhere around the other five points, a new Voronoi cell has to be created and the Voronoi Partition will have to be redrawn to look like Figure 3b. Two points are called neighbors if their Voronoi cells share a boundary. Natural neighbor uses the following equation to predict a variable at unknown locations.

$$G(x,y) = \sum_{i=1}^{n} w_i f(x_i, y_i)$$

Here $G(x,y)$ is the predicted value at a point with n neighbors, each with known value $f(x_i,y_i)$ and weight, w_i. For calculating the weight for a value of every neighbor, natural neighbor uses the Voronoi cells according to the following equation:

$$w_i = \frac{Area\ of\ i^{th}\ Voronoi\ cell\ inside\ the\ new\ Voronoi\ cell}{Area\ of\ new\ Voronoi\ cell}$$

For the example shown in (a) and (b), the variable z_6 will be defined as the following:

$$z_6 = \sum_{i=1}^{5} w_i z_i$$

z_i for $i = 1\ \text{to}\ 5$ is known and w_i will assigned according to following equation, where A_{xyz} denotes Area of polygon xyz:

$$w_1 = \frac{A_{agfe}}{A_{abcde}}$$

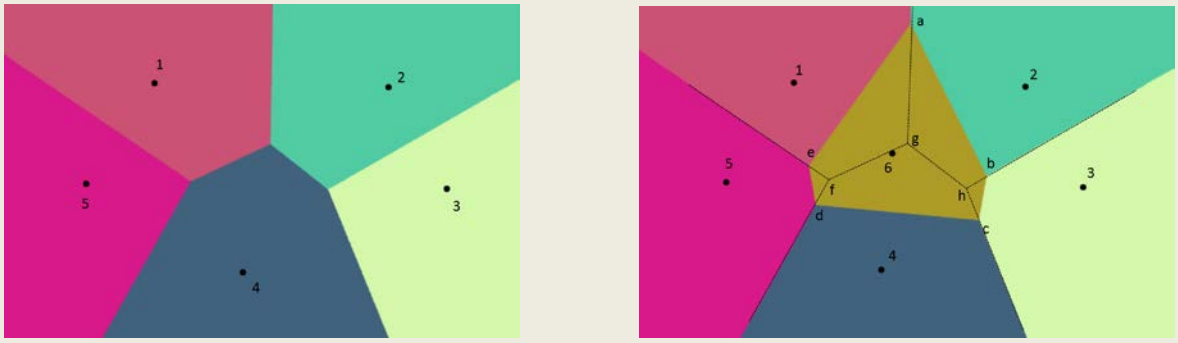

Figure 3. (a) Voronoi Tessellation for the original set of point (left). (b) New Voronoi Tessellation after the addition of point 6 (right)

The overburden above the upper most sand layer (layer 1) is simply the difference between the surface elevation and the sandstone layer's upper boundary. Adding the interlayered waste rock material between subsequent sand layers accounts for the additional overburden volume for layer 2 and layer 3. Equations 6, 7 and 8 illustrate the relationship,

$$OB_1 = Z_{surface} - Z_{1top} \quad [6]$$
$$OB_2 = OB_1 + P_{12} \quad [7]$$
$$OB_3 = OB_1 + P_{12} + P_{23} \quad [8]$$

where OB_1, OB_2 and OB_3 are overburden thickness values for layer 1, 2 and 3, respectively. P_{12} denotes the waste rock material between layer 1 and layer 2, and P_{23} denotes the waste rock material between layer 2 and 3. $Z_{surface}$ and Z_{1top} are elevation values for the surface and the first sand layer's upper boundary, respectively. To calculate volume, we make an approximate assumption that sandstone thickness is uniform within the fishnet grids of area 100 square meters or less, and the volume for sand and overburden is simply the product of respective thickness and grid area:

$$Volume(sand\ or\ OB) = Thickness(sand\ or\ OB) \times Grid\ area \quad [9]$$

4. DATA INTEGRATION AND PROSPECTIVITY MAPPING

We have used Fuzzy logic methodology to integrate the variables governing favorability. Zadeh (1965) defines the Fuzzy set theory, where each contributing member has a value from 0 to 1 to reflect its membership. Figure 4 shows the method of integration by Fuzzy operators listed in Table 1 (Bonham-Carter 1994; Singer and Menzie, 2005). The description for different Fuzzy members and explanation of how they are integrated in the analysis is as follows.

Geology

The geology of the appropriate quality sand resources in central Texas is perhaps the most important factor in determining the potential for new frac sand resources in the region (Figure 1). We have used the Cambrian-Ordovician formations that have sand resources as a defining limit to the spatial analysis, where those rocks (especially the basal sand units of the Hickory Sandstone in the Riley Formation, overlying the Precambrian basement rocks) have the appropriate geology and will be the only ones considered in this study for prospective resource sites.

Sandstone and overburden thickness

There are several locations in the Cambrian-Ordovician rock units that provide lower well density and are treated with less confidence, where factored into the spatial analysis. These locations may appear inferior due to the lack of information available and kept under consideration when evaluating the final analysis. The data retrieved from water well logs determined the thickness of overburden and thickness of sand units (3 separate layers). Overburden is a key factor in economic decision-making for surface extraction of resources. The more overburden that has to be removed, there is an increase in the cost of stripping that material and developing a new resource extraction site. The thickness of overburden was factored into the spatial analysis and weighted so that the thicker the overburden, the lower the weighted value becomes. The thickness of sand layers (individually as layer 1 – closer to the surface, layer 1 and 2, and layer 1, 2, and 3) was considered similarly, where the thicker the sand formations, the higher the weighted value becomes. The thickness, and therefore the volume, of sand material must be an adequate thickness to be economically feasible. In Figure 4, the *sandstone* raster assumes high membership in regions with thick sandstone layers (thickness ranges from 0m to greater than 30m), and the *overburden* raster assumes high membership in regions with thin overburden layers (thickness ranges from 0m to greater than 100m)

Railways

Railways are a major transportation network for the distribution of high volumes of frac sands around the U.S., especially in Texas. Many of the drilling operations that require frac sand resources procure their material from districts in the upper Midwest, from states such as Wisconsin, Minnesota and Illinois. Railways provide a much cheaper alternative to trucking when shipping very long distances. Railways have been incorporated in the spatial analysis, where locations close to the railways have a higher prospective value, and locations further away have a lower prospective value. Weighting between spatial constituents was not equal and the spatial distribution that railways received was small, due to a limited spatial coverage. There are only 2 areas in the Cambrian-Ordovician rock units that are intersected by railways: (1) in the northern part of the area and (2) in the eastern part of the area. The *railway* raster assumes high membership in regions close to railway lines (see Figure 4).

Roads

Major roads (state highways and Interstate highways) provide the majority of frac sand resource distribution from operations in the Central Texas Frac Sand district. Major roads have been incorporated in the spatial analysis,

where locations close to the roadways have a higher prospective value, and locations further away have a lower prospective value. Weighting between spatial constituents was given more consideration as it carries an inherent economical factor and frequency of use compared to railways. The spatial distribution of roads received a moderate contribution to prospectivity, where new sites near major transportation networks are more favorable when selecting a new resource extraction site. Therefore in Figure 4, the *highway* raster assumes high membership in regions close to highways.

We have used Fuzzy OR, Fuzzy PRODUCT and Fuzzy GAMMA for our calculations, described in Table 1. Fuzzy OR is the maximum operator that takes the maximum membership value of its members. For transportation purposes, it is sufficient for the sites to be close to either of the two facilities (i.e. highways and railways). Therefore we use Fuzzy OR operator to combine *highway* and *railway* rasters into a new raster that has high membership if a region is close to either highways or railways. We call this new raster *transport* (see Figure 4). For resource characteristics, we assert that while it is favorable to have either low overburden or high sandstone thickness, it is even more favorable for a region to have both the characteristics. To reflect this assertion we use Fuzzy PRODUCT (see Table 1) to combine the rasters: *sandstone* and *overburden.* The new raster formed as a result of Fuzzy PRODUCT is called *resource.* The two new rasters (*transport* and *resource*) are further combined by Fuzzy GAMMA operator (see Table 1) to derive the final favorability map. Fuzzy GAMMA operator combines the characteristics of two other operator: Fuzzy PRODUCT and Fuzzy ALGEBRAIC SUM. A high value of GAMMA causes a higher inclination towards Fuzzy ALGEBRAIC SUM (Bonham-Carter 1994). We have subjectively used a value of 0.8 for GAMMA in our calculations.

Table 1 fuzzy operators' descriptions, Bonham-Carter (1994)

Operator	Equation
Fuzzy PRODUCT	$\mu_{Combination} = \prod_{i=1}^{n} \mu_i$
Fuzzy OR	$\mu_{Combination} = Max(\mu_a \mu_b \mu_c, \dots)$
Fuzzy ALGEBRAIC SUM	$\mu_{Combination} = 1 - \prod_{i=1}^{n} (1 - \mu_i)$
Fuzzy GAMMA	$\mu_{Combination} = (\prod_{i=1}^{n} \mu_i)^{1-\gamma} (1 - \prod_{i=1}^{n} (1 - \mu_i))^{\gamma}$

Restricted Areas

There are several areas that have been eliminated from consideration in the evaluation of new site selection methodology (Figure 5). There are existing leases of operations that have been excluded, although the model is dynamic enough that changes in lease status can be modified for future iterations. Municipalities and areas directly adjacent, within 2km, to municipalities have been excluded from consideration, as permitting and public policy prohibit the likely establishment of new mining operations in or close to towns and cities. Surface water regulations prohibit surface extraction within 50m of major water bodies, rivers and streams, and groundwater regulations create permitting and regulatory hurdles that may be prohibitive. The spatial analysis and reserve calculations in this study only incorporate sand thicknesses and overburden thicknesses above the water table.

Existing Mining Operations

There are several existing frac sand mining operations in the Cambrian-Ordovician units of central Texas (Figure 6). Eleven operations with a total lease area exceeding 3600 acres, reporting an annual production of more than 9Mt of frac sand. These operations produce a variety of sand fraction products, but the typical distribution of grain sizes is 20% <80 mesh, 12% 60–80 mesh, 25% 40–60 mesh, 30% 20–40 mesh, 13% >20 mesh. The locations of existing frac sand mining operations have been utilized for the validation of prospectivity maps. The location of these proven prospects with respect to prospective locations predicted by the Fuzzy logic model reflects the accuracy of prediction and the range of favorability where new prospects are feasible. All frac sand mining operations have a favorability of 0.6 or higher in the final favorability map (see Figure 6).

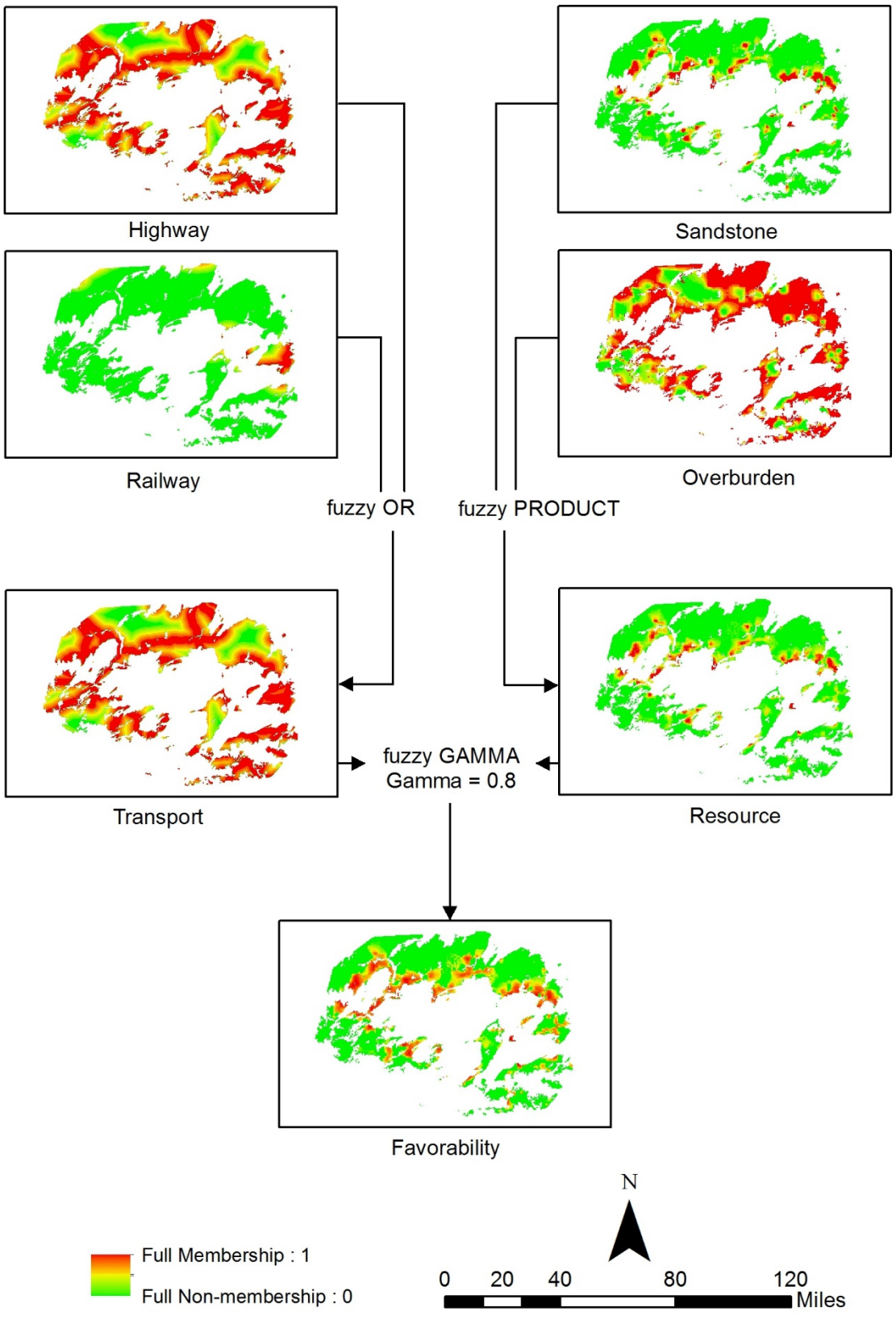

Figure 4. Methodology and memberships integrated into the Fuzzy logic model.

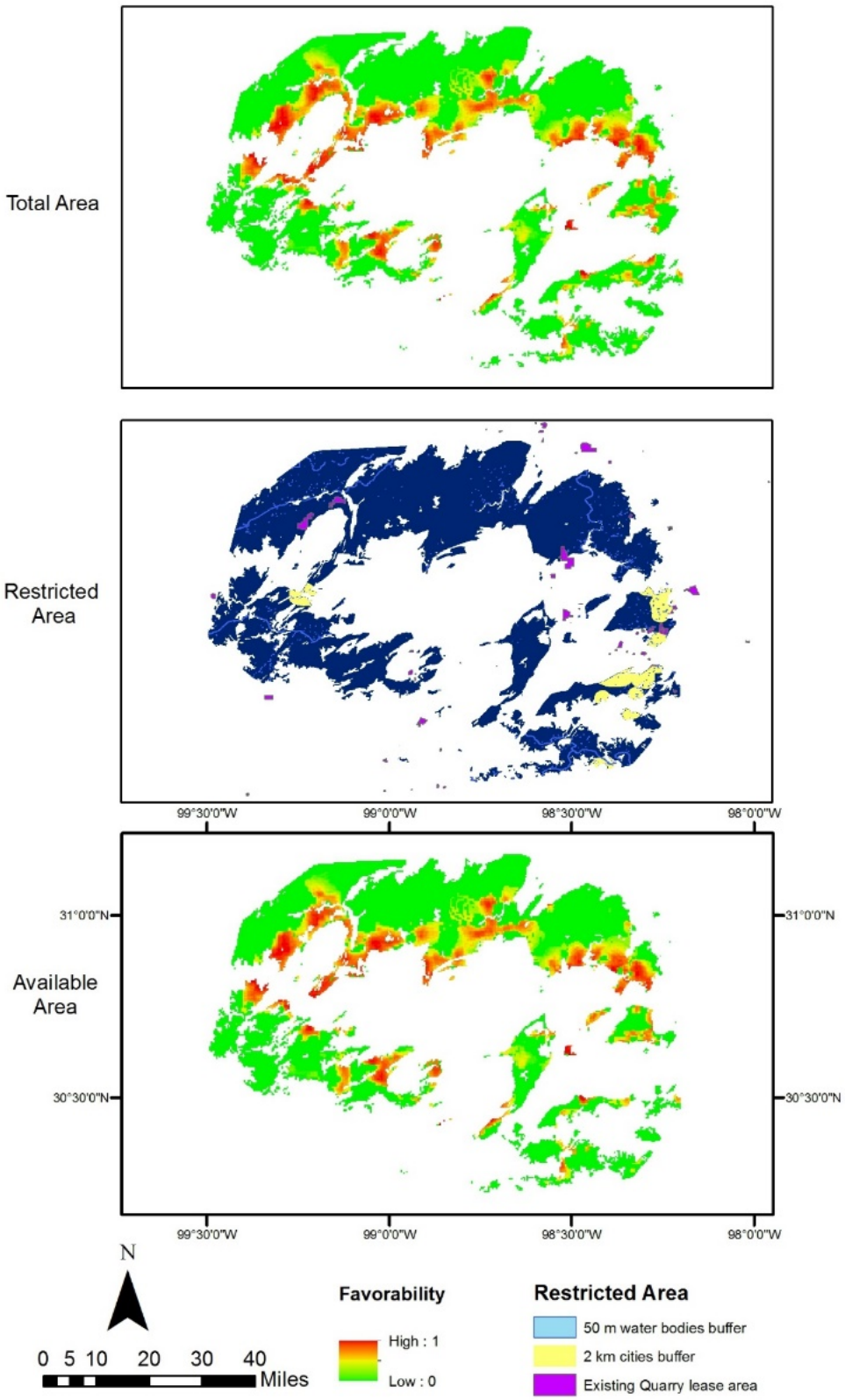

Figure 5. Map of predicted favorability for new sand resource development in central Texas.

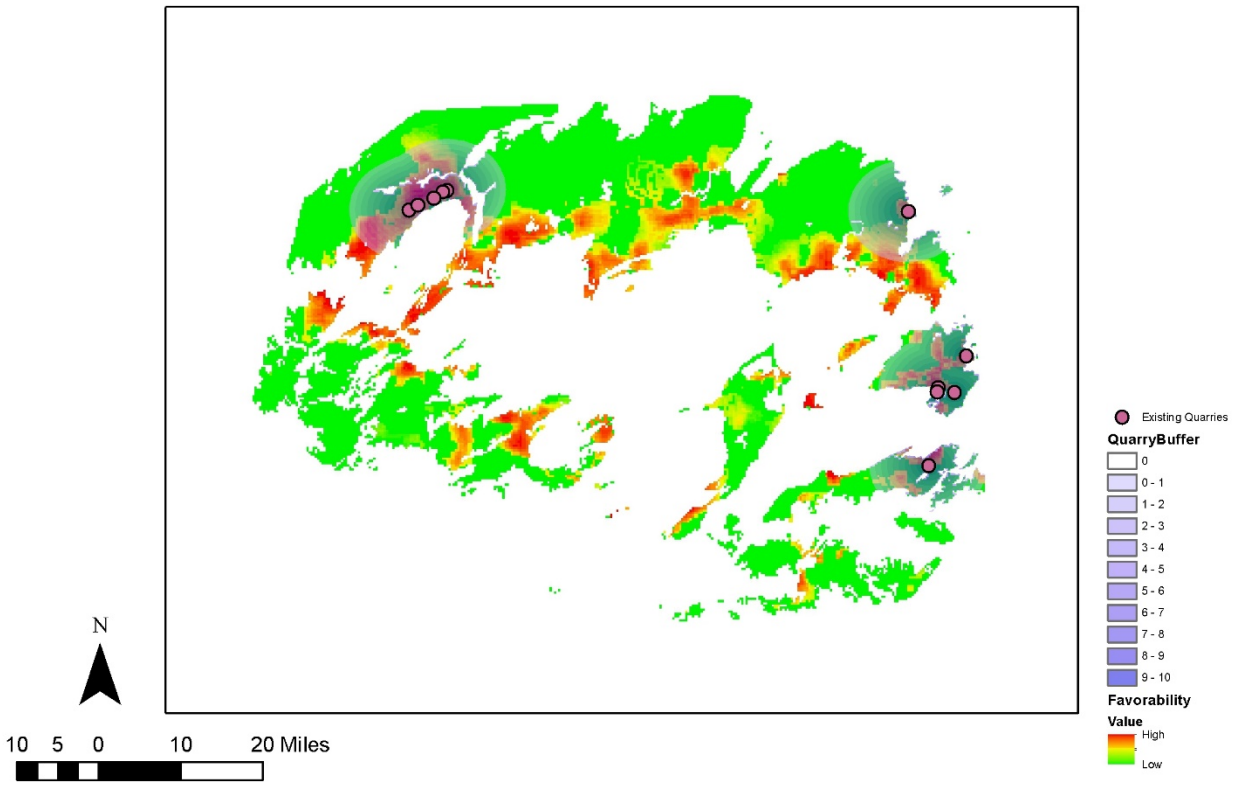

Figure 6. Final favorability map's comparison to existing mining operations

5. RESULTS AND DISCUSSION

The final area available for locating new sand mining facilities (see Figure 5) is scored on a scale of 0 to 1, with 0 being the least favorable and 1 being the most favorable. All existing mining activity is being done in areas with favorability equal to 0.6 and above. The total area with favorability equal to or greater than 0.6 spans over 185,000 acres and holds 20 Bt of sand resource according to our calculations derived from the Fuzzy logic model. The specialized sand used in hydraulic fracturing is an output of several crushing and filtering processes after mining. Interviews with industry sources estimate the yield of processing at only about 25 percent. The calculated volume of natural sand proppant in the Central Texas Frac Sand district, yet to be developed, is slightly less than 5 Bt of appropriate sand resources.

The applicability of sand from the Central Texas Frac Sand district to hydraulic fracturing through the state of Texas is of great interest. The central Texas sand resources could provide a more economical proppant than synthetic or premium natural sand products. There are a number of characteristics that define a material's suitability to the hydraulic fracturing process, but crush strength is primary concern. The Texas sands tend to have crush strength around 6,000 psi. Much of the northern white sands that are transported long distances by railway from Minnesota, Wisconsin and Illinois have a much higher rated crush strength. Figure 7 shows an estimate of basin closure stress in parts of Permian Basin, Eagle Ford, Barnett, and Haynesville basin. The estimate is made based on lower perforation depths (ft) in the shown regions and assuming a closure gradient (psi/ft) of 0.73 psi/ft in the Permian Basin, 0.54 in the Barnett basin, 0.70 psi/ft in the Eagle Ford basin, and 0.95 psi/ft in the Haynesville basin. Although there are many oil and gas wells in the basins across Texas that require a higher crush strength to withstand the immense pressures in deeper formations, most of the area in Texas has wells in more shallow produced formations, well suited to the lower crush strength and more cost effective central Texas frac sand.

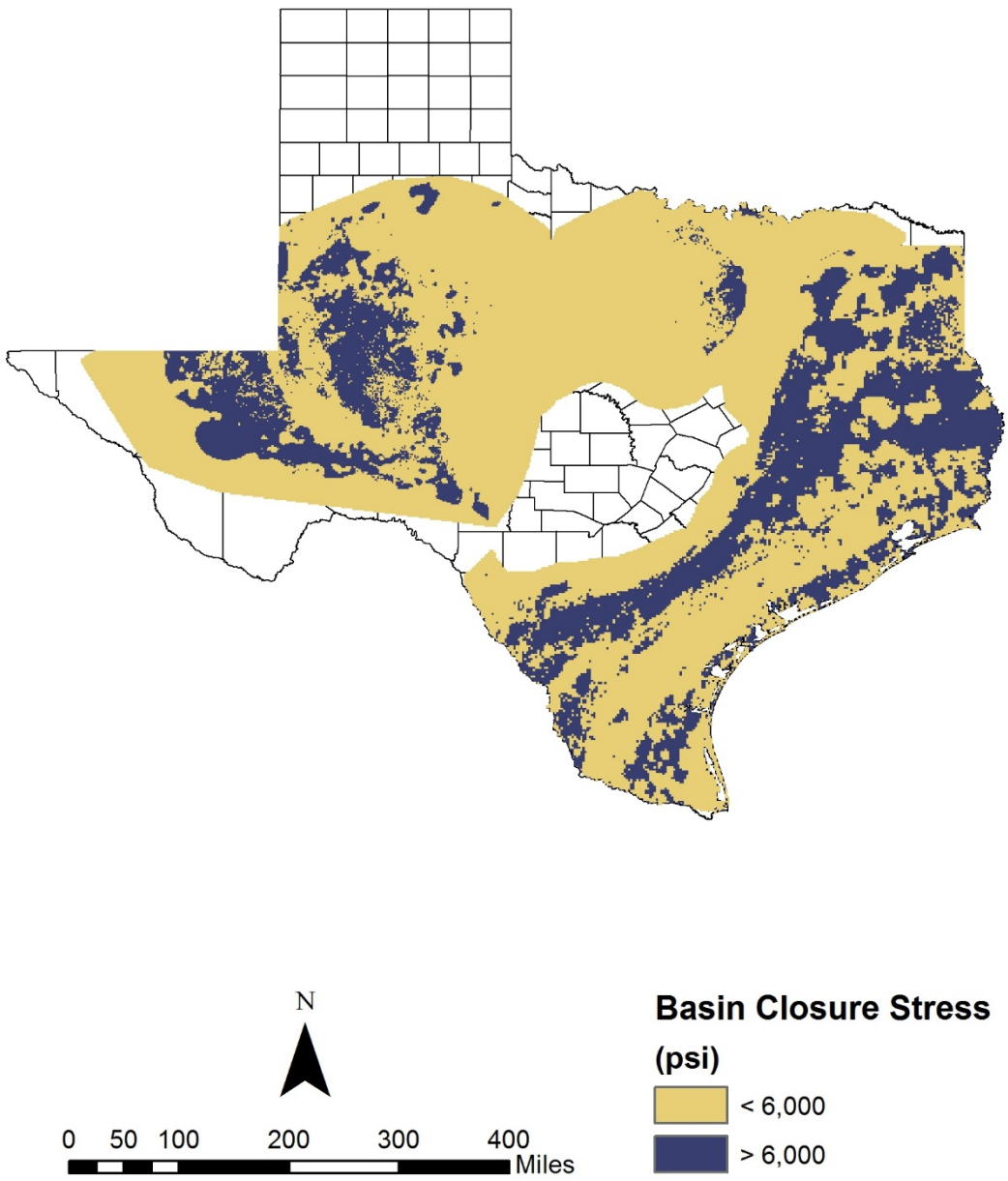

Figure 7. Prospective areas for using Texas' frac sand

6. CONCLUSIONS

The Cambrian-Ordovician sand resources in central Texas have been a source of specialty sand for hydraulic fracturing, and continue to provide an abundance of proppant to oil and gas producers and markets throughout Texas. This study has defined new locations for sand resource extraction in central Texas and estimated the district-wide potential for new developments with the integration of key geospatial characteristics. The following estimates have been formulated:

(1) There is great potential, covering a total of 185,000 acres of land surface, for new sand resource development in the Central Texas Frac Sand district (0.6 and higher on a scale of 0-1).
(2) These new sand resources have the potential to produce 20 billion tons of sand, or about 5 billion tons of frac sand product, from the uppermost sand layer alone.
(3) Overburden tonnage for identified new prospects is about 4.7 billion tons. The average combined stripping ratio for these areas is 0.94.

(4) There are potentially more prospects that could be developed for sand resource extraction, if infrastructure development increased, or more well control is established providing knowledge of the subsurface stratigraphy.

Spatial analysis and prospectivity mapping for resources aid the decision making process and provide an efficient and effective way to conduct exploration, by concentrating on areas of higher economic potential. For example, the spatial analysis of sand layers and overburden suggests that lateral expansion is preferable to vertical development of resources in the area, where extraction of deeper sand layers and removing the inter-layered waste rock is considerably less economical.

5. ACKNOWLEDGEMENTS

We would like to give thanks to the thoughtful suggestions from colleagues and reviewers, which greatly improved the manuscript. The funding for this study was provided by the State of Texas Advanced Resource Recovery program through the University of Texas at Austin, Bureau of Economic Geology, Mineral Resource Program. This study was greatly enhanced by regional mapping products, produced by the University of Texas at Austin Bureau of Economic Geology, and funded through the United States Geological Survey Mapping Cooperative Program, STATEMAP Award No. G14AC0020.

6. REFERENCES

Adams, J.E. (1954). Mid-Paleozoic paleogeography of central Texas. In San Angelo, Geological Society Guidebook, Cambrian (1st) Field Trip – Llano area, pp.70–73.

Barnes, V., Bell, W.C., Clabaugh, S.E., Rodda, P.U. & Young, K. (1972). Geology of the Llano Region and Austin Area. Field Excursion: Guidebook Number 12, Bureau of Economic Geology, p.75.

Barnes, V.E., & Bell, W.C. (1977). The Moore Hollow Group of Central Texas. University of Texas at Austin, Bureau of Economic Geology, Report of Investigations no. 88, 169 p.

Bonham-Carter, G.E. (1994). Geographic Information Systems for Geoscientists, Modeling with GIS. New York: Pergamon.

Carlson, W.D. (1998). Petrologic constraints on the tectonic evolution of the Llano Uplift. In J.P. Hogan, M.C. Gilbert (Eds.), Central North America and Other Regions; Proceedings of the twelfth International Conference on Basement Tectonics: Norman, Oklahoma, USA 1995, Basement Tectonics, 12 (6), (pp. 3–27). Dordrecht, Netherlands: Kluwer Academic Press.

Corrigan, J.C., Cerveny, P.F., Donelick, R.A., & Bergman, S.C. (1998). Postorogenic denudation along the Paleozoic Ouachita trend, south central United States of America: magnitude and timing constraints from apatite fission track data. Tectonics, 17, 587–603.

Elliott, J. (2012). Frac sand in the pipeline. Industrial Minerals, 533, February, 32–40.

Garrison, J.R., Jr., Long, L.E., & Richmann, D.L. (1979) Rb-Sr and K-Ar geochronologic and isotopic studies, Llano uplift, central Texas. Contributions to Mineralogy and Petrology, 69, 361–374.

Helper, M.A. (2000). Geology of the eastern Llano Uplift. In Kyle, J.R., (Ed.), Geology and Historical Mining, Llano Uplift Region, Central Texas: Austin Geological Society, Guidebook 20, 33–48.

Kier, R.S. (1980). Depositional history of the Marble Falls Formation of the Llano region, Central Texas. West Texas Geological Society Publication 80-73, Guidebook to the Annual Field Trip, 59–75.

Krause, S.J. (1996). Stratigraphic framework, facies analysis, and depositional history of the Middle to Late Cambrian Riley Formation, central Texas. Masters Thesis, University of Texas at Austin, 172 p.

Kyle, J.R., and McBride, E. F. (2012). Geology of the Voca frac sand district, western Llano Uplift, Texas. In Conway, F.M. (Ed.), Proceedings, 48th Annual Forum on the Geology of Industrial Minerals: Arizona Geological Survey Special Paper 9, Chapter 2, 1-13.

McBride,E.F., Abdel-Wahab, A.A., & Milliken, K.L. (2002). Petrography and diagenesis of a half-billion-year- old cratonic sandstone (Hickory), Llano region, Texas. University of Texas at Austin, Bureau of Economic Geology, Report of Investigation No. 264, 77 p.

Mosher, S. (1993). Exposed Proterozoic rocks of Texas. In J.C. Reed Jr., M.E. Bickford, R.S. Houston, P.K. Link, D.W. Rankin, P.K. Sims, W.R. Van Schmus (Eds.), Precambrian Conterminous U.S., The Geology of North America, C-2. (pp. 366–378). Boulder, Colorado: Geological Society of America.

Mosher, S. (1995). Geology of the eastern Llano Uplift. In S. Mosher (Ed.) Guide to the Precambrian Geology of the eastern Llano Uplift, A field trip organized by The University of Texas at Austin, in conjunction with the 12th International Conference on Basement Tectonics, (pp. 2–8). Austin, Texas.

Mosher, S. (1996). Geology of the eastern Llano Uplift. In S. Mosher (Ed.) Guide to the Precambrian Geology of the eastern Llano Uplift, Meeting of the South-Central Section of the Geological Society of America, (pp. 3–7), Austin, Texas.

Mosher, S. (1998). Tectonic evolution of the southern Laurentian Grenville orogenic belt. Geological Society of America Bulletin, 110, 1357–1375.

Mosher, S., Levin, J.S.F., & Carlson, W.D. (2008). Mesoproterozoic plate tectonics: A collisional model for the Grenville-aged orogenic belt in the Llano Uplift, central Texas. Geology, 36(1), 55–58.

Reese, J.F. (1995). Structural evolution and geochronology of the southeastern Llano Uplift, central Texas. Ph.D. dissertation, The University of Texas at Austin, 172 p.

Reese, J.F., Mosher, S., Connelly, J. & Roback, R. (2000). Mesoproterozoic chronostratigraphy of the southeastern Llano Uplift, central Texas. Geological Society of America Bulletin, 112(2), 278–291.

Roback, R.C. (1996). Mesoproterozoic polymetamorphism and magmatism in the Llano Uplift, central Texas Geological Society of America, Abstracts with Programs, 28, A377.

Salvador, A. (1991). Origin and development of the Gulf of Mexico Basin. In A. Salvador (Ed.), The Gulf of Mexico Basin, v. J, (pp. 389–344). Boulder, Colorado: Geological Society of America.

Sengupta, M. (1993). Environmental impacts of mining monitoring, restoration, and control. CRC Press.

Singer, D.A. & Menzie, W.D. (2005). Statistical guides to estimating the number of undiscovered mineral deposits: an example with porphyry copper deposits. In Q.Cheng and G. Bonham-Carter (Eds.), Proceedings of IAMG-The annual conference of the International Association for Mathematical Geology, Toronto, Canada, Geomatics Research Laboratory, York University, p. 1028–1033.

Sibson, R. (1981). A Brief Description of Natural Neighbor Interpolation. In Interpolating Multivariate Data, (pp 21–36). New York: John Wiley & Sons.

Smith, D.R., Barnes, C., Shannon, W., Roback, R. & James, E. (1997). Petrogenesis of Mid-Proterozoic granitic magmas; examples from central and west Texas. Precambrian Research, 85, 53–79.

Terracina, J.M., Turner, J.M., Collins, D.H. & Spillars, S.E. (2010). Proppant Selection and its Effect on Results of Fracturing Treatments Performed in Shale Formations. Society of Petroleum Engineers, Paper 135502, 17 p.

United States Geological Survey (2014). USGS Minerals Yearbook – Mineral Commodity Summaries 2014, Department of the Interior, p. 144–145.

Walker, N. (1992). Middle Proterozoic geologic evolution of the Llano uplift, Texas: Evidence from U-Pb zircon geochronometry. Geological Society of America Bulletin, 104, 494–504.

Watson, D. (1992). Contouring: A Guide to the Analysis and Display of Spatial Data. London, England: Pergamon Press.

Zadeh, L.A. (1965). Fuzzy Sets. Information and Control, 8, 338–353.

ASPECTS OF MINERALOGY AND GENESIS OF JAMAICA BAUXITE ORES

Richard D. Hagni[1], and Ann M. Hagni[2]
[1]Department of Geosciences and Geological and Petroleum Engineering, Missouri University of Science and Engineering, Rolla, Missouri,
[2]Ann Hagni Consulting, LLC, Rolla, Missouri

Abstract

The bauxite deposits of Jamaica formerly were the world's largest producers. They occur within karst sink structures and on karst surfaces of Tertiary limestones. Hypotheses on the origin of the bauxite have involved leaching of aluminum from: 1) residual clays in the host limestones, 2) older uplifted volcanic rocks, and 3) younger air-fall volcanic ash from volcanoes in the Lesser Antilles together with Sub-Saharan dust blown from Africa both deposited on the karst host limestones. The presence of altered bentonitic Miocene tuffs on the nearby ocean floor has provided support for the third hypothesis.

Because the bauxite ores contain up to 32% P_2O_5, cathodoluminescence (CL) microscopy was used to examine the character of the phosphorus-bearing grains. Apatite and collophane, that commonly exhibit distinct CL in other ores and rocks, were not observed in low-phosphorus Jamaican bauxite. Scanning electron microscopy (SEM) – energy dispersive spectroscopy (EDS) analyses indicate that phosphorus is instead present as rare earth (Ce, Nd, and Dy) phosphates in those bauxites. CL examination also revealed highly zoned zircon with a bimodal size distribution. By contrast, phosphatic bone fragments and 200-500 µm crandallite pellets, interpreted to represent oral pellets, deposited by sea birds such as cormorants were observed in high-phosphorus bauxites.

Reflected light and SEM-EDS study of opaque grains in a black sand concentrated at Blue Hole Spring, speculated to be derived from bauxite protore by underground drainage, identified hematite, martite, titaniferous magnetite, titaniferous hematite with abundant exsolution ilmenite, and ilmenite. The recognition of titanium iron oxides also in the bauxite ores suggests that the black sands at Blue Hole were indeed derived from the bauxite protores.

1. Introduction

This research project was undertaken shortly after the authors attended the annual Forum on the Geology of Industrial Minerals (FGIM, http://geologyofindustrialminerals.org/content/49th-annual-fgim-jamaica-2013) in Kingston, Jamaica on June 23-29, 2013. The Forum included a field trip to the Jamalco bauxite mines and reduction plant at Clarendon in south-central Jamaica, and one of the authors (R. D. Hagni) arranged a separate visit to one of Noranda's bauxite mines near Alexandria in north-central Jamaica during the Forum meeting. Although the authors had not intended to undertake research on the Jamaica bauxite, upon returning from the Jamaican Forum meeting, it was recognized that there was a need for a cathodoluminescence microscopy study of the bauxite to examine the presence and character of phosphatic grains in the bauxite. The Jamaican bauxite ores contain the highest contents of P_2O_5 in the world. Phosphorus is a deleterious element in the metallurgical treatment of bauxite, and it is eliminated during the Bayer Process by using limestone to increase the pH of the bath. General thinking was that the phosphorus was present predominantly as apatite, and apatite typically exhibits distinctive, intense cathodoluminescence under an electron beam.

In addition to the CL study, it was decided to also conduct an ore microscopic and SEM-EDS study of the mineralogy of black sands collected at Blue Hole (Lagoon) Spring near Negril, Jamaica. The sands were believed to possibly have originated from bauxite protore material by subsurface drainage.

2. Jamaican Bauxite

Jamaica is a world-class bauxite producer, and for many years Jamaica was the world's largest producer of bauxite (USGS mineral resources data). Jamaica placed 6th in world bauxite production in 2014, and Jamaica is the largest supplier of bauxite to the United States. Jamaica has the 4th largest bauxite reserves in the world with grades in excess of 50% Al_2O_3.

Based upon the shapes and occurrence of the deposits, two types of bauxite deposits have been distinguished. In the north and west portions of the island, bauxite deposits occur within steep-sided sink structures in highly karsted limestones. In the south portion of Jamaica bauxite ores occur as blanket-shaped deposits above highly karsted limestones.

Jamaican bauxite ores are very fine grained, with more than 50% of the grains less than 0.5 μm. In addition to containing more than 50% Al_2O_3, Jamaican bauxites are characterized by high iron contents, typically about 15% Fe_2O_3 and up to as much as 20% Fe_2O_3. They might best be referred to as ferruginous bauxites. With regard to their phosphorus contents, samples analyzed for this study ran from 0.2 to 32% P_2O_5.

3. Noranda Bauxite Mine, Alexandria

Noranda, Inc., mines bauxite from a number of deposits in the St. Ann area of northern Jamaica. The deposits are contained in steep-sided sink structures, such as the one at Alexandra (Figure 1). The karst sink structures may have sides about 300 feet (91 meters) high. The bauxite ore is contained in the bottom of the sink structure. Limestone occurs beneath the bauxite ore.

Figure 1. Noranda, Inc., bauxite mine at Alexandria, Jamaica.

The mined bauxite is transported by rail to the St. Ann shipping port at Discovery Bay, and then shipped by boat to a reduction plant at Gramercy, Louisiana, where the aluminum hydroxide is reduced to aluminum oxide (alumina). The alumina is shipped up the Mississippi River to an aluminum smelter at New Madrid in southeast Missouri, where the aluminum oxide is smelted to aluminum metal.

4. Jamalco Bauxite Mine and Reduction Plant, Clarendon

Jamalco is the largest bauxite and reduction operation in Jamaica. Jamalco is owned 55% by Noble Group and 45% by the Jamaican government. Noble recently (Jamaica Observer, 2014) bought their share of Jamalco from Alcoa, who had been the long-time operator. The bauxite deposits in the Clarendon area are blanket deposits typical of southern Jamaica (Figure 2a). Breccia fragments of limestone occur in the bauxite, observed where mining shovels have intersected the underlying limestone pinnacles (Figure 2b).

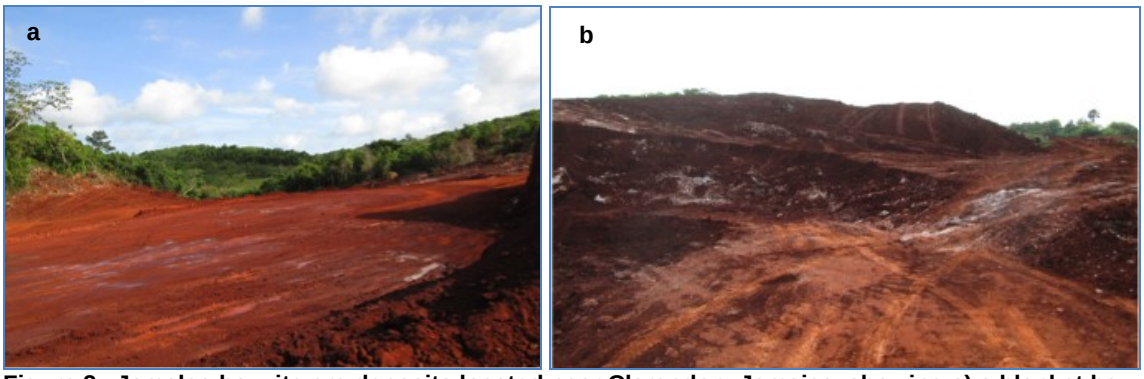

Figure 2. Jamalco bauxite ore deposits located near Clarendon, Jamaica, showing a) a blanket bauxite deposit, typical of southern Jamaica, and b) breccia fragments of limestone (white) from underlying limestone pinnacles.

The Bayer Process at the reduction plant at Clarendon reduces bauxite ore to alumina, and the alumina is shipped to alumina smelters abroad. The Bayer Process uses a hot solution of NaOH to digest the bauxite, converting alumina to sodium aluminate. The solid impurities that do not dissolve are filtered off to form red mud. Two tons of red mud is formed for each ton of sodium aluminate produced. The caustic red mud sludge is impounded in ponds, and it is the greatest environmental problem of the bauxite industry. Four billion tons of red mud has accumulated worldwide.

5. Nippon Light Metal Rare Earth Elements (REE) Extraction Pilot Plant at St. Andrew

One possible use of the waste red mud is to extract by-products, such as rare earth elements (REE). Nippon Light Metal Holdings Company, Ltd., built a pilot plant at St. Andrew in 2013 to evaluate the possibility of extracting REE's from Jamaica red muds (Jamaica Observer, 2013). They chose Jamaica for the plant location because Jamaican bauxites and red muds are higher in REE than others worldwide (McFadden, 2013). Although Nippon has not disclosed the REE contents of Jamaican red muds, Wagh and Pinnock (1987) have previously published analytical results for ten Jamaican red mud samples (refer to Table 1 for averaged data). The cerium (Ce, a light REE) concentration is about 600-700 ppm. Nippon's main target was dysprosium (Dy, a heavy REE), which averaged 76.5 ppm.

Table 1. Concentration (ppm) of Rare Earth Elements (REE) in Jamaica Red Mud*

LREE:	**Concentration (ppm)**
Lanthanum (La)	140
Cerium (Ce)	726
Neodymium (Nd)	392
Samarium (Sm)	90
Europium (Eu)	14
HREE:	
Terbium (Tb)	12.7
Dysprosium (Dy)	76.5
Ytterbium (Yb)	23.3
Lutetium (Lu)	6.1

* Data from (Wagh and Pinnock, 1987)

The plant was completed in September, 2013, but China restored their REE exports and REE prices declined dramatically. Nippon put the REE extraction plant on hold in July, 2014, and then turned the plant over to the Jamaican government in October, 2014 (McIntosh, 2014).

6. Genesis of Jamaican Bauxite Ores

Although the origin of bauxite worldwide is understood to involve deep lateritic weathering under tropical weathering conditions, the character of the original rock (protore) that was weathered differs from bauxite district to district. In the Arkansas bauxite district of northern Arkansas, formerly the largest bauxite producer in the United

States, the protore was nepheline syenite. The fact that nepheline syenite contains little or no quartz made it an ideal rock for bauxite development. In contrast, the Darling Range bauxite district of western Australia developed by weathering of granite, a rock that requires a significant amount of quartz leaching to form bauxite. In contrast to both of those bauxite districts, the bauxite ores on an island in the Trombetas River, a tributary to the Amazon River, formed by lateritic weathering of clay shale. In contrast to all three of the above bauxite districts, the bauxite ores in the Eufaula District of Alabama formed by the weathering of clay residues formed through the dissolution of the host limestones. The Alabama bauxite ores are similar to Jamaican bauxite in that they occur within limestone sink structures.

Three principle hypotheses have been proposed as a source of the aluminum in the Jamaican bauxites. 1) An early hypothesis interpreted the alumina to have been derived from insoluble clay residues from the dissolution of the host Tertiary limestones (Hill, 1955). Although the geographical coincidence of bauxite ores and white Tertiary limestone is remarkably close, the Al_2O_3 content (0.009-0.04%) of the limestone is clearly too low. Jamaican limestones are characterized by their high purity and that makes them useful for many high-purity calcium carbonate industrial uses. 2) Another hypothesis holds that the aluminum was derived from volcanic tuffs exposed in a central inlier that was uplifted by faulting (Comer, 1974). Although spatial distributions of the inlier and the bauxite ores would allow for this interpretation, it is unlikely that the inlier was denuded by the time of bauxite formation. 3) The currently favored hypothesis was first proposed by John Comer (1974), and further developed by Comer (1984), Lyew-Ayee (1984, 1986), and Comer and Jackson (2004). Comer noted that minor bentonite beds occur stratigraphically high in the limestone sequence, and speculated that additional ash may have fallen on the limestones and was concentrated in karst depressions. This interpretation has been further supported by the discovery of numerous beds of volcanic ash in Miocene marls of northern Jamaica (Jackson and Scott, 2014). A recent modification of the third hypothesis is that African dust blown from the Saharan desert may form an additional component in Jamaican terra rossa soils and bauxite protores (Muhs and Budahn, 2009). These writers show that the distribution of African dust extends to Jamaica, and that plots of immobile elements in terra rossa soils occur on or close to compositional areas for African dusts on triangular diagrams.

7. Causes of High P_2O_5 in Jamaican Bauxite

Several possible sources have been suggested for the exceptionally high P_2O_5 contents of Jamaican bauxites. It is unlikely that any significant amount of phosphorus was derived by leaching of the host Tertiary limestones, because they contain only 0.1% P_2O_5. A significant amount of the phosphorus may well have derived from the volcanic ash that probably was the main constituent of the bauxite protores (Jackson and Scott, 2004). The average Jamaican volcanic ash contains 0.75% P_2O_5. The African dust may have contributed some phosphorus. Although carbonatite deposits tend to be small in areal extent, there are many carbonatite deposits in Africa and they typically are rich in apatite. Most of the phosphorus in some Jamaican bauxites was derived from phosphorite bird guano that is especially rich in P_2O_5.

Bird guano was first reported by Garrett et al. (2008) to be plastered on the top of a limestone pinnacle beneath bauxite ore at the Hope bauxite mine in south-central Jamaica. They speculated that sea birds, mostly cormorants, had deposited the guano at roosts on the island. They believe the cormorants had been eating fish offshore, mostly anchovies that had flourished in nearby favorable oceanic currents. Fish bones and fish teeth were among the phosphatic constituents that they observed in the guano.

A similar situation occurs today along the coast of Peru where anchovy flourish in upwelling cool waters of the Humboldt Current, which attracts large numbers of cormorants that feed on the anchovies. The birds huddle close to each other on their roosts as they drop massive amounts of phosphatic bird guano deposits that are put into bags by miners to be sold commercially as fertilizer.

More recently Garrett et al. (2010) reported the presence of phosphate rich “nodules” in bauxitic material at Spitzbergen about seven miles northwest of the Hope mine. By SEM they found very small prismatic crystals of apatite and crandallite [$CaAl_3(PO_4)_2(OH)_5.H_2O$] in the phosphatic bauxitic material. Platy fluorapatite crystals up to 5 µm long occurred in rosettes. Platy crandallite crystals up to 3 µm long were clustered densely together.

8. Purpose of Current Research

This current research was aimed at further examining the mineralogy of the phosphorus content of the Jamaican bauxite. Apatite is a mineral that typically shows a strong and characteristic cathodoluminescence (Figure 3) and no previous cathodoluminescence microscopic examination had been conducted on the Jamaican bauxites. It was anticipated that some of the phosphorus might well be present in the bauxites as the amorphous variety

collophane, and collophane had been found to show strong cathololuminescence in previous studies of the Birmingham iron ores in Alabama (Figure 4; Hagni and Cooper, 1982) and in the Alsace-Lorraine iron ores of France (Figure 5; Musa Karakus et al., 1990). Crandallite had not been studied by CL previously. It was speculated that the character of the phosphate mineral grains might provide information not only on the origin of those grains but also might provide useful information on the character of the bauxite protores.

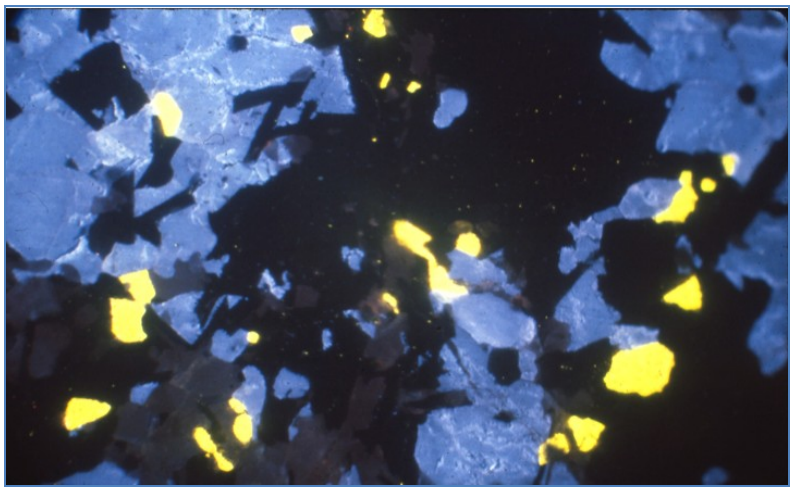

Figure 3. Cathodoluminescence photomicrograph of sample from Charnockite, Adirondack Mountains, New York, showing apatite (yellow CL), orthoclase (blue CL), quartz (black), and biotite (black, platy).

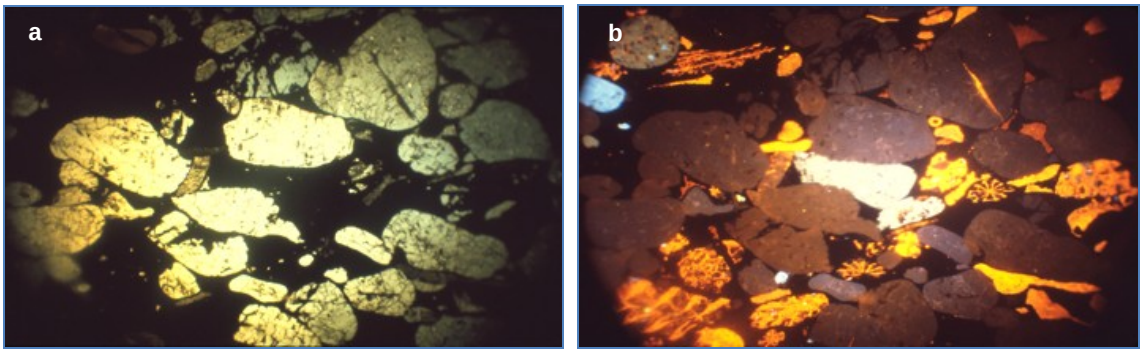

Figure 4. Photomicrographs of Birmingham iron ores, showing a) fine-grained hematite occludes collaphane in transmitted light, and b) collaphane (strong white CL), calcite fossils (yellow CL), quartz grains (dull red CL) and one orthoclase grain (blue CL) by cathodoluminescence microscopy.

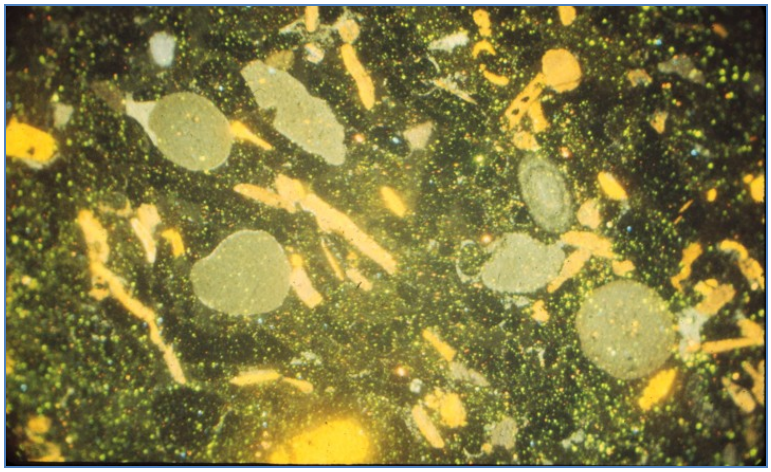

Figure 5. Cathodoluminescence micrograph of Alsace-Lorraine sedimentary iron ores, France showing many large collophane fecal pellets (light gray) and calcite fossils (yellow CL).

A total of five Jamaican bauxite samples have been analyzed not only by cathodoluminescence microscopy (CL), but also by transmitted light microscopic (TL), reflected light microscopic (RL), scanning electron microscopy (SEM), back scattered image (BSI), energy dispersive spectroscopy (EDS), and X-ray diffraction (XRD). The initial bauxite sample, from a Jamalco mine near Clarendon, contained only 0.2% P_2O_5. Concerned that the very low-phosphorus bauxite sample might not be representative of Jamaica bauxite, the authors contacted Shanti Persuad to request intermediate to high phosphorus bauxite samples. The writers thank Shanti Persuad for providing two intermediate-level phosphorus bauxite samples (drill hole samples from two orebodies at Maggotty in St. Elizabeth Province in southwest Jamaica with 7.7 and 9.2% P_2O_5), and Tony Porter for providing high-level phosphorus samples with 30-32% P_2O_5 from the Hope mine and Spitzenberg site previously discussed.

Finally, black sands at Blue Hole (Lagoon) were examined by reflected light microscopy and by SEM to determine their mineralogy and textures. It had been speculated that the black sands might have been derived from the protore material that was weathered to bauxite.

9. Causes for Elevated Rare Earth Elements (REE) Content of Jamaican Bauxite and Red Mud

Prior to discussing our microscopic results it is appropriate to discuss possible sources of the rare earth elements (REE) present in the Jamaican bauxites. The host Tertiary limestones are essentially devoid in REE's and cannot be considered to be a viable source for REE's. The most likely source of REE's is from the air-fall volcanic tuffs that are speculated to have formed the protore for the development of the bauxite. Another possible contribution might be from the Sub-Saharan dust blown from Africa (Simon Mitchell, University of the West Indies, oral communication, 2013). Elevated amounts of REE's commonly occur in African carbonatites.

The concentration of light and heavy REE's in ten (10) Jamaican red mud samples have been analyzed by Wagh and Pinnock (1987). Those analyses were averaged and are presented in Table 1 (refer to Section 5). The light REE's are much more abundant than the heavy REE's, and dysprosium is the most abundant of the heavy REE's at 76.5%.

10. Occurrence of Phosphorus in Low-phosphorus Jamaican Bauxite

CL study of the bauxite sample from the Jamalco mine near Clarendon that contained only 0.2% P_2O_5 did not reveal any apatite. SEM-EDS maps for the sample showed that calcium and phosphorus do not occur in the same phases, confirming that neither apatite nor collophane were present. SEM-EDS probes of the same sample identified four rare earth phosphates (oxygen identified and hydrogen assumed to be present in three of these four phases): $NdPO_4 \cdot 2H_2O$, $CePO_4 \cdot H_2O$, $(Nd,Y)PO_4 \cdot 2H_2O$, and $DyYPO_4$. Thus the phosphorus in low-phosphorus Jamaican bauxites does not occur as calcium phosphates, but rather as rare earth phosphates.

The CL study did show the presence of zircon crystals. Most of the zircon crystals probably were derived from the air-fall volcanic tuffs, but some zircon crystals were contributed to the bauxite protores from alluvial sources (Comer et al. 1980A,B).

11. Microscopy of High-phosphorus Bauxite at Spitzenberg

The microscopy of the Spitzbergen high-phosphorus bauxitic material provides the most information regarding phosphatic minerals and their character. It contains 30% P_2O_5, and XRD indicated the presence of 48% crandallite [$CaAl_3(PO_4)_2(OH)_5 \cdot H_2O$] and 27% apatite. By transmitted light microscopy, rather large (200-500 µm) abundant, rounded grains of crandallite appear to be fecal pellets (Figure 6a) dropped by invertebrate organisms. The pellets may be closely clustered together to form much larger areas of crandallite that only locally reveals the shapes of individual pellets (Figure 6b). Some crandallite grains are more irregular in shape (Figure 6c). The crandallite pellets are much too small to represent true fecal pellets (up to two-feet long) dropped by the large cormorants. They may represent droppings of some small invertebrate organism. Alternatively, they may represent oral pellets regurgitated each morning by cormorants. Those oral pellets contain indigestible components from the former day's feasting on anchovies and other small fish. However, such oral pellets have sizes that exceed those observed in the bauxite. SEM-EDS analyses confirm that the crandallite pellets contain major amounts of calcium, aluminum, and phosphorus. Examination of many crandallite pellets by CL showed that they are non-cathodoluminescent.

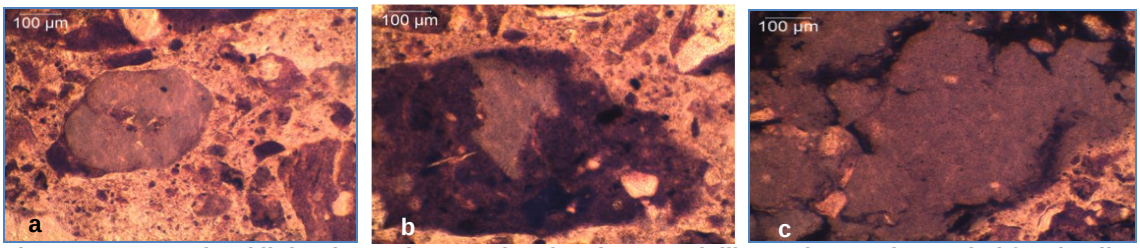

Figure 6. Transmitted light photomicrographs showing crandallite grains as a) rounded fecal pellet, b) irregularly-shaped fecal pellet, and c) clustered fecal pellets.

Phosphatic bones also are common in the Spitzenberg sample. The bones originally were collophane, but they are commonly partly replaced by apatite that may be radial-acicular spherulitic and spherulitic crandallite (Figure 7). The bones typically are crudely rounded. In contrast to the Birmingham and Alsace-Lorraine collophane grains that readily cathodoluminesced, the Jamaican bauxite collophane do not catholuminesce. The term "collophane" is used here in the petrographic sense. That is, it is used for material that under transmitted light microscopy appears to be isotropic but in reality is very fine-grained cryptocrystalline apatite.

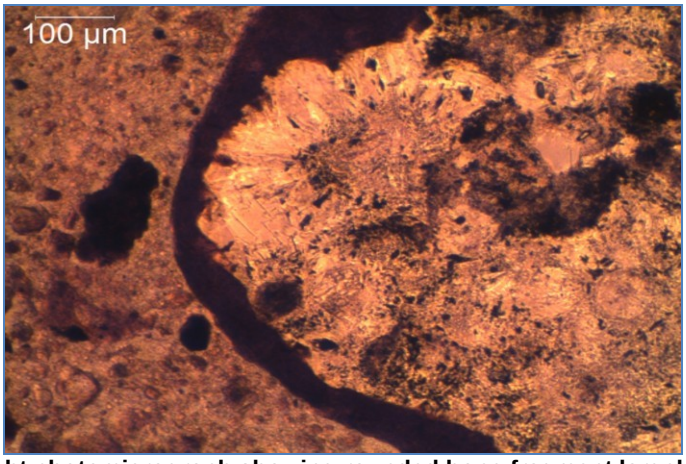

Figure 7. Transmitted light photomicrograph showing rounded bone fragment largely replaced by radial acicular boehmite.

A SEM-BSI photomicrograph shown in Figure 8a includes two phosphatic bones that are elongate and partly rounded at their ends. The bones originally consisted of collophane (medium gray), but they have been largely replaced by apatite (bright white). SEM-EDS maps of Al, Ca, and P, are overlain and shown as a composite (selected phase map) in Figure 8b. The larger bone (green, right center) shows a chemical composition for the collophane portion that is essentially equivalent to that to the apatite portion of the bone. Smaller grains of apatite (green) occur within bauxite grains. The three large grains (pale purple) to the left of the large bone are crandallite pellets. Areas of Al-rich bauxite are shown by bright purple colors

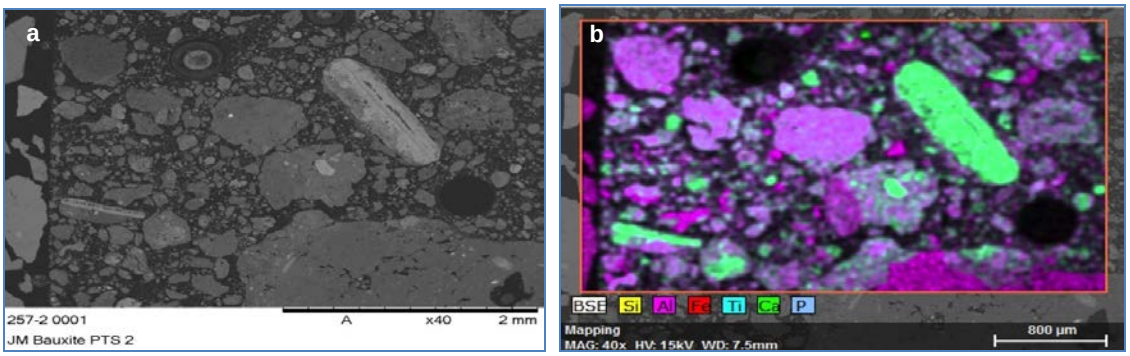

Figure 8. Scanning electron microscopy (SEM) photomicrographs, showing a) back scattered image (BSI), and b) energy dispersive spectroscopy (EDS) composite of Al, Ca, and P elemental maps.

Limestone fragments in this bauxitic material show no tendency to be replaced by apatite or crandallite. Interestingly, in contrast to most limestones that cathodolumionesce brightly, the limestone fragments in the Jamaican bauxite are largely non-cathodoluminescent. Limestones that do not show CL usually are the result of excessive amounts of quencher elements such as ferrous iron. In the case of Jamaican limestones, which are especially pure, it is more likely due to the deficiency of activator elements such as manganese.

12. Microscopy of High-phosphorus Bauxite at the Hope Mine

The microscopy of the Hope mine high-phosphorus (32% P_2O_5) bauxitic material is similar to that at the Spitzbergen site, but no apatite was detected by transmitted light microscopy nor by CL. Crandallite pellets are abundant and similar to those at Spitzbergen (Figure 9).

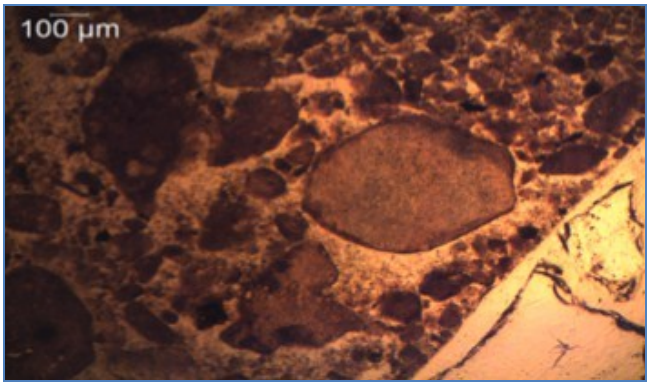

Figure 9. Transmitted light photomicrograph of bauxite from the Hope Mine, showing crandallite fecal pellet.

13. Microscopy of Bauxite Samples with Moderate Amounts of Phosphorus

Drill core samples from two separate orebodies, Maggotty 315 and Maggotty 316 in St. Elizabeth parish in southwest Jamaica, differ from both low and high phosphorus bauxite samples. Maggotty 315 contains 7.7% P_2O_5, and Maggotty 316 contains 9.2% P_2O_5. Neither sample contains crandallite pellets. Apatite was not detected by CLM or XRD. No REE-phosphates were detected by SEM-EDS. XRD indicates that all of the phosphorus is present as crandallite. The crandallite appears to occur as non-cathodoluminescent, micron-sized, very fine grains in the bauxite.

14. Ore Microscopy and SEM Examination of Black Sands at Blue Hole, Negril

Black sand currently concentrating at the edge of subsurface waters emerging at Blue Hole Spring near Negril, Jamaica, were examined for their mineralogy by reflected light microscopy and SEM. The minerals are dominantly very coarse-grained magnetite, ilmenite, and hematite (Figures 10a and 10b). Some ilmenite grains exhibit well-developed exsolution textures in which abundant hematite laths have exsolved from the ilmenite host grains (Figure 11). Secondary fine-grained martite and goethite have developed by oxidation of the primary Fe-Ti oxide minerals.

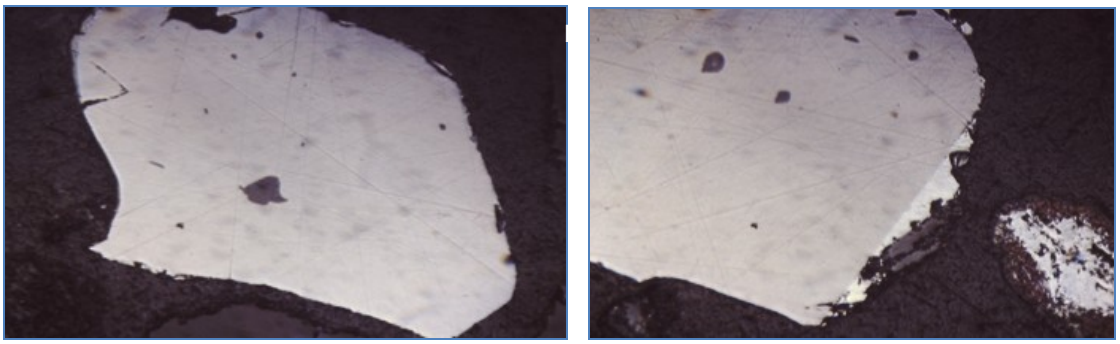

Figure 10. Reflected light photomicrographs of samples from Blue Hole, Negril, Jamaica, showing coarse-grained a) magnetite, and b) ilmenite.

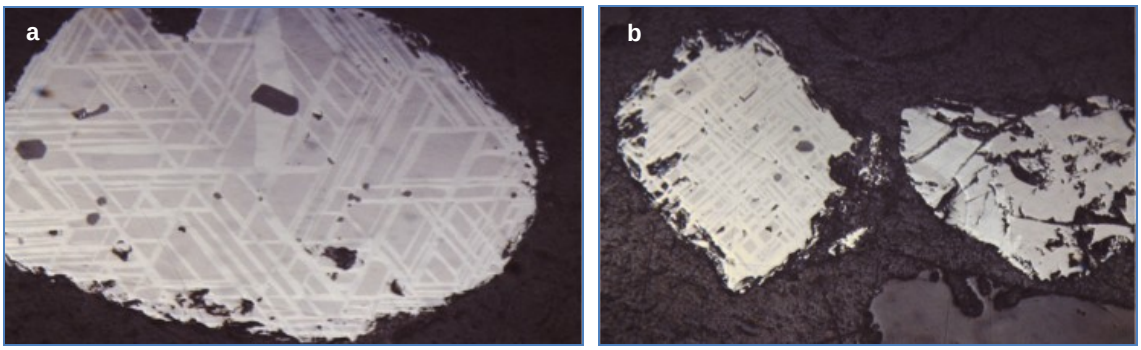

Figure 11. Reflected light photomicrographs of samples from Blue Hole, Negril, Jamaica, showing extensive exsolution of hematite lamellae from host ilmenite grains.

The coarse-grained nature of the Fe-Ti oxides and the well-developed exsolution textures are not what would be expected to occur in volcanic air-fall tuffs or in Sub-Saharan African dusts. A likely source would be the igneous intrusive and metamorphic rocks in the nearby Blue Mountains of northeast Jamaica. The additional recognition of exsolution-textured ilmenite-hematite grains in the Jamaican bauxites (Figure 12) confirms that the black sands at Blue Hole do represent a component present in the protores for the bauxite deposits. The black sands are important because they represent a third (alluvial) source of material in the protores from which the bauxite deposits were developed by lateritic weathering. Muhs and Budahn (2009) also postulated a third source based on chromium present in Jamaican terra rossa soils.

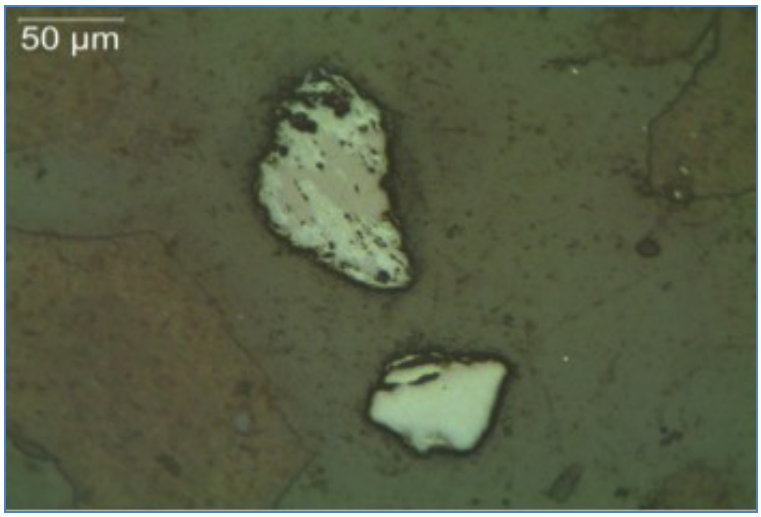

Figure 12. Reflected light photomicrographs of Jamaican bauxite, showing exsolution of hematite lamellae from host ilmenite grain.

15. Summary and Conclusions

Cathodoluminescence microscopy did not reveal any apatite nor collophane is low-phosphorus (0.2% P_2O_5) Jamaican bauxite. SEM-EDS study shows that the small amounts of phosphorus occur instead as REE phosphates. The CL study did recognize zircon crystals that probably were derived mainly from the air-fall tuffs, but perhaps partly also from alluvial sources.

The rounded “concretions” at Spitzbergen probably are bones composed of collophane that has been relatively easily replaced, due to its very fine-grained character, by boehmite. The Al for the formation of boehmite was introduced from fluids in the adjacent bauxite. The bones are anchovy and other fish bones dropped by roosting cormorants.

Crandallite grains that appear like fecal pellets are too small to be regurgitated cormorant oral digestive pellets. Instead, they appear to be fecal pellets dropped by invertebrate organisms foraging in the organic-rich bauxitic material.

The coarse-grained magnetite, ilmenite, and hematite, together especially with well-developed ilmenite-hematite exsolution textures in black sands at Blue Hole Spring points to an alluvial source in addition to those of air-fall volcanic tuffs and wind-blown African dusts. These grains probably indicate an origin from coarse-grained intrusive igneous and metamorphic rocks in the nearby Blue Mountains of northeast Jamaica. The fact that such ilmenite-hematite exsolution textured grains were also found in the examined bauxite samples shows that the black sands represent the bauxite protores, and that they form a third, alluvial, contribution to the protores. This third source may well be equivalent to the third source of Muhs and Budahn (2009), who postulated such a source based upon the presence of chromium in Jamaican terra rossa soils of Jamaica.

The results of these microscopic studies are consistent with the hypothesis that the Jamaican bauxites have originated by deep lateritic weathering of volcanic air-fall tuffs from the Lesser Antilles, dusts blown from Africa, and a third alluvial source from the Blue Mountains.

16. References

Comer, J.B. 1974. Genesis of Jamaican Bauxite: Economic Geology 69 (8), p. 1251-1264.

Comer, J.B. 1984. Geological and Geochemical Constraints on the origin of Bauxite in Jamaica, in Jacob, L., Jr., ed., Bauxite Symposium: American of Mining, Metallurgical and Petroleum Engineers Proceedings, p. 152-164.

Comer, J.B., C.W. Naeser, and F.W. McDowell. 1980A. Fission-track ages of zircon from Jamaican Bauxite and Terra Rossa: Economic Geology, 75 (1), p. 117-121.

Comer, J.B., C.W. Naeser, and F.W. McDowell. 1980B. Fission-track ages of zircon from Jamaican Bauxite and Terra Rossa, reply: Economic Geology 75 (1), p. 947-948.

Comer, J.B. and T.A. Jackson. 2005. Miocene bentonites in the white limestone group, Jamaica: Cainozoic Research 3, p. 31-37.

Forum on the Geology of Industrial Minerals (FGIM), 2013. http://geologyofindustrialminerals.org/content/49th-annual-fgim-jamaica-2013, Kingston, Jamaica, June 23-29, 2013, accessed September 29, 2015.

Garrett, R., A. Porter, P. Hunt, and G. Lalor. 2008. The Presence of Anomalous Trace Element Levels in Present Day Jamaican Soils and the Geochemistry of Late-Miocene or Pliocene Phosphorites: Applied Geochemistry 23, p. 822-834.

Garrett, R., A. Porter, and P. Hunt. 2010. An Occurrence of Cadminiferous Phosphorite Soil Concretions in Jamaica: Applied Geochemistry 25, p. 1047-1055.

Hagni, R.D. and M. Cooper. 1982. The Nature of Phosphorous-Bearing Mineral Grains in the Birmingham, Alabama Sedimentary Iron Ores and an Assessment of Their Potential Liberation by Beneficiation: Process Mineralogy II, TMS-AIME, p. 95-117

Hill, V.G. 1955. The Mineralogy and Genesis of the Bauxite Deposits of Jamaica: American Mineralogist 40, p. 676-688.

Jackson, T.A. and Scott, P.W. 2014. The provenance of volcanogenic sediments in the Miocene Buff Bay Member, Buff Bay, Jamaica. Caribbean Journal of Earth Science, 47, 9-13. © Geological Society of Jamaica. Available online 17th September 2014.

Jamaica Observer. 2014. Alcoa Sale of Stake in Jamalco to Noble Group Completed, December 7, 2014, http://www.jamaicaobserver.com/latestnews/Alcoa-sale-of-stake-in-Jamalco-to-Noble-Group-completed, accessed September 9, 2015.

Jamaica Observer. 2013. A Rare Find: A Japanese Firms says Jamaica's Earth Minerals could help them break China's hold on Market, October 24, 2013, http://www.jamaicaobserver.com/news/A-rare-find_15313316, accessed September 11, 2015.

Karakus, M., R.D. Hagni, and A.C. Spreng. 1990. Phosphate Mineralogy of the Alsace-Lorraine Iron Ores and the Potential for Phosphate Liberation by Beneficiation: Process Mineralogy IX, TMS-AIME, p. 93-110.

Lyew-Ayee, P.A. 1984. Bauxites in the Caribbean, in Jacob, L., Jr., ed., Bauxite Symposium: American of Mining, Metallurgical and Petroleum Engineers Proceedings, p. 262-296.

Lyew-Ayee, P.A. 1986. A case for the Volcanic Origin of Jamaica Bauxites: Proceedings of Bauxite Symposium VI, Geological Society of Jamaica Journal, p. 9-39.

McFadden, D. 2013. Jamaica breaks Ground on Rare-Earth Project, The Washington Times, February 4, 2013, http://www.washingtontimes.com/news/2013/feb/4/jamaica-breaks-ground-on-rare-earth-project/, Accessed September 10, 2015.

McIntosh, D. 2014. Jamaica has Full Ownership of Rare Earth Element Plant, Jamaica Information Service, October 10, 2014, http://jis.gov.jm/jamaica-full-ownership-rare-earth-element-plant/, accessed September 9, 2015.

Muhs, D. R., and J.R. Budahn. 2009. Geochemical Evidence for African Dust and Volcanic Ash Inputs to Terra Rossa Soils on Carbonate Reef Terraces, Northern Jamaica, West Indies: USGS, Digital Commons, University of Nebraska-Lincoln, 35 p.

USGS. 2013. National Minerals Information Center: Mineral Industry Surveys, Bauxite and Alumina.

Wagh, A.S., and W.R. Pinnock. 1987. Occurrence of Scandium and Rare Earth Elements in Jamaican Bauxite Waste: Economic Geology 82, P. 757-761.

ICE: THE COOLEST (FORGOTTEN) INDUSTRIAL MINERAL

Stanley T. Krukowski, Oklahoma Geological Survey, Norman, OK 73019; 405-325-8033; skrukowski@ou.edu

Abstract

Ice production in the United States was big business in the 19th and first half of the 20th centuries. It led all US exports in the 19th century with the exception of cotton. Most ice production occurred in the northern tier of states where lengthy, cold winters were necessary for ice to form in ponds and lakes.

Ice is a mineral in a geological sense: occurs naturally; is inorganic; has definite chemical composition (H2O); has regular internal structure (hexagonal). Ice is an economic mineral as it is extracted from the earth for a useful purpose, i.e., a refrigerant. It is ranked as an industrial mineral, because it is a non-fuel and nonmetallic.

The earliest known ice harvesting was in Persia around 400 BC. Harvested in nearby mountains in winter, it was stored underground in summer, and reserved for royalty. Ice harvesting thrived for centuries in Europe and Asia. For example, Switzerland exported ice to France, and England imported ice from Norway. The first commercial ice shipment in North America was from New York City to Charleston, South Carolina, in 1799. Local ice production occurred earlier, but prospered in the 19th century.

Frederick Tudor, the 'ice king,' made a fortune exporting New England ice to the tropics. Packed in sawdust, one third of the cargo melted, but enough survived for a profit. Ice was readily available (low unit value, high place value), but shipped to warmer climes it was a rare item (high unit value). Ice houses were standard in most US towns for 150 years, disappearing in the 1950s as mechanical ice production became efficient. The first refrigerated railroad cars in 1851 used harvested ice to preserve perishables.

Early harvesting tools were simple hand saws, scrapers, axes, pikes, and tongs. Heavier work was by horse drawn plows, sledges, and conveyors. Later internal combustion engines powered large saws, and transported ice to storage by conveyor and trucks. Because work was seasonal, crews usually found summer work locally on farms, quarries, and forests.

Introduction

Little thought is given today about refrigeration and how we rely on it. It preserves the food we eat, from household refrigerators and freezers to meatpacking plants; enhances the flavor of beverages and keeps them cool during consumption; keeps buildings cool during summer (air conditioning); is responsible for advances in cryogenics, from industrial to medical applications. The discussion herein, however, will restrict itself to the origins of refrigeration concentrating on the utilization of naturally harvested ice from lentic environments. The trade in frozen water was so great an enterprise that it was second only to cotton as a major US export. American ice made its way to the southern tropical isles, India, and as far away as Australia in the 19th century.

Ice is a Mineral

Ice is considered a mineral in the geological sense and in terms of economics. It is also an industrial mineral. Geologists define a mineral as a naturally occurring, inorganic substance, usually a solid, with a definite chemical composition and with a regular internal structure. Ice fits this description forming an inorganic solid at temperatures below 0^o C (32^o F), has a definite chemical composition of hydrogen dioxide (H_2O) with hexagonal internal structure (I_h; under high pressure, for example in glacial ice, its internal structure is cubic, I_c). See Figure 1. An economic mineral is any substance extracted from the Earth for a useful purpose, usually at a profit. It is obvious from its history of harvesting, that ice is also an economic mineral. Lastly, ice is an industrial mineral because it is a nonmetallic and a nonfuel.

Early History

In ancient times, people would preserve ice from winter months usually by burial—ancient civilizations would dig pits to bury ice and snow, using the preserved ice for various refrigeration applications. Ancient records from Mesopotamia report how to build an icehouse (Dalley, 2002). Archeological evidence supports the existence of ice pits in China in the 7th century BC while other evidence suggests their use some 400–500 years earlier. In the eastern

Mediterranean ancient Greeks also stored snow in such pits, harvesting it from mountains in the winter. Likewise during the Roman Empire, snow and ice was imported from the mountains and stored in underground pits purposely dug for this reason.

The enduring example of ancient ice harvesting and storage comes from ancient Persia (modern-day Iran). Persian engineers devised and built a structure called a *yakhchal* (Figure 2) for the storage of ice harvested in the winter from surrounding mountains. Yakhchals have been under construction and used in Iran since the 4th century BC. The yakhchal was constructed ingeniously so that stored ice could be utilized in summer, but also could produce additional ice each winter day. Walls of the yakhchal were made of a special mortar of sand, clay, egg whites, lime, goat hair, and ash in exact proportions and acted as an insulating material, resistant to heat and impervious to water. Ancient royalty used the yakhchal to cool off during hot summer days. The ice also was used to cool royal treats such as *faloodeh*, which today is the traditional frozen dessert of Persia. (Anonymous, 2009)

Prior to the 19th century, snow and ice was harvested wherever it was available in small amounts, and stored for use in summer. The Alps and Andes mountains provided ice and snow in the Mediterranean and in South America, respectively. Russians had a long history of harvesting ice from rivers and lakes during winter for use during summer. Other Europeans, particularly royalty and the wealthy, had ice harvested during the winter and stored on their estates using it to cool drinks and other food. The same was done in North America, ice cream being a favorite treat of the well-to-do. The northern Scandinavian countries exported ice in small quantities to England in the 17th and 18th centuries, but only the rich could afford it.

Frederic Tudor — "The Ice King"

Frederic Tudor was born in 1783, the year of the Peace of Paris, a treaty of which, part of, ended the hostilities between England and its North American colonies in rebellion—it marked the end of the American Revolutionary War. Born into a well-to-do family, Frederic determined to make his mark in the world. His father William, a successful lawyer and Harvard alumnus, sent three sons to that institution of higher learning. However, Frederic would have none of it. He apprenticed himself at age 13 to a retailer in Boston to learn the ways of the business world. In 1801, when his brother John suffered a broken leg, Frederic accompanied him to Havana, as a warmer climate was recommended for his recovery. Back in Boston in 1805, his brother William off-handedly made the suggestion that ice harvested from New England ponds could be sold in the tropics. Frederic committed himself to the idea despite the ridicule and incredulity he suffered.

Frederic Tudor recognized that New England ice was an underused commodity—ice was free for the taking. Further, New England farmers idled most of the winter away; Tudor understood, therefore, that farmers represented an underemployed labor force. Also recognized was an underserved market for the New England ice—the tropics. To complete the scenario, two additional conditions had to be met: ballastless ships and ice storage facilities (icehouses). The ice would provide the ballast for the ship, even though melting would decrease the amount of ice that reached its destination. Ice required insulated storage to minimize its melting. The forests of Maine and its logging industry provided the lumber for icehouse construction and the abundance of sawdust needed to insulate the ice in storage and onboard ship.

In 1806 Tudor purchased the brig *Favorite* to transport his first cargo of ice to St. Pierre, Martinique. It was a financial disaster. His brother William with the help of a cousin, James Savage, were supposed to prepare the way. Unfortunately, they had left the island prematurely failing to obtain the proper subscriptions for the sale of the ice, and also neglected to prepare for its storage. Despite these letdowns, Frederic secured the proper permission to sell his ice, but without suitable storage. Unfortunately this first endeavor was not a financial or marketing success. Despite handbills instructing the consumer about the care and use of the commodity, customers carried the ice home in the noonday sun; stored it in tubs of water; stored it with salt. All proved detrimental. It was clear that the endeavor needed rethinking.

Icehouses were built in Havana, Cuba, for Tudor's next attempt at the ice trade. He secured exclusive rights from the government to sell his ice there (Figure 3). He then expanded his trade in a similar manner in Jamaica. Despite the financial losses incurred during these ventures and constant indebtedness, Tudor continued with his aspirations. Finally after the War of 1812 and renewed efforts in Havana, Tudor's enterprise finally turned a profit. About 90% of his trade consisted of sales to coffeehouses where ice was used for making ice cream and cooling drinks.

During this period, Tudor traveled to Charleston, South Carolina, to establish trade relations. His marketing plan included convincing everyone that ice was a necessity even though it never had been. He visited boarding houses, taverns, meat and fish packers, and farmers markets. He offered tavern owners free ice for a year with the

proviso that they charge no more for cooled drinks than those purchased at ambient temperatures. Customers typically preferred the cooler versions, helping to convince proprietors of the necessity of ice for refrigeration and cooling drinks. One marketing ploy was to stay in boarding houses, where he would use ice to cool his drink during meals. At first others boarders thought the practice odd, but curiosity got the better of them and before too long they preferred iced drinks, too.

By 1820, Tudor had established trade with the southern tropical isles and states in the southern US. He had finally met with success and was on his way to making his fortune. (Oddly enough, Tudor was willing to take commercial risks, one of which again almost brought him to ruin: his investments in toothpick-making inventions [Petroski, 2008]). Tudor's success depended on two aspects of the trade. First he tried to obtain from local government authority exclusive rights to sell his frozen product. He was not always successful at this, but managed to sell his wares just the same. Those who also shipped ice could ill afford to compete with Tudor, however, because he maintained his edge in superior storage technology. When a competitor arrived to sell ice, Tudor simply lowered his price making it cheaper to buy from him. Competitors' ice, sold on the spot market without the advantage of icehouse storage, simply melted away at which point Tudor would raise his prices to sustain a healthy profit margin.

Beginning in 1833, Tudor began exporting ice to Calcutta, India. Successfully establishing his enterprise there, Tudor began further expansion in the 1830s to such places as Brazil. With the success of this globalization in the frozen water trade, competitors could not be kept out any longer as demand continued to increase. Other New England frozen water traders opened markets in England and as far away as Australia. The California Gold Rush during the 1850s created new demands in west coast cities for the New England frozen water. As the new global markets began to expand, additional markets in fresh produce expanded as well. Ships transporting the ice essentially were refrigerated. So entrepreneurs were able to include in their shipments produce kept fresh by the temperatures maintained aboard by the frozen cargo.

During this early period of expansion and accomplishment, the demand for ice and its uses began to spread down the Atlantic seaboard. In eastern states, particularly the urban areas, the frozen water trade made its product available first for commercial use (mechanical ice cream makers were introduced in the 1840s), and then for private consumption. Frederic Tudor manufactured refrigerators for domestic use in the first 10–15 years of his frozen water enterprise. These were little icehouses used in the Boston area at first, but later in the century (1840s) mass storage and marketing of ice made these iceboxes essential for domestic use and not merely a convenience for the wealthy. Even after manufactured ice overtook harvested ice as a matter of economics, ice still needed to be stored prior to domestic use. Icehouses, therefore, remained a common site in the US for nearly 150 years; nearly every town had one, testament to the impact of the frozen water industry.

Frederic Tudor's legacy was his entrepreneurial spirit, commercial risk-taking, and his vision, all of which were maligned during his early attempts to establish the frozen water trade. When Tudor came up against an impediment, he learned from his mistakes. Slowly through trial-and-error practice, he refined his methods and became successful, enough so that despite the early ridicule and incredulity, his inspiration led others to follow in his footsteps, perhaps his greatest legacy.

Place Value, Unit Value, and Time Value

Place value is the value imparted on an industrial mineral based on its location relative to the point of consumption (Barker and others, 1999). Otherwise stated, if a large part of the value of an industrial mineral is the result of its relative geographic position, it is said to have high place value (Bates, 1969). Sand and gravel is an example of a product whose value depends on its proximity to its end use. Because sand and gravel, a common construction material, has a low unit value, the cost of shipping it over large distances diminishes its value even further.

Unit value is determined by an intrinsic property or properties of a substance unique to it. Rare occurrences of an industrial mineral also may impart high unit value. Bates (1969) used industrial diamonds as an example of a substance with high unit value irrespective of its geographic position. Because of its hardness, high resistance to abrasion, and low reactivity, industrial diamonds are in high demand for a variety of applications. This gives them a high unit value and a low place value. Their worth does not diminish despite remote geological occurrence or high processing costs.

Barker and others (1999) defined commodity minerals as industrial minerals that are characterized by large volume, lower value, relatively simple processing and high place value. They are widespread in distribution and use. They further describe specialty minerals as industrial minerals that are characterized by smaller volume, higher value, and value added generally by more complex processing, and are commonly unique and used by one consumer or a few. Sand and gravel is an example of a commodity mineral; industrial diamonds are examples of specialty minerals.

Similar to sand and gravel, therefore, ice has high place value relative to its point of consumption, particularly because it is produced, stored, and used locally. This was the case in the early 19th century when ice was harvested in New England, stored locally in icehouses, and consumed there. Its unit value was low because lakes and ponds were relatively numerous and close at hand, processing was simple, and storage was proximal.

The difference for 19th century harvested ice, however, was its seasonal or time value. Even locally, as summer waned, ice could become scarce through high usage (demand) and higher rates of melting (it became scarce). Shipping abroad also complicated the issue in this regard. It had high place value in New England, but lower in the tropics—it melted (disappeared) relatively quickly once exposed to ambient temperatures. Furthermore, shipping the ice to the tropics would make ice a commodity mineral, because shipping was done initially in large volumes, with low unit value, and high place value. But once delivered to warmer climes, such as India and the southern tropical islands for example, the ice became a specialty mineral—smaller volumes from melting; higher value because of its scarcity; complex storage and handling to prevent or forestall its melting; fewer applications, namely cooling drinks and making small quantities of ice cream.

So ice had seasonal value or time value as well. In New England where the ice was harvested in the early 19th values shifted from winter to summer. Demand was low in the winter as was its value; in summer harvested ice was in higher demand so its value was relatively higher. Because harvested ice was stored in huge icehouses in New England, it lasted into the summer months and, therefore, shipping could be accomplished throughout the year, but preferably in the cooler months.

Ice Harvesting and Production

The harvesting of ice in the early 19th century depended on the cold weather conditions typical of the northern tier of states. This meant the winter months of December into March. Limnic waters were the primary sources of frozen water. New England was originally where mass harvesting and marketing occurred, chiefly because the northeastern ports supported the export of large volumes of product. Yankee sailing and shipping was well known throughout the world, and entrepreneurs such as Frederic Tudor even helped design ships expressly for the ice, or frozen water, trade.

New England lakes and ponds provided clean unpolluted water for the harvesting of ice. As the demand for ice grew throughout the US, states farther west, such as Ohio and Minnesota, became large harvesters of ice. As industrialization progressed through the 19th century, availability of clean fresh water diminished. Also, later in the 19th century, artificially manufactured ice became more available and more efficient. Railroads demanded huge amounts of ice for refrigerated railcars (a refrigerated railcar was called a *reefer*) and so the railroad companies devised ways to manufacture large quantities of ice.

The frozen pond and lake water attained a thickness of 9 –12 inches before it was ready for harvesting Figure 4). Various tools were improvised specifically for the harvesting of ice (Figure 5). First a snow plough removed any snow that had accumulated on the surface of the ice. Then the ice was scored by horse-drawn saws or by hand with a specially designed saw. Other hand saws were then used to cut the ice into long strips prior to breaking them into 28–32-inch-long blocks with ice chisels. Each block weighed about 120 pounds and were guided along the pond or lake surface using long-handled pikes. Using ice tongs and pikes, the blocks were loaded into icehouses directly or onto wagons, carts, or sleds for the trip to the icehouse for storage. Ramps outside the icehouses guided the large blocks up and into the storage facility. Workers inside, armed with long-handled pikes, intercepted the large blocks of ice, stacking them up to the ceiling (Figure 6). This clearly was the most dangerous job during the ice harvest, as the blocks would slide around at great speeds and those stacking the ice tried to avoid contact. The fast moving ice collided with other blocks causing ice chips to fly through the air. In addition, caroming blocks sliding from side to side could easily mean broken toes, feet, ankles, and legs.

Few statistics survive from the 19th century frozen water trade. It was never decided at several levels of government, how to regulate or tax the production of harvested ice. Was it an agricultural product or the result of mining? Frozen water production, therefore, continued its large scale operations unregulated. As a result of government indecision, no official records of production, domestic use, or exports were ever documented. The information available today in this regard comes from company records, bills of laden, ships logs, etc. Most production figures, therefore, are estimates. Table 1 (Smith, 1961) is an estimate of ice production in the US during the 19th century. The data was gleaned from various sources.

Ice Storage

Harvested ice had to last through the summer months, so proper storage was required to prevent it from melting. Simple ice pits represent the simplest form of storage, and the yakhchal is an example of a more sophisticated structure. These were discussed earlier.

When Frederic Tudor began his ice harvesting enterprise, he realized the need for storage that could survive ambient summer temperatures. He also knew that he had to insulate his cargo when shipping harvested ice abroad. After many attempts to build suitable storage, particularly in Havana, Cuba, he came up with a basic design. Icehouse construction preferably had walls of stone; later concrete or stucco. In northern climes the outer walls were of double 2 x 4-inch construction. A base or floor of loose sand and/or gravel allowed for drainage when ice began slowly to melt. Tiled channels or gutters could also be used to aid subterranean drainage. Packed between the walls and the ice was a thick layer of insulating straw or sawdust, 18–24 inches thick (sometimes hay was used). The roof was constructed similar to the walls with a space under the peak for ventilation (Figure 7).

Brick, stone, and concrete of course were preferred over wood for icehouse construction. These provided better insulation properties, but also they were more fire resistant than wooden structures. Fire was the major hazard for icehouses, particularly because of the significant amount of sawdust and hay used for packing and insulating.

Transporting

Before the railroads, ships were the major means of transporting ice over long distances. Ballastless ships were the first choice for shipping harvested ice. The ice provided the ballast, and over long voyages a certain amount of melting occurred, despite a thick cover of sawdust insulation. Ships would typically lose about one third of their icy cargo due to melting, but losses of ice due to melting depended on the length of the journey and the geography of its destination.

Later as railroads became more prevalent in the US, it was believed that, just as ships took on fresh produce along with their frozen water payload, railcars could do the same. The first refrigerated railcar (reefer) was packed with harvested ice in 1851, making possible the transportation of fresh produce by rail over long distances. Ice used by railroads was not actually used to ship the ice itself, but rather, ice was used as a refrigerant to maintain interior temperatures for the preservation of perishables such as meat, dairy, and produce (Figure 8).

Refrigerated shipping methods are beyond the scope of this article. It is important to note, however, that with increased refinement of reefers and refrigerator ships, marketing of perishable items became less dependent on location. This meant the centralization of fisheries and meatpacking plants. This also allowed more widespread growing of farm products, namely fruits and vegetables. Once restricted to serving only local markets, refrigerated rail transport delivered fresh produce to more numerous, distant, and diverse urban markets.

Summary

The frozen water business in the United States was a huge industry in the 19th century. As an industrial mineral it was a significant part of the economy ranked second in US exports behind only cotton during that period. Despite its high place value and low unit value, one New England entrepreneur, Frederic Tudor, had the vision and marketing skills to trade a local product successfully on both domestic and global bases. Traded as a commodity mineral, Tudor raised it to that of a specialty mineral, creating markets where none had existed previously. Alone and together with business partners, he improvised tools, harvesting methods, storage facilities (icehouses), and shipping methods. Towards the end of the century, manufacturing ice became more efficient and economic, displacing the need for harvested frozen water. But the frozen water trade left behind a legacy of an expanded agricultural economy, scientific and engineering advances in refrigeration, and a perceived need for an iced tea on a sweltering summer's day.

References and References Cited

Anonymous, 2009, Yakhchal: Ancient Refrigerators *downloaded on November 9, 2015 from* http://eartharchitecture.org/, page: http://www.eartharchitecture.org/index.php?/archives/1045-Yakhchal-Ancient-Refrigerators.html.

Barker, J. M., Austin, G. S., and Santini, K., 1999, What geologists (and perhaps others) should know about marketing industrial minerals, Proceedings, 34th Forum on the Geology of Industrial Minerals, 1998, K. S. Johnson, ed., Oklahoma Geological Survey Circular 102, p. 281–295.

Bates, R. l. 1969, Geology of the industrial rocks and minerals, Dover Publications Inc., New York, NY, 459 p.

Dalley, S., 2002, Mari and Karana: two Babylonian cities, Gorgias Press, LLC, 91 p.

Petroski, Henry. 2008. The toothpick: technology and culture. Random House, New York, NY, 464 p.

Smith, P. C. F., 1961, Crystal blocks of Yankee coldness, http://www.iceharvestingusa.com/crystalblocks1.html, downloaded November 13, 2015.
Bibliography

Cummings, Richard O. (1949). The American ice harvests: a historical study in technology, 1800–1918. California University Press, Berkeley, CA, 184 p.

Dickason, David G., 1991, The nineteenth-century Indo-American ice trade: an hyperborean epic, Modern Asian Studies 25 (1): 55–89.

Herold, Marc W., 2011, Ice in the tropics: the export of 'Crystal Blocks of Yankee Coldness' to India and Brazil, Revista Espaço Acadêmico, no. 126, p. 162–177.

Weightman, G., 2003, The frozen water trade: a true story, Hyperion, New York, 254 p.

Table 1. US 19th Century Ice Exports (Smith (1961)

YEAR	QUANTITY (TONS)
1806	130
1816	1,200
1826	4,000
1836	12,000
1846	65,000
1856	146,000
1860	142,463
1865	131,275
1866	124,751
1872	69,500
1873	70,370
1874	69,80
1884	60,000

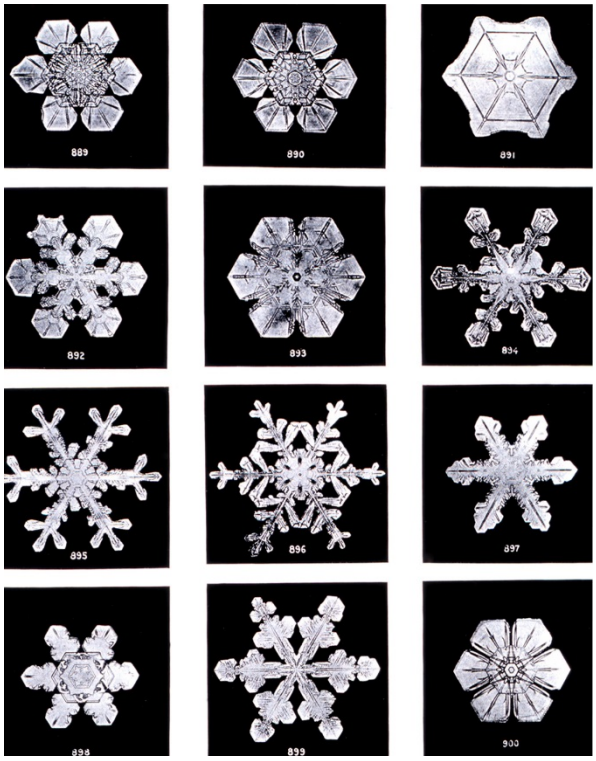

Figure 1. Snowflakes are the most illustrative example of the hexagonal crystal structure of ice. (Wikimedia Commons)

Figure 2. Yakhchal, a Persian ice storage structure in the Iranian desert. The Yakhchal is an ancient, but efficient, method of preserving ice in the deserts of Iran. The walls of the Yakhchal are impervious to water and insulate against heat transfer. (Wikimedia Commons)

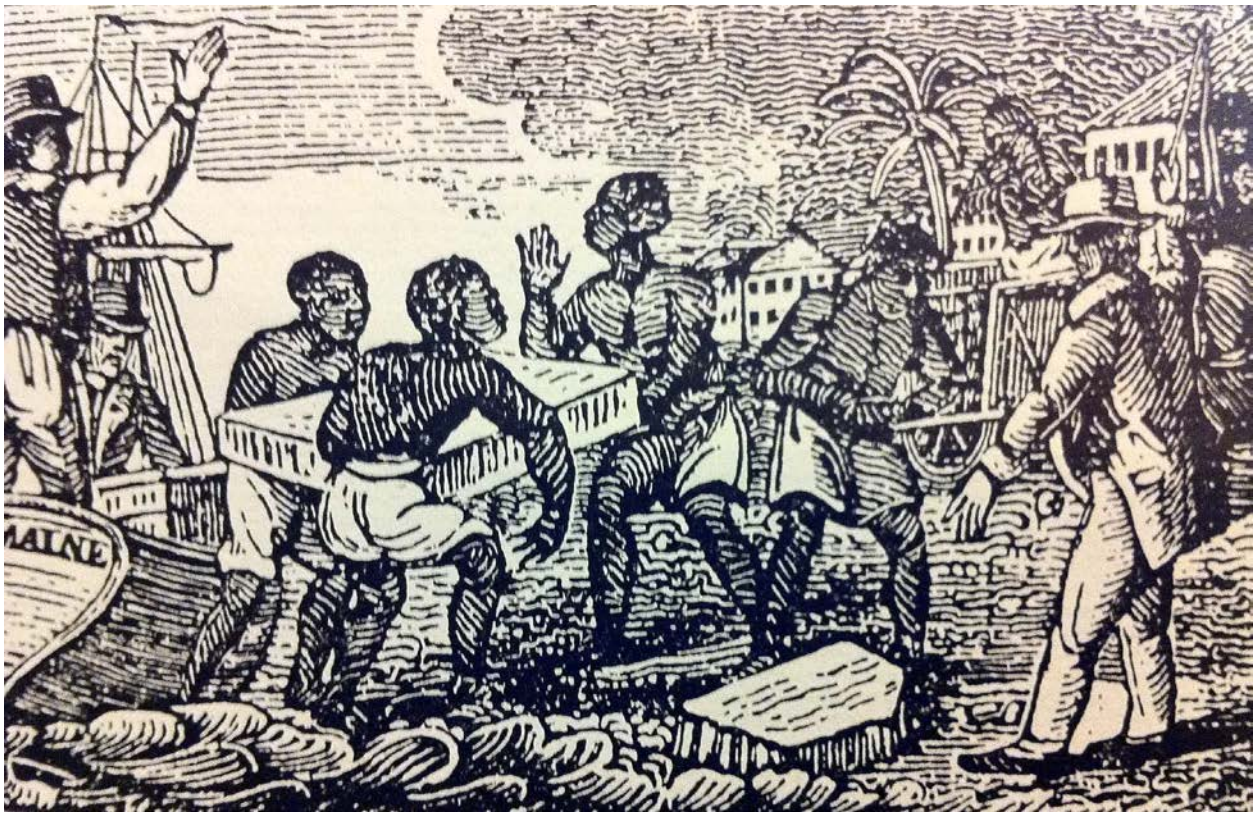

Figure 3. Slaves in Cuba unloading ice from Maine. (Wikimedia Commons)

Figure 4. Ice harvesting in Massachusetts, early 1850s. Note the division of labor and the variety of tools. (Wikimedia Commons)

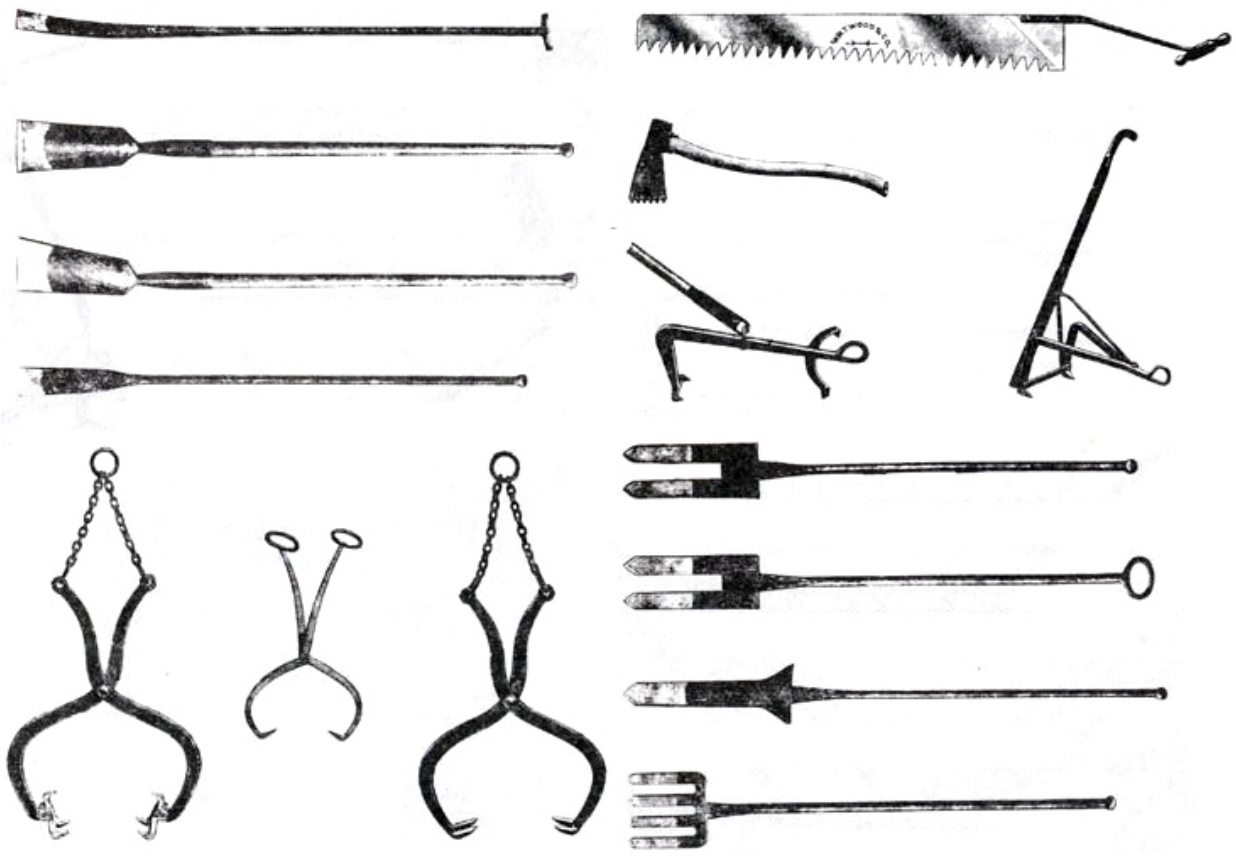

Figure 5. A selection of late 19th century specialist ice tools; clockwise from top left, chisels; ice saw, ice adze, grapples; bars; tongs. (Wikimedia Commons)

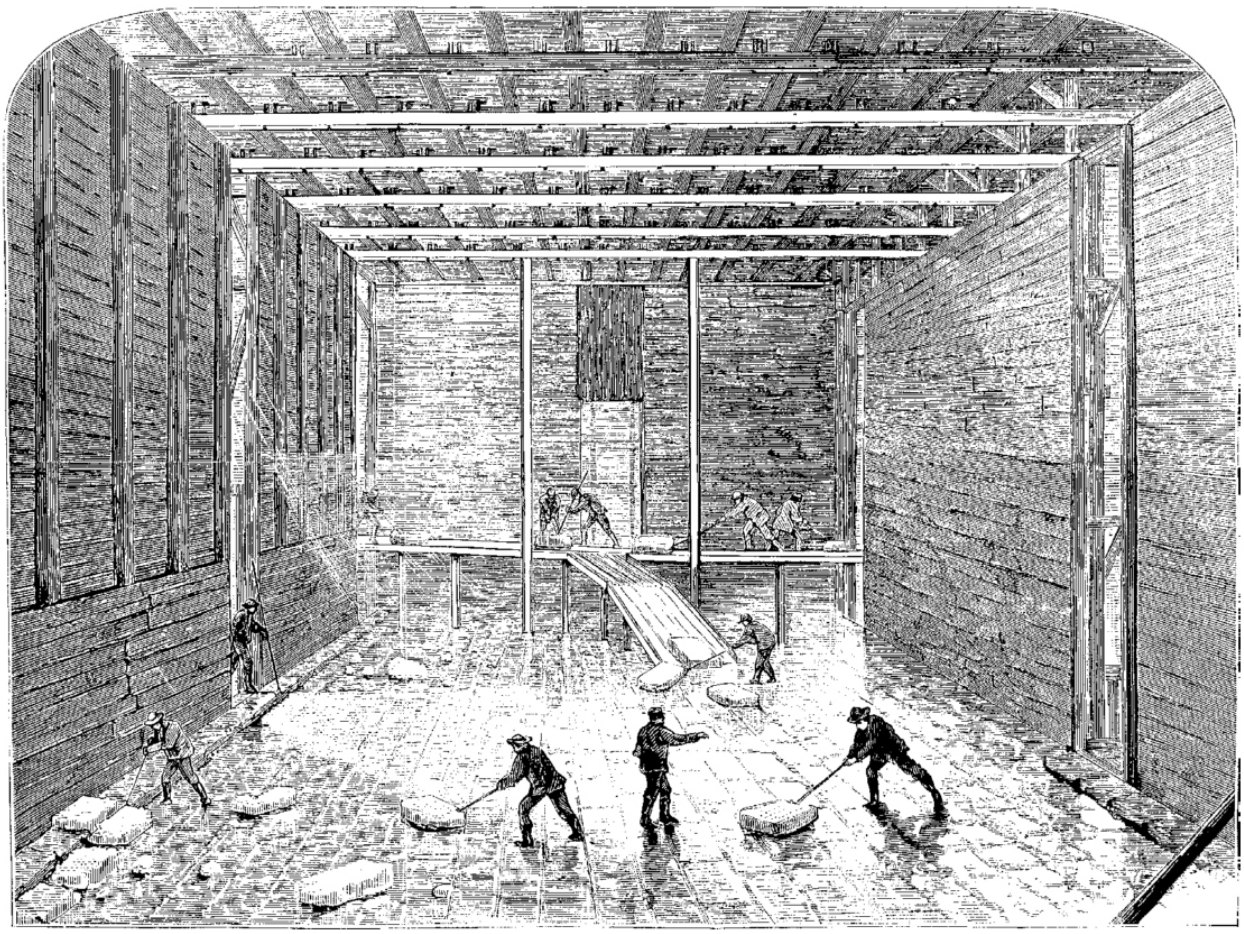

Figure 6. Stacking ice inside an icehouse in Barrytown, NY, on the Hudson. (Wikimedia Commons)

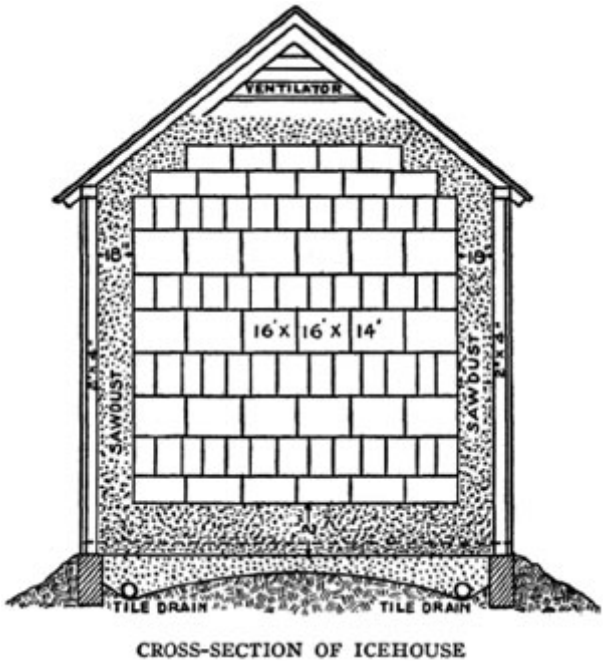

Figure 7. Cross section of typical icehouse. (Printed with permission from Phoenix Garage Doors)

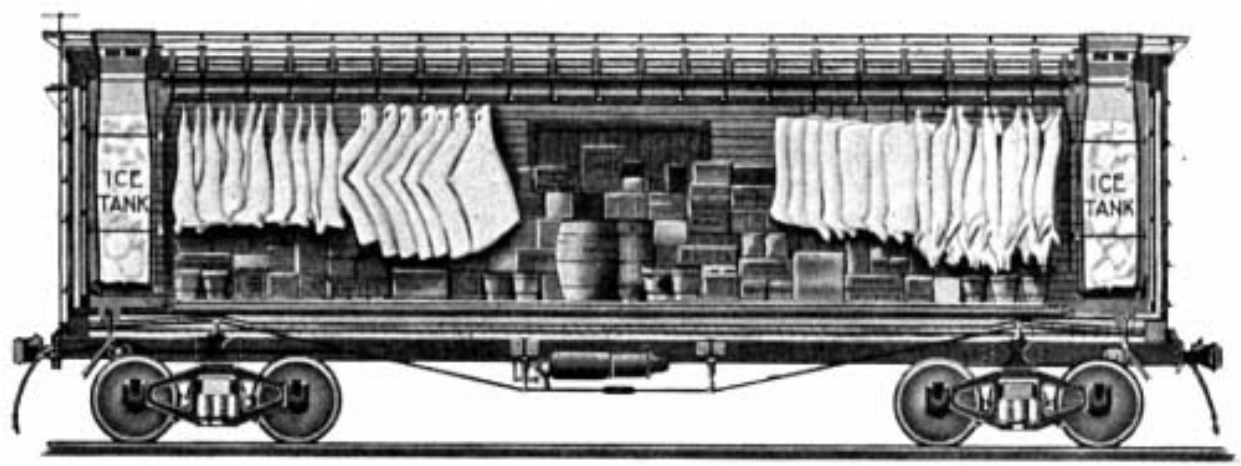

Figure 8. Early refrigerator railcar (reefer) circa 1870. (Wikipedia Commons)

ENVIRONMENTAL IMPACTS OF INDUSTRIAL SAND MINING

Mark J Krumenacher, PG, CPG, CGWP; Senior Principal/Senior Vice President, GZA GeoEnvironmental, Inc., 20900 Swenson Drive, Suite 150, Waukesha, Wisconsin 53186
mark.krumenacher@gza.com

Abstract

Mining is a unique industry that has in recent decades transitioned from a private business operating behind tall fences to one of the most heavily regulated industrial businesses with increased public exposure and public control over the permit to operate. One of the primary concerns of the general public pertains to potential environmental impacts. This presentation focuses on three general environmental impacts; water quality, water quantity, and mine reclamation. Federal and state regulations address water quality across the US whereas mine reclamation is generally addressed at the local land use level. History has shown that mining can be done in a responsible manner without sacrificing the environment.

Introduction

The rate of industrial sand mining in the United States has increased in recent years, due in large part to the tremendous growth in hydraulic fracturing for oil and gas using horizontal drilling techniques. As a means to advocate against mining, some environmental activist groups and community organizers contend silica sand mining presents significant threats to human health and the environment. Scientific evidence strongly refutes such claims.

Experience shows that industrial sand mining has minimal environmental impact, involves virtually no public health risk, and is an important part of domestic energy production that has substantial economic benefits. Heartland Policy Study No. 137, "Environmental Impacts of Industrial Silica Sand (Frac Sand) Mining," documents the following facts:

Overwhelmingly, the publicly available information available on the impacts of industrial sand mining is negative. Although presentations are made and papers written that factually report on the impacts, that information is commonly presented to narrow groups during permitting, or to industry, and not the policy makers and the general public. This presentation provides a partial overview of a much broader attempt by the presenter to develop a comprehensive technical fact based document with the potential of a much broader audience that will go beyond preaching to the choir. The outline for the paper may be substantial enough to be a book, but instead, is being prepared in a series of Policy Studies published by the Heartland Institute. Teaming with the Heartland Institute provided the added support of experienced technical writers and reviewers and a well-developed and diverse publishing and distribution network. The rationale for publishing as a series is that the information is timely, and can be published and shared as the technical papers are developed.

The first paper addressed environmental impacts[1] and was published in May 2015 and the second paper addressed economic impacts[2] and was published in June 2015. In September 2015 the third paper in the series was published addressing road use[3] and the fourth paper addressing social impacts focused on land use and value[4] will be published before the end of January 2016. The most notable benefit of these papers is that a simple internet search for impacts of industrial sand mining will now yield fact-based technical papers within the first search results instead of pages of anti-mining social media websites, Facebook pages and blogs.

Environmental Impacts

Some of the primary concerns commonly raised pertain to potential environmental impacts. This presentation focused on three general environmental impacts; water quantity, water quality, and mine reclamation. Federal and state regulations address water quality across the US whereas mine reclamation is generally addressed at the local land use level. History has shown that mining can be done in a responsible manner without sacrificing the environment. The summary provided as presented at the August 2015 SME Twin Cities 2015 Annual Conference, 51st Forum on the Geology of Industrial Minerals was copied directly from the May 2015, paper referenced above.

---

[1] May 2015, Environmental Impacts of Industrial Silica Sand (Frac Sand) Mining, Isaac Orr and Mark Krumenacher
[2] June 2015, Economic Impacts of Industrial Silica Sand (Frac Sand) Mining, Isaac Orr and Mark Krumenacher
[3] September 2015, Roadway Impacts of Industrial Sand (Frac Sand) Mining, Isaac Orr and Mark Krumenacher
[4] In process, expected January 2016, Social Impacts of Industrial Sand (Frac Sand) Mining - Land Use and Value, Mark Krumenacher and Isaac Orr.

Water Quantity

Silica sand mining is often portrayed as a water-intensive industry due to the volumes of water used for washing, processing, suppressing fugitive dust, and, at some facilities, transporting sand as a slurry. The amount of water used varies greatly depending on the facility and the extent to which water is recycled, as closed-loop systems that recycle 90 percent of the water used can consume as little as 18,000 gallons per day, whereas open-loop systems can consume as much as two million gallons per day.[5]

The growth of the industrial sand industry in recent years has generated concern among some members of the public that mining and processing operations will permanently alter groundwater aquifers and water use will compete with residential, municipal, and agricultural use of groundwater and ecological systems such as springs, streams, rivers, and lakes.

However, when compared to other uses of water in Wisconsin, such as power generation, municipal public water, and agriculture, water consumption by industrial silica sand mining accounts for a very small percentage of the water used in the state. Data from the Wisconsin Department of Natural Resources (DNR) shows all nonmetal mining in the state, which includes quarry dewatering, washing sand and gravel, and industrial sand mining, accounted for just 0.71 percent of all water withdrawals in 2013 (see Figure 1).[6]

Furthermore, water consumption by industrial silica sand operations constituted just a fraction of the amount used by all nonmetallic mining operations, as water withdrawals associated with industrial sand activity used only 1.99 billion gallons of water in 2013, just 0.09 percent of the 2.121 trillion gallons consumed for all purposes throughout the state (see Figure 2). In comparison, agricultural irrigation accounted for 5 percent of total water withdrawals, using 55 times more water than industrial sand operations for mining and processing.

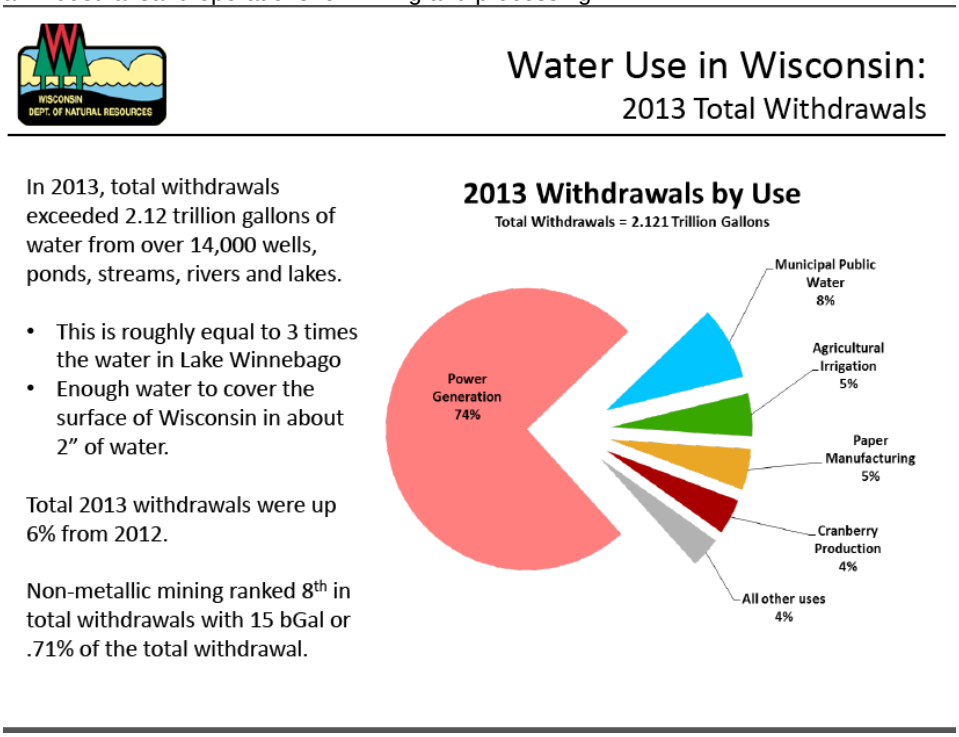

Figure 1. Total water withdrawals in the state of Wisconsin were 2.121 trillion gallons. Power generation accounted for 74 percent of this total, meaning more than 100 times as much water was used to generate electricity as all nonmetallic mining operations, which includes quarries and gravel pits in addition to industrial sand mines.

[5] Kate Prengaman, "A sand plant by the numbers," Wisconsinwatch.org, August 19, 2012, http://wisconsinwatch.org/2012/08/a-sand-plant-by-the-numbers/.

[6] Robert Smail, "Mining and Water in Wisconsin: Water Use for Non-Metallic Mining," presentation at SME Wisconsin Annual Conference, October 7th, 2014, http://higherlogicdownload.s3.amazonaws.com/SMENET/1b517024-bb1c-4b2c-b742-0136ce7a009c/UploadedImages/TCjointConference/Robert%20Smail%20-%20Water%20Usage%20in%20Non-Metallic%20Mining.pdf .

One reason industrial sand mines use so little water is the majority of plants operate closed-loop systems, which is why industrial-sand washing and processing was only the sixth-largest source of water use in the ten counties reporting presence of industrial-sand washing operations.[7] Modern, efficient closed-loop systems recycle 90 percent of the water used on site, and as a result, water consumption at sand facilities can vary between 18,000 and 250,000 gallons per day. The 10 percent of water lost in these systems results primarily from evaporation from ponds, drying moist sand, and placement of wet sand and fines (silt and clay particles) during mine reclamation.

Except for relatively small amounts of water that evaporate during the mining and processing, essentially all the groundwater pumped from the aquifer is retained in the geographic basin that comprises the surface-water-groundwater aquifer system. For example, water discharged from a mine during dewatering is kept within the basin, under a permit issued by the WDNR. As a result, there is no material net loss of water from the surface-water-groundwater system.

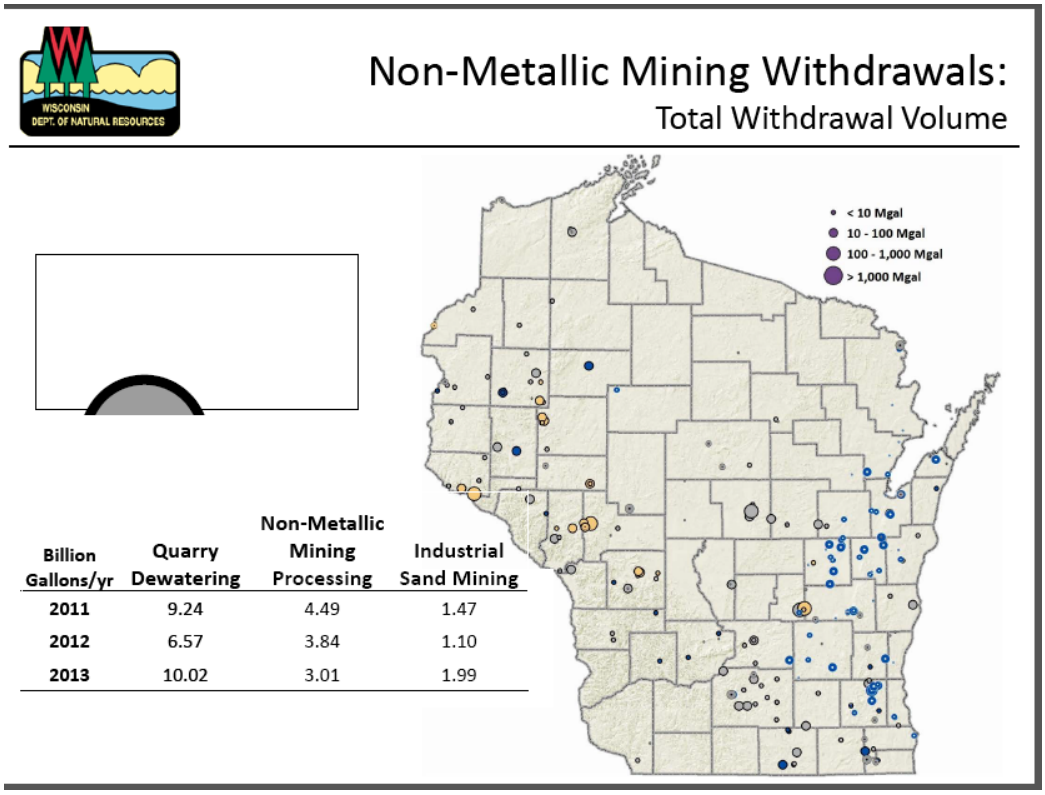

Billion Gallons/yr	Quarry Dewatering	Non-Metallic Mining Processing	Industrial Sand Mining
2011	9.24	4.49	1.47
2012	6.57	3.84	1.10
2013	10.02	3.01	1.99

Figure 2. Industrial sand washing, transporting, and dust suppression accounted for 0.09 percent of all water consumed in the state of Wisconsin in 2013. Because industrial sand mining accounts for such a small percentage of total water consumption in Wisconsin, by far the largest producer of industrial sand in the country, these numbers suggest industrial sand operations will not deplete water resources in other states with humid climates.

Additionally, groundwater quality and quantity are carefully considered in every stage of a mine's existence, before permitting, while operating, and after mine closure. Groundwater experts (hydrogeologists) study the groundwater for federal, state, and local governments as well as the sand mining industry, and WDNR hydrogeologists and engineers evaluate all permits for high-capacity wells.

Sand processing operations operating high capacity wells (a well capable of pumping more than 100,000 gallons per day) must pump groundwater in accordance with a high capacity well permit from WDNR. In addition, the local mine permitting authority requires scrutiny of groundwater during development of Conditional Use Permits and reclamation plans.

[7] Emily Chapman *et al.,* "Communities at Risk: Frac Sand Mining in the Upper Midwest," September 2014, www.civilsocietyinstitute.org/media/pdfs/092514 CSI BAR frac sand mining report FINAL2 - EMBARGOED.pdf.

Ultimately, the impact of groundwater pumping is site-specific and is based on ground surface and groundwater elevation, geology, hydrogeologic characteristics of the groundwater aquifer, proximity to surface water, and presence of other nearby groundwater users. However, the available data from Wisconsin, the largest producer of industrial sand in the nation, indicates industrial sand production accounted for just 0.09 percent of all water use in the state, demonstrating that sand mining will not deplete water resources in the communities in which it occurs.

Surface-Water and Groundwater Quality

Industrial sand mines have several potential interactions with water. Surface water may be present at or near mining operations in the form of wetlands, ditches, streams, ponds, or lakes, and water from silica sand facilities may infiltrate downward and encounter groundwater. As a result, surface water and groundwater quality are two of the most commonly cited environmental concerns expressed by the general public, because they are generally the most visible.

The most obvious surface water quality impacts arise when untreated storm water or process water is discharged directly to surface water bodies through a structural failure of storm water retention ponds or wash water storage ponds. These types of negative impacts due to structural failures have occurred on more than one occasion from a variety of sources and have resulted in the discharge of clay, silt, and fine sand into nearby waterways. Some of the affected waterways appeared cloudy for a matter of days until the fine silt and clay particles settled out of the water. Fortunately, because of the nontoxic nature of these pollutants, the impacts of these discharges were temporary.

Despite the benign and temporary nature of these incidents, Wisconsin has several environmental regulations intended to restrict mining activities to protect the state's waters. The two main regulations are the Wisconsin Pollutant Discharge Elimination System (WPDES) Storm Water Permits and the Chapter 30 and 31 Wis. Stats. waterway permits. These permits adequately address and protect surface water in the state but cannot prevent all accidents or the results of inadequate designs, construction, or procedures.

The authors of this study presume these incidents are instances of systems being improperly designed or constructed or failures to follow procedures. Whatever the case, the incidents could have been avoided by better engineering practices and strict adherence to applicable standards and industry best-practices. Unfortunately, there have been and presumably always will be bad actors in virtually any industry that can have a negative impact on the environment. The existence of a bad actor should not serve as indictment of an entire industry sector. For example, would an environmental organization argue that metals recycling should be banned because a few metals recycling companies have been found to be in violation of environmental standards? The same logic should apply to the sand mining industry. Bad actors should be identified and punished. But, the vast majority of companies that respect and adhere to applicable standards and best practices should not be condemned in the process.

Although the discharge of sediment into surface waters is a form of pollution, it differs from other forms of pollution in that sand, silt, and clay particles are naturally transported by water systems on a daily basis and do not represent catastrophic events from which a stream cannot recover once the discharge has been stopped and the suspended particles have settled. In fact, these sediments are found in substantially larger proportions during and after rain events. However, despite the lack of serious long-term consequences for these discharges, the industry must achieve better compliance with surface water discharge rules.

Groundwater Pollution Concerns

Private wells are the primary source of drinking water in many rural areas, and as industrial sand mines have begun operations, local citizens have sought to understand the potential impact of these operations on the quality of their groundwater. The main concerns regarding groundwater quality are the potential for pollution from the use of polyacrylamide and acid mine runoff from operating and reclaimed sand mines. Although there have been no documented cases of contamination of groundwater aquifers or potable water supply wells from industrial sand mining operations, these concerns merit serious discussion.

A vital step in recycling water for frac-sand processing is the removal of the small clay particles from the water through the use of water-soluble polymers, one of which is polyacrylamide, a safe chemical used by most municipal drinking water and wastewater treatment facilities, to get the clay particles to "clump together" and settle out of the

water faster than they would otherwise.[8] However, polyacrylamide can contain trace amounts of the chemical acrylamide, a known neurotoxin and carcinogen.

Although acrylamide is a neurotoxin, it does not present a threat to public health because acrylamide degrades into carbon dioxide, ammonia, and nitrogen oxides quickly in the environment. In oxygen-rich soils, 74 to 94 percent of the acrylamide breaks down within 14 days. In oxygen-poor soils, 64 to 89 percent breaks down in 14 days. In river water, 10-20 ppm levels of acrylamide degrade completely in 12 days. Because horizontal groundwater flow velocities are typically on the order of centimeters per day, acrylamide does not persist in groundwater. The rapid degradation of acrylamide greatly reduces, in fact essentially eliminates, the chances of adverse human health impacts from polyacrylamide use at industrial sand mining operations.[9]

Again, this reasoning applies to a great many industrial processes. Consider, for example, polyvinyl chloride, commonly known as "PVC". PVC is commonly used in plumbing, medical applications and a wide variety of other familiar products. PVC tubing is ubiquitous in the medical sector because it is easily sterilized, durable and provides a strong protective barrier from potential contaminants. Thus PVC polymer has significant value to the public. However, production of PVC also involves the use of vinyl chloride, a highly toxic and carcinogenic chemical. Any batch of PVC will contain a very small, but measurable, concentration of "free" vinyl chloride monomer. Yet, this concentration is so small, and breaks down so quickly in the environment in any case, that no rational judge would say that tiny risks presented by minute concentrations of residual vinyl chloride monomer in freshly-produced PVC outweigh the many benefits of PVC products.

The same holds true with respect to polyacrylamide. Acrylamide is a potentially toxic compound that may be present in exceedingly small concentrations in polyacrylamide for a short period of time. Environmental organizations may attempt to inflate this particular "risk" to monumental proportions, but the reality is that the actual risk is hardly worth considering.

The water-soluble polymers used at industrial sand operations are also approved by the National Sanitation Foundation (NSF) and American National Standards Institute (ANSI) NSF/ANSI Standard 60 for treatment of drinking water. For comparative purposes, it is worth noting municipal drinking water treatment facilities add polyacrylamide directly to the drinking water; industrial sand operations add polyacrylamide to the sand wash water, which is part of the industrial sand process and not a source of drinking water.

Additionally, WDNR regulations protect surface water and groundwater by regulating storm water and surface water discharges, well drilling, and the application of materials to the land surface with the potential to impact groundwater. Any storm water or surface water discharge of industrial sand wash water is regulated by WDNR under Ch. NR 216. WDNR approves the application of products containing polymers for sediment control purposes under DNR Conservation Practice Standard 1051 to protect surface waters. WDNR has not established specific groundwater standards for polymers under Ch. NR 140, but there is minimal danger of groundwater pollution if the wash water is held in a pond, WDNR reports: "Sealed ponds will have very little potential for groundwater impacts. Unsealed ponds will likely seal themselves with the fines that are removed from the frac sand." [10]

One report on silica sand mining suggests operating and reclaimed sand mine sites could lead to acid mine drainage, but frac-sand mining does not generate acid mine drainage.[11]

The long history of nonmetallic mining and the very large number of existing nonmetallic mines in Wisconsin indicate nonmetallic mines, including industrial sand mines, do not degrade groundwater quality and quantity in Wisconsin, and thus nonmetallic mining such as industrial sand mining is compatible with the state's goal of protecting groundwater quality and quantity. Aquifers, private water supply wells, municipal wells, springs, trout streams, and exceptional and outstanding resource waters are protected through USEPA and WDNR regulations and permits, and in many instances community-oriented industrial sand mining companies enhance these efforts.

---

[8] Dr. Kent Syverson, "Environmental Impacts of Sand Mining in Wisconsin," presentation, December 2012, https://www.wicounties.org/uploads/legislative_documents/kent-syverson-wi-counties-frac-sand-commision-talk-dec-2012.pdf.

[9] Dr. Kent Syverson, "Water Resource Impacts Associated with the Sand-Mining Boom in Western Wisconsin: A Comparison Between Agricultural Activities and Sand Processing," Geological Society of America, ***Abstracts with Programs*** 45:4, p. 69, May 2013, https://gsa.confex.com/gsa/2013NC/webprogram/Paper218689.html.

[10] Wisconsin Department of Natural Resources, "Silica Sand Mining in Wisconsin," January 2012, p. 28, http://dnr.wi.gov/topic/Mines/documents/SilicaSandMiningFinal.pdf.

[11] Dr. Kent Syverson, *supra* note 52.

Land Reclamation

Wisconsin state law requires all nonmetallic mines be reclaimed in accordance with NR 135 Wis. Administrative Code. These rules are implemented and administered by Wisconsin counties, as the counties are required to implement a nonmetallic mining reclamation permit program in accordance with the administrative code, including adoption of an ordinance and administration of a mining reclamation program. The purpose of this program is to ensure mining sites are reclaimed to a post-mining land use, which can be agricultural, wildlife habitat, prairie, a cranberry bog, or another use the mining company and property owner agree on.

Nonmetallic mining permits are subject to uniform reclamation standards provided in NR 135 Wis. Adm. Code. These standards require the replacement of topsoil to minimize compaction and erosion, the stabilization of soil conditions and slope, establishment of vegetative cover, control of surface water flow and groundwater withdrawal, prevention of environmental pollution, and development and restoration of plant, fish, and wildlife habitat if needed to comply with an approved reclamation plan.[12]

NR 340 Wis. Adm. Code also includes mine reclamation requirements administered by WDNR, which apply to a mine or portions of a mine that affect or are adjacent to navigable waterways. Because large industrial sand mines are designed to be mined in phases (typically 30-40 acres of permitted mine are actively mined at a given time)[13] there will, in most cases, be ongoing reclamation in some areas of the mine while mining continues in others, resulting in a type of "reclaim-as-you-go" strategy.

Mine owners or operators are also required to provide the county with a bond or some other form of financial assurance as a condition of the NR 135 permit in the event an operator fails to fulfill its obligation under the reclamation plan, so the county will have sufficient funding to carry out the reclamation plan. The financial assurance must be in place before initiating mine development.

Although activists occasionally raise concerns about the quality of reclamation plans, the Wisconsin administrative code ensures mines are reclaimed and vegetated to protect air quality and prevent wind erosion of the reclaimed area. This example is typical of the way that other states address land reclamation issues, whether related to sand mining or a myriad of other human activities.

Reclaiming Farmland

Because agriculture is such a vital industry in rural communities across the Upper Midwest, there has been a considerable degree of concern about whether industrial silica sand mining will cause permanent damage to the quality of soil for agricultural purposes, such as providing pasture for livestock and growing row crops.

Studies investigating the agricultural productivity of reclaimed sand mine sites have found crop yields at reclaimed sites produced 73 to 97 percent of their original yields within three years of reclamation, suggesting silica sand mining does not cause a long-term decline in farmland productivity.[14] The best yields were achieved in areas where the original topsoil was returned to the land.

Yields on reclaimed mine sites varied, depending on the type of crop grown, with certain crops faring better than others. On average, corn yields achieved 73 percent of the control group productivity, average winter wheat yields were 77 percent of control, soybean yields averaged 97 percent of control group productivity, and average cotton yields were 80 percent of control, but the quality of the cotton was reduced in all the reclamation treatment scenarios.[15]

These production trends have been affirmed by other studies examining the long-term results of crop production on reclaimed sand-mine soils from 2005 to 2012. These studies proved reclaimed mine soils consistently exceed local countywide five-year average yields for all crops (corn, wheat, soybeans, and cotton) but are typically 15 to 20 percent lower than adjacent prime farmland under identical management.[16] In 2012, however, soybean yields on

---

[12] N.R. 135 Nonmetallic Mining Reclamation, Wisconsin State Legislature, January 2012, http://docs.legis.wisconsin.gov/code/admin_code/nr/100/135/II/10.

[13] Dr. Kent Syverson, *supra* note 52.

[14] W. L. Daniels, et al, "Reclamation of Prime Farmland Following Mineral Sands Mining in Virginia," SME Annual Meeting, February 25-27, 2002, http://landrehab.org/UserFiles/DataItems/5A706850676C79516461343D/Daniels%20et%20al%202002%20SME%20Reclamation%20of%20Prime%20Farmland.pdf.

[15] *Ibid.*

[16] Comparisons between reclaimed mine soils and countywide production are complicated by the fact reclaimed soils received irrigation, whereas some but not all crops throughout the county were irrigated.

reconstructed mine soils were higher than on the unmined, adjacent prime farmlands and higher than the five-year county average, for the first time.[17]

These results are of particular interest in regard to silica sand mining in the Upper Midwest because corn, soybeans, and wheat are among the major row crops planted in the region, whereas the climate is unsuitable for growing cotton.[18] Lower corn yields were attributable to low levels of nitrogen, which were the result of the researchers' desire to study the long-term nitrogen supply of the biosolids by not adding additional supplies of nitrogen-based fertilizer.[19]

A likely factor in the high levels of soybean production is the fact soybeans are nitrogen fixers, meaning they are able to create their own supply of nitrogen by converting nitrogen from the air into a form the plant can use.[20] Although the study did not investigate alfalfa growth on reclaimed sand-mine soils, alfalfa is also a nitrogen-fixing plant, which suggests alfalfa too may be highly productive on reclaimed soils. Additionally, because alfalfa is a perennial plant, it develops a deeper root system than crops such as corn and soybeans. Such a root system can help prevent soil compaction, which has been recognized as a challenge for reclaiming farmland. These findings are particularly important because soybeans are a vital component of crop rotation in the Midwest, and alfalfa is important feed for dairy cows, which are the basis of the western-Wisconsin economy.

In all of these studies, soil compaction has been recognized as a limiting factor for crop yields, as compaction can limit the extent to which roots can grow downward in the soil, thus limiting the growth of grain, particularly wheat. Chisel plowing and disking the fields, as well as growing crops with longer root systems, can be an effective way to reduce soil compaction and crusting at the surface, and can also increase water retention.

Finally, faculty and students from the University of Wisconsin River Falls are undertaking additional studies of the effectiveness of agricultural land reclamation in Chippewa County, Wisconsin. These studies will examine reclamation best practices and provide valuable information for silica sand mining companies' future reclamation efforts.

Conclusion

The United States has achieved dramatic growth in industrial silica sand mining since the technological breakthrough of horizontal drilling combined with the established technique of hydraulic fracturing transformed once-uneconomic oil and gas deposits into profitable drilling operations. Silica sand production more than doubled between 2005 and 2014, increasing from 31 million metric tons in 2005 to more than 75 million in 2014. Sand for hydraulic fracturing, or "frac sand," now accounts for 72 percent of all industrial silica sand mined in the United States.

Concerns of industrial sand mining depleting groundwater and surface water resources are not supported by the data, as industrial sand operations use only a small fraction of the amount of water used for other, more prevalent, purposes, such as power generation and agriculture. Water quality is also unlikely to be seriously degraded by industrial sand operations, because acrylamide breaks down in aerobic environments in a short amount of time. Stormwater runoff events involving sand mining and other industries have temporarily reduced surface water quality with suspended particles of silt and clay, but these incidents can be mitigated by enforcement actions directed at operators who fail to adhere to state and federal standards, and improved stormwater runoff plans.

Finally, Wisconsin N.R. Code 135 requires all nonmetallic mines to be reclaimed, and concerns that sand mining will have negative, long-term impacts on agricultural land have not been supported by scientific research. Studies have found reclaimed sand mine sites produced 73 to 97 percent of their original yields within three years of reclamation. Industrial silica sand mines have been active in the upper Midwest for more than a century and can be operated in a safe and environmentally responsible manner. State governments and environmental protection agencies are capable of enforcing reasonable rules – already in place – that are designed to protect the environment and public health while allowing for the responsible development of silica sand resources.

---

[17] W. Lee Daniels and Z. W. Orndorff, "Indicators of reclamation success for mineral sands mining in the USA," 6th International Conference on Sustainable Development in the Minerals Industry, June 30, 2013- July 3, 2013, http://landrehab.org/UserFiles/DataItems/71702B51452B63547134343D/Daniels%20and%20Orndorff%20Indicators%20for%20Mineral%20Sands%202013.pdf.

[18] U.S. Census Bureau, Statistical Abstract of the United States, Agriculture, 2012, https://www.census.gov/prod/2011pubs/12statab/agricult.pdf

[19] W. Lee Daniels and Z. W. Orndorff, *supra* note 61.

[20] University of New Mexico State University, "Nitrogen Fixation by Legumes," May, 2003, Accessed February 28, 2015, http://aces.nmsu.edu/pubs/_a/A129/.

LIMESTONE FINES AND LIME SLUDGE: FROM BY-PRODUCT WASTE TO POTENTIAL BENEFICIAL USE—A KEY TO SUSTAINABILITY

Zakaria Lasemi[1], Shane K. Butler[2], Shadi Ansari[3]
[1]zlasemi@illinois.edu Illinois State Geological Survey, Prairie Research Institute, University of Illinois at Urbana-Champaign
[2]Illinois State Geological Survey, Prairie Research Institute, University of Illinois at Urbana-Champaign
[3]Illinois State Geological Survey, Prairie Research Institute, University of Illinois at Urbana-Champaign; present address: MilliporeSigma, St. Louis, MO 63118

Abstract

Limestone fines and lime residue waste (lime sludge) may contain more than 95 wt% calcium carbonate ($CaCO_3$), making them highly desirable for many beneficial uses. In this paper, we explore the sustainable utilization of by-product waste materials that are normally disposed of, namely, fines from limestone quarries or lime sludge from water treatment plants that are converted into a potentially effective flue gas desulfurization sorbent. Each year, millions of tons of by-product fines are produced during the crushing and processing of limestone and dolomite quarried in the United States. Similarly, a large amount of lime sludge is produced in the United States from water treatment plants that use lime softening to reduce the calcium and magnesium hardness of the source water. Because these by-products currently have limited uses, large portions end up in landfills or, in the case of fines, are used to backfill mined-out areas. Some of the fines and a small portion of the lime sludge materials are used in agriculture to control soil pH. Our recent studies, funded by the Illinois Clean Coal Institute, demonstrate that these potentially valuable, yet largely unknown, resources could provide an affordable and highly reactive sorbent for desulfurization in coal-fired power plants.

1.0 Introduction and background

Each year, millions of tons of fines (Figure 1) are produced from the crushing of limestone in quarries and mines, and most remain unutilized. Similarly, large amounts of lime residue waste (lime sludge), a by-product of water softening, are landfilled because of limited use (Figure 2). A few attempts have been made to find ways to utilize these by-product wastes in construction or for the manufacture of concrete and the production of portland cement, but thus far, such uses have been limited. To assess the large-scale utilization of quarry fines or lime sludge, a more detailed characterization of the fines and lime sludge is needed, as well as further experimental work on the quality of concrete and other products that could potentially be manufactured from these materials.

One potential application of these materials could be their utilization as sorbents in scrubber systems for sulfur capture in coal-fired power plants. However, the use of quarry fines or lime sludge in scrubber systems has been very limited, partly because many in the power-generating or construction industries are not aware of the availability or suitability of these potentially valuable resources. The quality of these resources is generally poorly known, and their suitability as sulfur-scrubbing agents or for construction has not been extensively investigated.

The overall objective of this project was to identify and characterize by-product fines from limestone quarries and lime sludge from water treatment plants in Illinois and to assess their potential beneficial use. Our main focus was to characterize and determine the suitability of these by-product waste materials for the removal of sulfur oxides from flue gases of coal-fired power plants. The data derived from this study complement those from our earlier Illinois Clean Coal Institute (ICCI)-funded studies to expand the database on sorbent resources for sulfur dioxide (SO_2) scrubbing in coal-fired power plants in Illinois (Lasemi 2004, 2005, 2008; Lasemi et al. 2011, 2012).

2.0 Methods

Limestone fine samples (Figure 1) from 36 quarries were subjected to sieve analysis to determine the proportions of various size fractions. The Tyler mesh sieves and intervals used for this initial analysis included 4–20, 20–40, 40–60, 60–100, 100–200, 200–325, and less than 325. On average, about 49% of the fines were found to be in the less than 4 to 20 mesh fraction, 17% were in the 20 to 40 mesh fraction, and 15% were in the less than 200 mesh fraction. Using this information, we split all 36 samples and grouped them into 4–60, 60–200, and less than 200 mesh sieve fractions for chemical and mineralogical analysis. Each of these size categories was characterized chemically (major, minor, and trace element constituents), mineralogically (calcite, dolomite, clay minerals, quartz, etc.), and petrographically.

Figure 1. Limestone fines or agricultural lime stockpiled for application on farmland to control soil acidity.

Figure 2. Lime sludge production: (left) lime (CaO) is added to water to remove Ca and Mg ions. (right) Lime slurry (mainly $CaCO_3$) is deposited in sedimentation lagoons; after dewatering, the lime sludge is removed and processed to be landfilled or, in limited cases, applied to farmland for pH control.

Lime sludge samples (Figure 2) from 28 water treatment plants in Illinois were also subjected to chemical (major, minor, and trace element constituents), mineralogical (calcite, dolomite, clay minerals, quartz, etc.), and petrographic (scanning electron microscopy) analyses. Because lime sludge materials are naturally very fine grained, they were tested as received, without subdividing them into different size fractions.

A pH-stat auto-titration technique, ASTM Designation C 1318-95 (ASTM 2001), was used to investigate the performance of limestone fine and lime sludge dissolution in an acid solution at a controlled pH value. The reactivity measured by this method provides a comparison of the relative performance of a limestone fine and lime sludge for removal of SO_2 in wet flue gas desulfurization (FGD) processes. For a detailed discussion of the experimental procedures and theoretical background, see the final technical reports submitted to the ICCI (Lasemi 2004, 2005, 2008; Lasemi et al. 2011, 2012).

3.0 Results and discussion

3.1 Limestone fines

A detailed characterization of by-product fines from Illinois limestone quarries showed that, on average, about 74% of the fines were in the 4–60 mesh fraction, 12% were in the 60–200 mesh fraction, and 14% were in the less than 200 mesh fraction (Figure 3). X-ray diffraction (XRD) results showed that quartz (SiO2) was the major impurity in the quarry fines examined. The fines with a high silica (or quartz) content were mainly from quarries that extract cherty limestones. Clay did not appear to be a major component of the fines studied. A moderately positive correlation was found between the amount of aluminum oxide (Al_2O_3) and silica in the 60–200 and less than 200 mesh size fractions (Figure 4). This result suggests a contribution from clay minerals. However, the XRD results

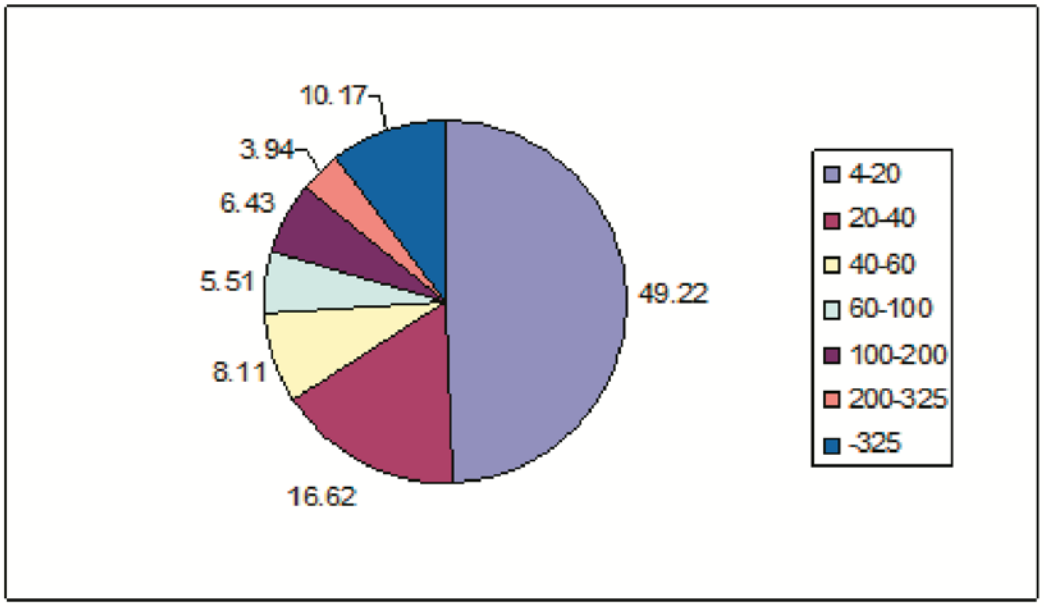

Figure 3. Average particle size distribution of by-product limestone fines; wt. %, Tyler mesh.

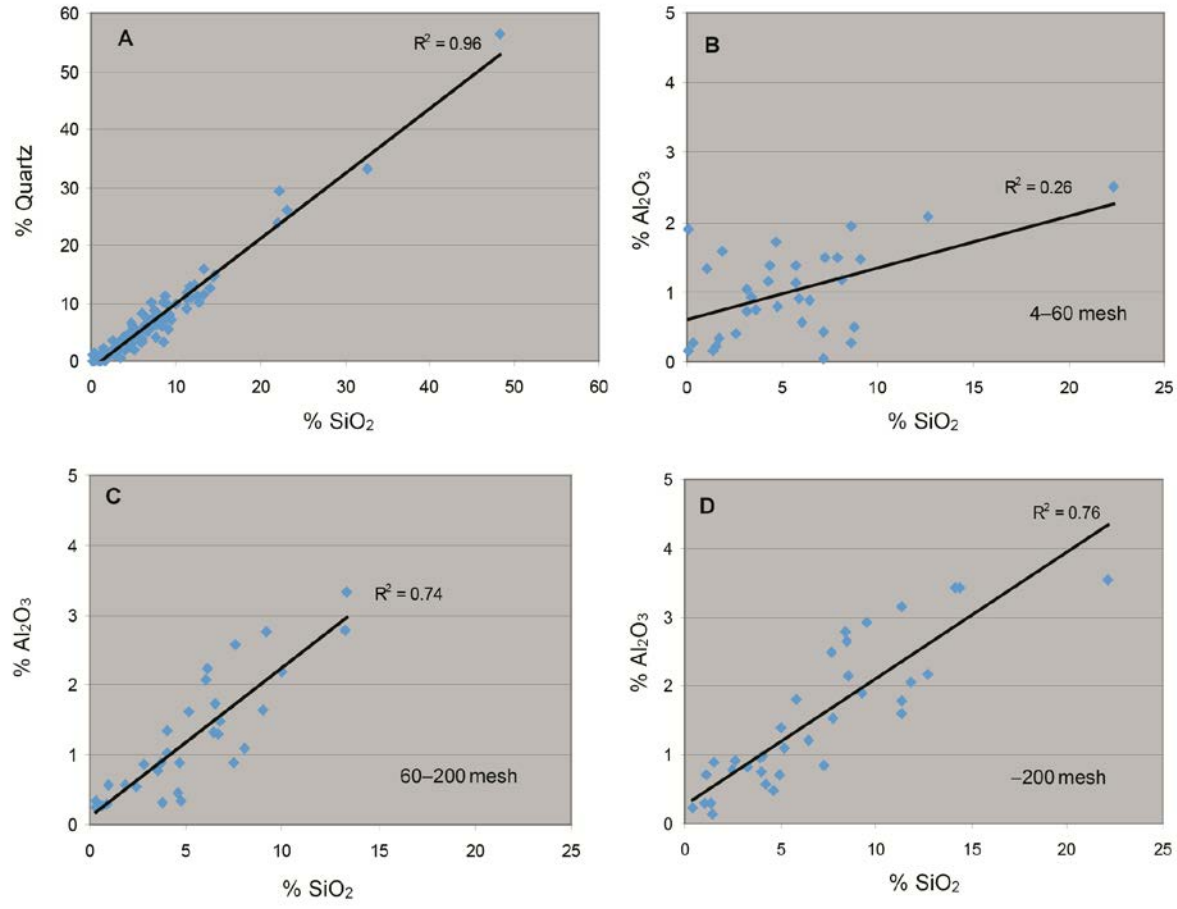

Figure 4. (A) Relationship between percentages of quartz and silica (SiO_2; XRD and XRF data); (B, C, D) relationship between percentages of aluminum oxide (Al_2O_3) and SiO_2 (XRF data).

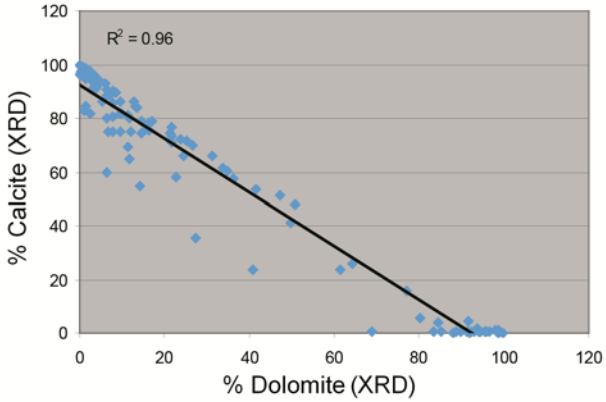

Figure 5. Relationship between dolomite and calcite. Samples below the trend line are impure (generally rich in silica).

indicated that, except for a few samples, the amount of clay minerals was low (below the detection limit). The amount of $CaCO_3$ calculated from the chemical analysis ranged from 0.7% to 95%. The higher calcium limestones come from quarries in the central, western, and southern parts of the state. A number of samples are magnesium (Mg) rich, containing up to 97% dolomite. Dolomitic samples are mainly from quarries in the northeastern part of the state. A strong positive correlation was found between magnesium oxide (MgO) and calcium oxide (CaO) and calcite and dolomite values, indicating that the source of the MgO and CaO was primarily carbonates.

Both the chemical analysis and XRD showed that by-product fines ranged from a relatively pure limestone to dolomite; some fines were a mixture of both limestone and dolomite (Figure 5). Calcite and dolomite contents in the by-product fines correlate with the geology of the parent material (Figure 6). Fines from quarries in the northern part of the state are dominated by dolomite, whereas those from the central, western, and southern parts of the state are predominantly limestone. The calcite or dolomite content was similar in all three size fractions examined. However, only 4 samples in the 4–60 mesh, 2 samples in the 60–200 mesh, and 3 samples in the less than 200 mesh size fractions had a calcite content greater than 90%. The number of samples with greater than 80% calcite ranged from 12 in the 4–60 mesh fraction, to 8 in the 60–200 mesh fraction, to 7 in the less than 200 mesh fraction. Samples with less than 70% calcite contained a substantial amount of dolomite. Except for the few samples with a high silica content, the calcite and dolomite contents could be used to determine the suitability of fines for use in FGD systems.

3.2 Lime Sludge

The lime sludge from Illinois water treatment plants is characterized by a very fine particle size, mostly averaging less than 15 µm. Particle sizes are, however, quite variable but rarely reach greater than 30 µm in diameter. The larger particle size in this study, as determined by a laser particle size analyzer, was, for the most part, due to the aggregation of carbonate crystals into larger particles. Lime sludge also had a large surface area, ranging between 4.5 and 11 m2/g, which was much larger than that of limestone (mostly less than 2 m2/g) even in samples ground to less than 325 mesh, the particle size range generally used in FGD systems.

Lime sludge ranged in color from white, to light gray, to pale yellow, to pale brown as perceived visually according to a Munsell color chart. The color was, for the most part, related to the water source used in the treatment plants. If the source was groundwater, then the sludge tended to be very light gray to white. The light color also correlated with a sludge of higher purity. In plants where surface water was used, the sludge tended to be darker and was generally somewhat less pure.

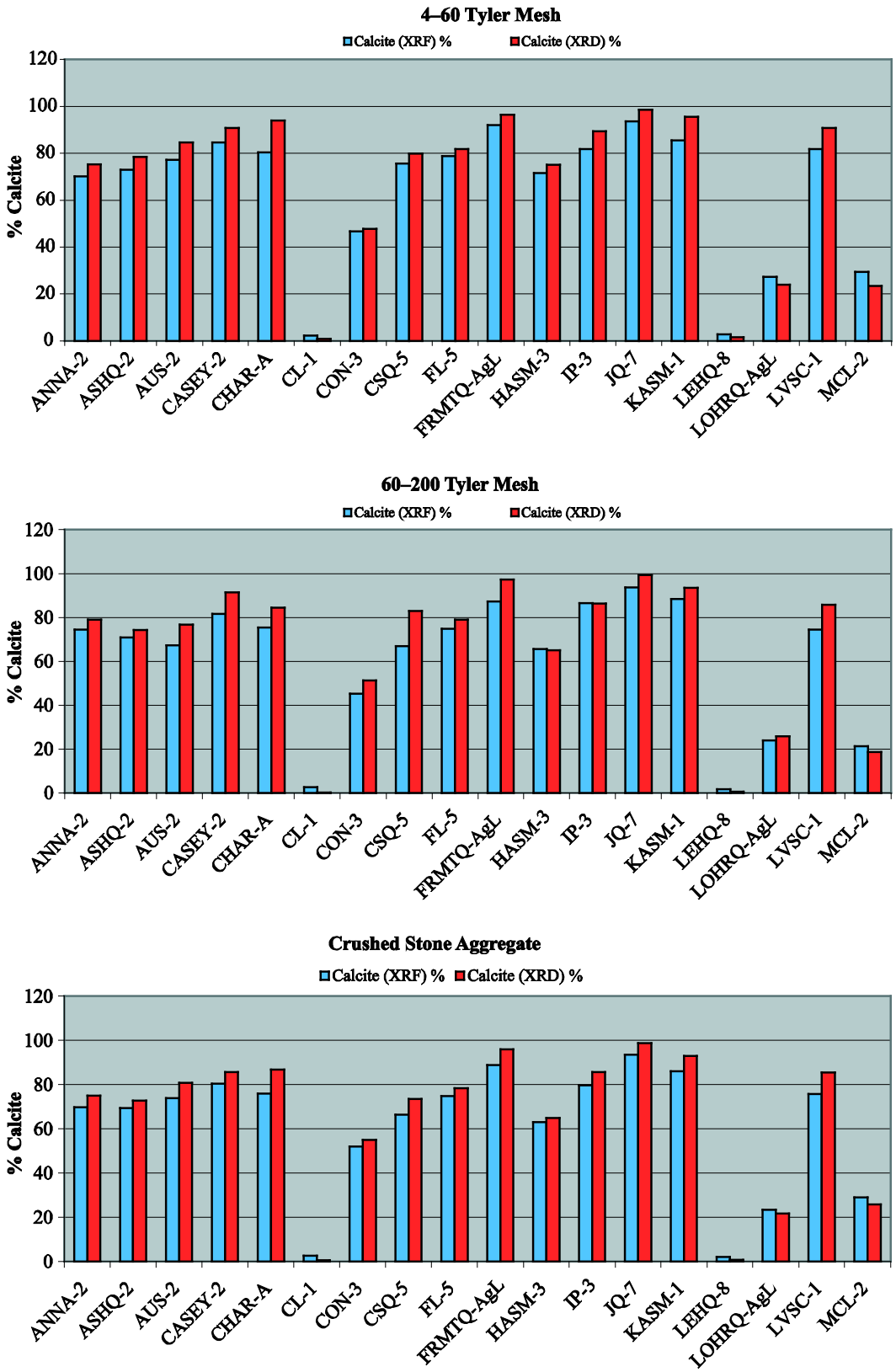

Figure 6. Comparison between $CaCO_3$ content of by-product fines (top two panels) and the parent material (crushed stone aggregate, bottom panel). Quarry names are withheld.

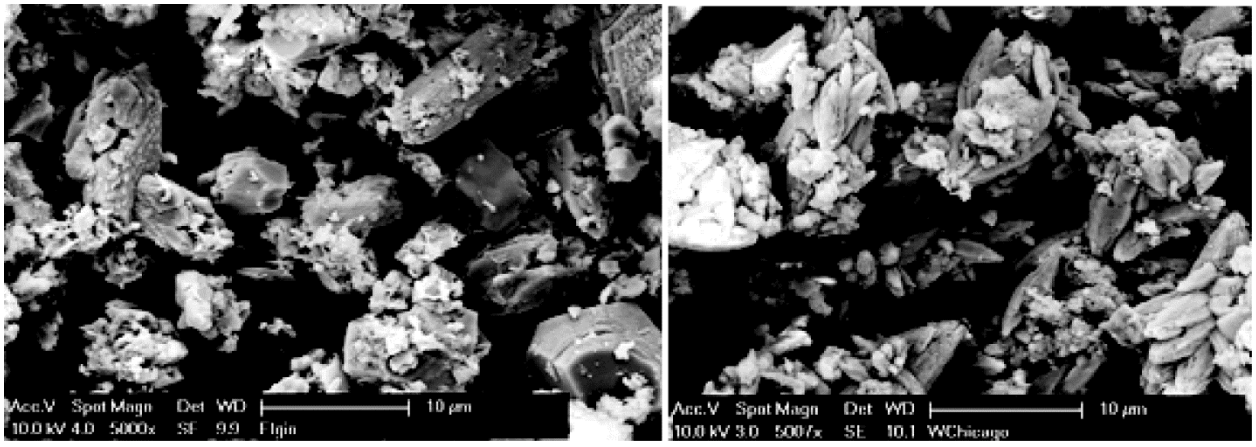

Figure 7. SEM photomicrographs of representative lime sludge samples studied. (left) A calcite-dominated lime sludge; (right) an aragonite-dominated lime sludge. Aragonite is a calcium carbonate polymorph similar in composition to calcite ($CaCO_3$) but with a different crystal morphology. Crystal shapes in the calcitic sludge are mainly blocky, some with well-developed rhombohedron and scalenohedron morphologies. Aragonitic sludge, on the other hand, mainly consists of finely crystalline, needle-shaped to acicular crystal habits.

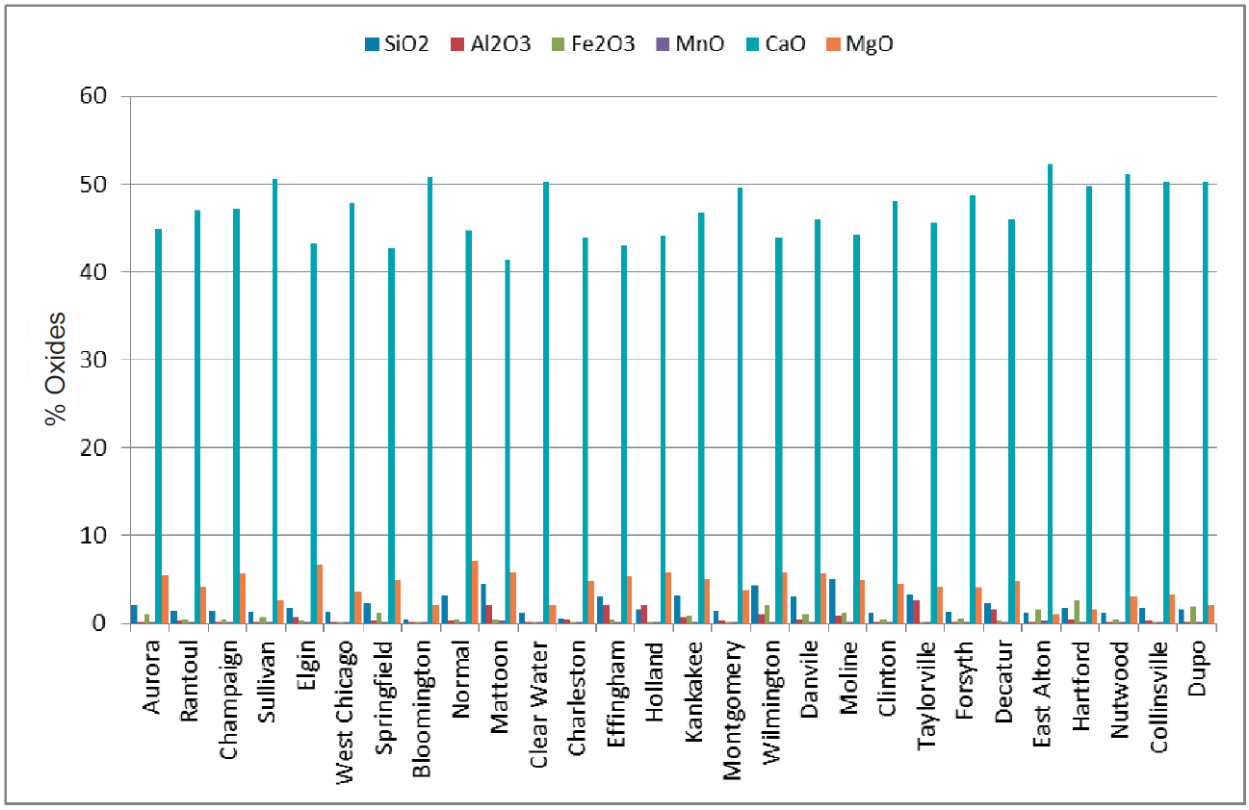

Figure 8. Major oxides in lime sludge studied.

Scanning electron microscopy (SEM) showed that the lime sludge was made up of very fine crystals, some of which had well-developed crystal faces (Figure 7). However, many crystals were less well developed, possibly because of rapid precipitation. Scanning electron microscopy also showed that, in most cases, the crystal diameter was much smaller than the particle size measured in the laboratory with the particle size analyzer. This was likely due

to the clustering of crystals into larger aggregates. Both SEM and pore volume data further demonstrated the very finely crystalline and porous nature of these materials. The small crystal size and high porosity contributed to the high surface area measured for lime sludge samples.

X-ray fluorescence (XRF) analysis indicated that CaO was the dominant oxide present in the lime sludge we studied. Magnesium oxide was the next dominant oxide present (Figure 8). Also present in some samples was SiO_2. Other impurities were minor and included Al_2O_3, ferric oxide (Fe_2O_3), and MnO.

The XRD and chemical analyses further showed that the lime sludge from Illinois water treatment plants consisted primarily of acid-soluble calcium carbonates. A calcium carbonate polymorph, aragonite, was the dominant mineral in a few lime sludge samples studied. Another major component was magnesium carbonate ($MgCO_3$), which ranged between 2 and 15 wt% and primarily occurred as a solid solution within calcite rather than as a separate mineral phase. The total acid-soluble carbonates ($CaCO_3$ + $MgCO_3$) in most of the lime sludge samples examined ranged between 90 and 95 wt%. As with $CaCO_3$, both $MgCO_3$ and aragonite were highly soluble in dilute acids, an important property for the desulfurization process. The magnesium hydroxide [$Mg(OH)_2$] content of lime sludge in other studies has generally been between 2 and 3 wt% (Che et al. 1988; Shannon et al. 1997). However, we did not detect any $Mg(OH)_2$ in the samples we examined.

Because of the high $CaCO_3$ content, very fine particle size, and high pore volume and surface area, lime sludge residues tend to have high reactivity with respect to sulfur capture (Baker et al. 2005; Che et al. 1988; Goodwin et al. 1982; Lasemi et al. 2011; Shannon et al. 1997). Very few reports have been published on the use of lime sludge for desulfurization. Test trials of the sludge from two power plants in Iowa and Kansas showed a significant efficiency of the material in capturing SO_x from the flue gas of coal-fired power plants (Baker et al. 2005; Shannon et al. 1997). This potentially valuable resource presently has limited use for two reasons. First, many in the coal-fired power plant industry are not aware of the availability of these resources. Second, the quality of these resources may be quite variable, depending on the method of water softening used.

The utilization of lime sludge as a sulfur oxide scrubbing agent provides two major cost-saving advantages. First, the material is very fine, having an average particle size ranging between 8 and 20 μm in diameter. As a result, it can be used as is, thus eliminating the additional energy cost associated with grinding. Second, lime sludge is a waste material that may be available at no cost except for that incurred for removal and transportation. This can reduce, or possibly eliminate, the need for limestone sorbents, especially in areas where limestone deposits are generally unavailable.

4.0 Reactivity with respect to sulfur capture

The acid dissolution rate of limestones has been used as an indicator of limestone reactivity with respect to sulfur capture in FGD conditions. A pH-stat auto-titration experiment was conducted to measure the relative reactivity of a selected number of limestone fine and lime sludge samples for removal of SO_2 in wet FGD processes. The dissolution fractions and the neutralizing capacities for a selected number of limestone fine and lime sludge samples were calculated based on the titration results.

The dissolution performance of the fines varied significantly. The calculated dissolution fraction [based on the calcium (Ca) and Mg contents of the samples] ranged from 2% to 75% in 10 minutes and from 5% to 99% in 60 minutes. A strong correlation was observed between the dissolution fraction of limestone and the MgO content: the dissolution fraction decreased with increasing MgO content because of the low reactivity of dolomite, the source of MgO in quarry fines (Figure 9).

Data from the acid titration tests indicated that lime sludge was highly reactive compared with dolomites and even some limestones. The results showed that lime sludge reactivity had a weak to no correlation with MgO content, as shown in Figure 10. This result is in contrast to titration results from limestone and dolomite, in which a strong negative correlation was found between reactivity (acid-neutralizing capacity) and MgO content. The higher reactivity of lime sludge, regardless of the MgO content, was due to the $MgCO_3$ contribution in the lime sludge and not from the much less reactive dolomite source in dolomitic limestones and dolomites. We suggest that $MgCO_3$ in the lime sludge occurs as a solid solution within the calcite lattice without significantly altering the calcite structure. Our results showed not only that $MgCO_3$ in a solid solution with calcite did not reduce the calcite reactivity, but also that it might even have enhanced it.

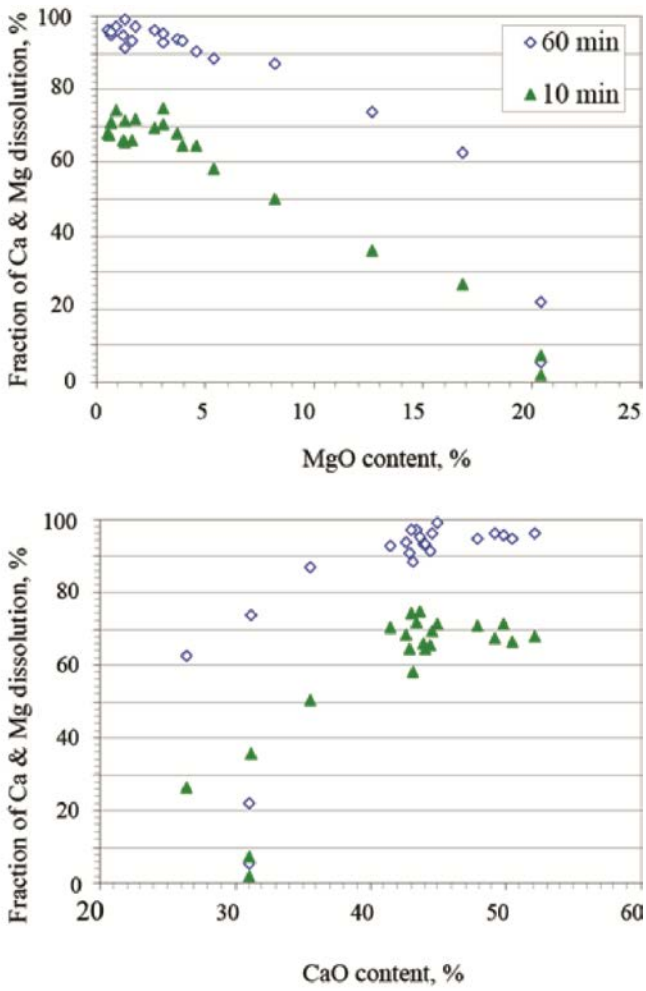

Figure 9. Correlation between the dissolution fraction and MgO (dolomite) and CaO contents of limestone fines after 10 and 60 minutes of reaction. The MgO content in pure dolomite is about 21.86%.

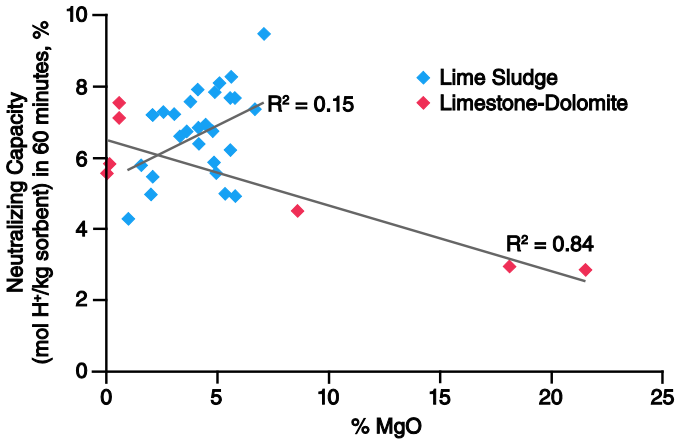

Figure 10. Correlation between neutralizing capacity and MgO content in limestone-dolomitic limestone-dolomite (red diamonds) and lime sludge (blue diamonds). The weak to slightly positive correlation between MgO content and neutralizing capacity of lime sludge samples (blue diamonds), in contrast to that in limestone-dolomite samples, indicates that the Mg in lime sludge is from acid-soluble compounds (e.g., $MgCO_3$).

5.0 Conclusions

Results of this study indicate that abundantly available by-product limestone fines and lime sludge waste materials could be used as affordable sorbents for desulfurization in coal-fired power plants, as agricultural lime for pH control, or potentially as raw materials in the manufacture of portland cement and concrete. The utilization of quarry fines and lime sludge as scrubbing agents or for other beneficial purposes would offer two major cost-saving advantages: (1) because the material has already been crushed substantially (quarry fines) or is naturally very fine grained, the energy cost associated with grinding would be reduced if these by-products were used as sorbents for desulfurization; and (2) because, in many cases, the fines and lime sludge are considered waste materials, they are widely available at quarries or water treatment plants free or at a relatively low cost. Reactivity tests suggested that the desulfurization reactivity was higher in limestone fines than in the parent material. Reactivity tests further showed that lime sludge was highly reactive compared with dolomite and dolomitic limestone. In contrast to dolomite and dolomitic limestone, $MgCO_3$ in lime sludge did not have a negative effect on reactivity because the contribution of $MgCO_3$ was not from a less reactive dolomite source.

Acknowledgments

This paper is an excerpt from two reports prepared with support, in part, by grants made possible by the Illinois Department of Commerce and Economic Opportunity through the Office of Coal Development and the Illinois Clean Coal Institute. Neither the authors and the University of Illinois at Urbana-Champaign, nor any of its subcontractors, nor the Illinois Department of Commerce and Economic Opportunity, Office of Coal Development, the Illinois Clean Coal Institute, nor any person acting on behalf of either, (1) makes any warranty of representation, express or implied, with respect to the accuracy, completeness, or usefulness of the information contained in this report, or that the use of any information, apparatus, method, or process disclosed in this report may not infringe privately owned rights; or (2) assumes any liabilities with respect to the use of, or for damages resulting from the use of, any information, apparatus, method, or process disclosed in this report. Yongqi Lu and Seyed A. Dastgheib are acknowledged for helpful discussions regarding reactivity measurements and for providing the surface area data. Special thanks also go to Susan Krusemark and Michael Knapp for their invaluable assistance with editing and layout of the final document. The paper benefited from helpful review by Brett Denny and Yongqi Lu, both at the Illinois State Geological Survey.

References

ASTM. 2001. C1318-95: Standard Test Methods for Determination of Total Neutralizing Capacity and DissolvedCalcium and Magnesium Oxide in Lime for Flue Gas Desulfurization (FGD): West Conshohocken,Pennsylvania, ASTM. Available at: https://docs.google.com/folderview?pli=1&id=0BySAaSKrtUDnS2JuUXBRRF9US1E [accessed 2 2 2016].

Baker, R.J., J. van Leeuwen, and D.J. White. 2005. Applications for Reuse of Lime Sludge from Water Softening: Ames, Iowa State University, Final Report TR-535, 142 pp.

Che, M.D., T.J. Logan, S.J. Traina, and J.M. Bigham. 1988. Properties of water treatment lime sludges and their effectiveness as agricultural limestone substitutes: J. Water Pollution Control Federation, v. 60, no. 5, p. 674–679.

Goodwin, J.H., I.G. Krapac, P.C. Reed, and W.R. Roy. 1982. Assessment of potential agricultural and industrial uses of lime-water softening waste slurry, *in* Fifth Annual Madison Conference of Applied Research and Practice on Municipal and Industrial Waste [proceedings]: Madison, Department of Engineering & Applied Science, University of Wisconsin–Extension, pp. 495–521.

Lasemi, Z., S.B. Bhagwat, G.B. Dreher, S.P. Koenig, H.E. Leetaru, Y. Lu, D.G. Mikulic, R.D. Norby, M. Rostam-Abadi, and J.D. Steele. 2004. Champaign, Illinois State Geological Survey, Final Technical Report to Illinois Clean Coal Institute, 30 pp. plus appendices.

Lasemi, Z., S.B. Bhagwat, G.B. Dreher, A.G. Ianno, S.P. Koenig, Y. Lu, D.G. Mikulic, R.D. Norby, M. Rostam-Abadi, G.L. Salmon, L.R. Smith, and J.D. Steele. 2005. Champaign, Illinois State Geological Survey, Final Technical Report to the Illinois Clean Coal Institute, 30 pp. plus appendices.

Lasemi, Z., Y. Lu, M. Rostam-Abadi, S.K. Butler, and D. Ruhter. 2008. Limestone Fines—An Economically Viable Source of Sorbents for Desulfurization? Champaign, Illinois State Geological Survey, Final Technical Report to Illinois Clean Coal Institute, 30 pp. plus appendices.

Lasemi, Z., S. Ansari, S. Butler, G. Durant, and W. Roy. 2012. Lime Softening Sludge—A Potentially Important Source of Sorbent for Wet FGD Systems: Champaign, Illinois State Geological Survey, Final Contract Report to Illinois Clean Coal Institute, 38 pp. plus appendices.

Lasemi, Z., G. Durant, S. Butler, B. Denny, S. Maddix, and S. Raduha. 2011. Mapping High-Calcium Limestone Resources near Illinois Coal-Fired Power Plants: Champaign, Illinois State Geological Survey, Final Technical Report to Illinois Clean Coal Institute, 39 pp. plus appendices.

Shannon, L.D., C.H. Yu, R.E. Eieklinski, J.B. Jarvis, and D.P. DeKraker. 1997. Beneficial Reuse of Lime Softening Residuals for Flue Gas Desulfurization: Denver, Colorado, American Water Works Association, p. xvii.

METHODS FOR ASSESSING THE ALKALI-SILICA REACTIVITY OF AGGREGATES FOR USE IN CONCRETE

Laura Simandl[1], Rishi Gupta[2], Alireza Biparva[3]
[1] lsimandl@uvic.ca Civil Engineering Department, University of Victoria, Victoria, B.C. Canada
[2] Civil Engineering Department, University of Victoria, Victoria, B.C. Canada
[3] Kryton Corporation Canada, Vancouver, B.C. Canada

Abstract

The world population is rapidly increasing and resources of prime aggregates near major urban centres have been depleted or are dwindling. The construction industry has two choices: 1) use more distant sources of raw materials and pass the associated cost to consumers (e.g. imports of aggregate to San Francisco Bay area, California from Texada Island, British Columbia), or 2) resort to the use of non-ideal raw materials. Unless low cost transportation corridors link urban centres to distant low-cost suppliers of aggregate, the use of non-ideal raw materials is the only competitively available solution to maintain the cost of concrete at a reasonable level. This solution carries higher risk of premature deterioration of buildings and infrastructure made from sub-standard concrete. Alkali-silica reaction (ASR) is one of the deterioration mechanisms at risk of taking place. ASR produces cracks in hardened concrete when the following three conditions are present: alkali-reactive siliceous aggregates, a highly alkaline pore fluid, and moisture. Significant cracking can lead to loss of strength and compromise the structural integrity of the infrastructure. To reduce such risks, the construction industry resorts to new innovative concrete mix designs involving the addition of cementitious materials and chemical additives, in combination with preventive testing. To test the suitability/durability of concrete produced using unproven mix designs, preventative tests can be performed prior to large-scale batching and wide-spread use. This document discusses and compares the suitability of tests used by industry for assessing the alkali-silica reactivity of aggregates for use in concrete.

1.0 Introduction

Concrete is the most used man-made material (de Brito and Saikia. 2012). Globally, over 11.5 billion tonnes of concrete are being produced annually and by year 2050 it is expected to reach 16 billion tonnes (Mehta and Monteiro. 2006).

This document gives a brief overview of concrete as a construction material, and discusses its strengths, in particular, its durability. Subsequently, it focuses on the chemical deterioration mechanism of alkali silica reaction (ASR). Discussion as to why ASR may be a concern for the concrete and construction industries in North America is included; mainly with regards to how new or less-suitable aggregate sources will need to be used in concrete as non-reactive aggregate sources near urban centres are depleted. The suitability of these aggregates will need to be tested before widespread use in construction of infrastructure. This document summarizes and briefly reviews the several well-established ASTM test standards, guides and practices relevant for determining the alkali-silica reactivity of these sources of aggregate in concrete. Recommendations for industry professionals are included.

2.0 What is concrete?

Concrete is a composite material. Its three main components are: aggregate (usually sand, gravel and/or crushed stone), cement, and water (Figure 1). The cement used is typically Portland cement. Sometimes supplementary cementitious materials (such as fly ash, blast furnace slag, and silica fume), chemical admixtures and ground limestone are also added. The combination of water and cementitious materials forms a paste, which coats the aggregate. The paste hardens as a result of a chemical reaction called hydration, and binds the aggregate together.

Concrete is the most used construction material in the world. Twenty five billion tons (22.7 billion metric tonnes) of concrete are placed each year (World Business Council for Sustainable Development. 2009). Twice as much concrete is used in construction around the world than the total of all other building materials (Kosmatka et al. 2011).

The main reasons why concrete is so widely used as building material are:

1. The ingredients are readily available in most geographic regions.
2. Aggregate, a relatively inexpensive material, is the main constituent of concrete. In USA, the price of construction-grade sand and gravel averaged US $7.7/metric ton free on board at the mine site (Bennett. 2015). Where local sources of aggregate can be used, the cost of concrete at construction sites remains very competitive relative to other construction materials.
3. Concrete is a versatile building material. It can be cast to any shape or configuration for which a form is available.

4. Concrete is fire resistant.
5. The properties of concrete (strength, workability, density, setting time, etc.) can be modified for an application.
6. It is recyclable.
7. Concrete is durable. If properly designed and placed, it is able to resist deterioration caused by chemical and physical attacks, and maintain satisfactory performance for long periods of time.

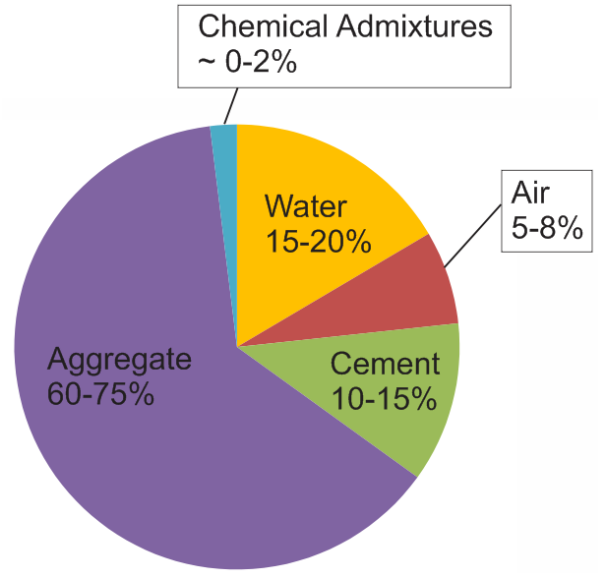

Figure 1. Concrete components and approximate proportions. Proportions used to construct this diagram were obtained from Portland Cement Association (n.d.).

3.0 Concrete durability and factors affecting durability

Concrete durability is defined by Kosmata et al. (2011) as "the ability of concrete to resist weathering action, chemical attack, and abrasion while maintaining its desired engineering properties with minimal loss of mass in an aggressive environment".

Factors affecting durability include: the exposure environment, the mix design, the placement, and curing of the concrete. If the concrete is not properly designed for the exposure environment or the ingredients are inadequate, the concrete will become susceptible to premature physical and/or chemical deterioration, and will not last the target lifespan of the project. Similarly, no matter how well a concrete mix is designed, if the workmanship and placement are not adequate, the concrete will not meet its target lifespan.

An example of the effect of adverse environments on concrete structures is the concrete seawall at Dallas Road in Victoria, B.C. (Figures 2 and 3). Over the years, the concrete in this environment has been subjected to abrasion and erosion from wave action in addition to steel reinforcement corrosion (likely due to abundance of chloride ions in seawater), as well as sulfate attack. The design of a concrete for this environment requires significantly different considerations than a concrete wall in the interior of a building.

Figure 2. Concrete seawall at Dallas Point, Victoria B.C.

Figure 3. Close-up of corrosion of steel reinforcement

As already evident from the example presented above, there are several deterioration mechanisms that can affect the durability of concrete. Besides corrosion of steel reinforcement, erosion, abrasion, and sulfate attack, there are other deterioration mechanisms to which concrete may be subjected. ASR is one of them, and is discussed in the following section.

4.0 Alkali Silica Reactivity (ASR)

ASR is a deleterious chemical reaction which occurs when siliceous aggregates in concrete react with the concrete's alkaline pore fluid reference. For ASR to occur, there are three requirements: 1) the presence of alkalis, 2) a source of reactive silica, and 3) sufficient moisture as shown in Figure 4 (Farny and Kerkhoff. 2007). The main source of alkalis in concrete is typically the cement, which contains minor amounts of sodium and potassium (Lindgård et al. 2012). Additional alkalis may be supplied by aggregates, admixtures and supplementary cementing materials (SCMs), or from external sources such as seawater (Folliard et al. 2003). The most reactive forms of silica are generally those with a more disordered crystalline structure, such as opaline chert and strained quartz (Farny and Kerkhoff. 2007).The third condition for ASR is sufficient moisture. The minimum limit for relative humidity is approximately 80-90% (Lindgård et al. 2012). If one of these three conditions is not met, expansive ASR is unlikely to occur. So in order to prevent ASR, one of these factors (or more) should be eliminated.

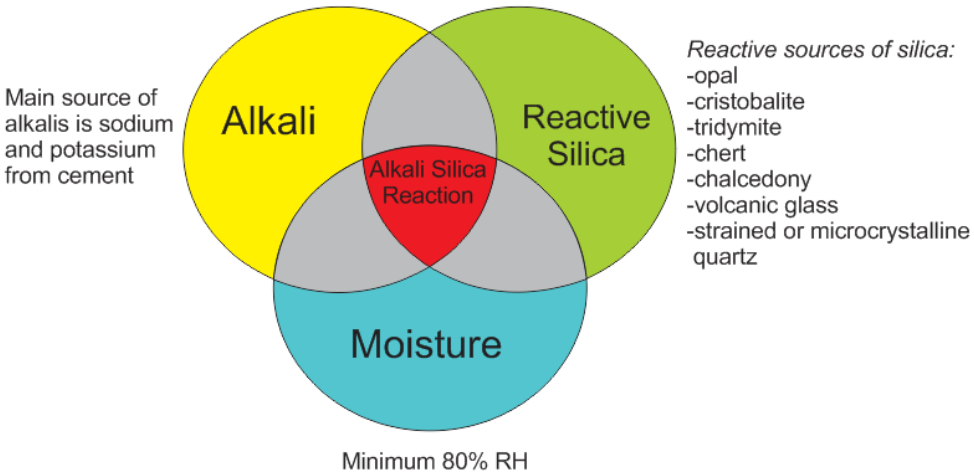

Figure 4. Requirements for alkali silica reaction. Diagram modified from Du. (2010)

The following mitigation measures are recommended to reduce the potential of ASR:

1) Avoid using reactive aggregates
2) Use low-alkali cement
3) Limit the total alkali content of concrete (aggregates and SCMs included)
4) Use SCMs such as slag, fly ash, and silica fume
5) Use lithium-based admixtures

6) Reduce movement of moisture and alkalis into and within the concrete. (Farny et al. 2007)

In some regions, it may not be practical to use non-reactive aggregates. In this case, reactive aggregate can be blended with non-reactive aggregate to produce an aggregate combination with limited **reactivity** (Fournier and Bérubé 2000)**.** Since ASR reaction is dependent on the availability of **moisture** (Multon and Toutlemonde 2010) (Olafsson 1986) (Kurihara and Katawaki 1989)**,** reduction in water infiltration may reduce ASR. This may be achieved by reducing the water to cementing materials ratio or adding a permeability reducing admixture, as this in turn reduces the porosity of the matrix.

The mechanism of ASR is outlined in Figure 5. As mentioned previously, ASR requires the presence of alkalis and a reactive source of silica (Figure 5a). Concrete's highly alkaline pore fluid (i.e. pH **≥**12.5) (Fournier and Bérubé 2000)**,** leads to the dissolution of the silicates from the alkali-reactive aggregates, and produces a hygroscopic (able to attract and hold water from the surrounding environment) gel (Figure 5b). Ultimately, the pressure generated by expansion of the gel leads to cracking (Figure 5c). 'Map-cracking' is the signature cracking pattern of ASR (Figure 6). Extensive cracking of the concrete results in premature deterioration of the structures. The presence of surface cracks caused by ASR may also accelerate the deterioration of concrete by other processes, such as corrosion of steel reinforcement and freeze and thaw (Fournier and Bérubé 2000)**.** The combination of these mechanisms can create major structural problems in infrastructure.

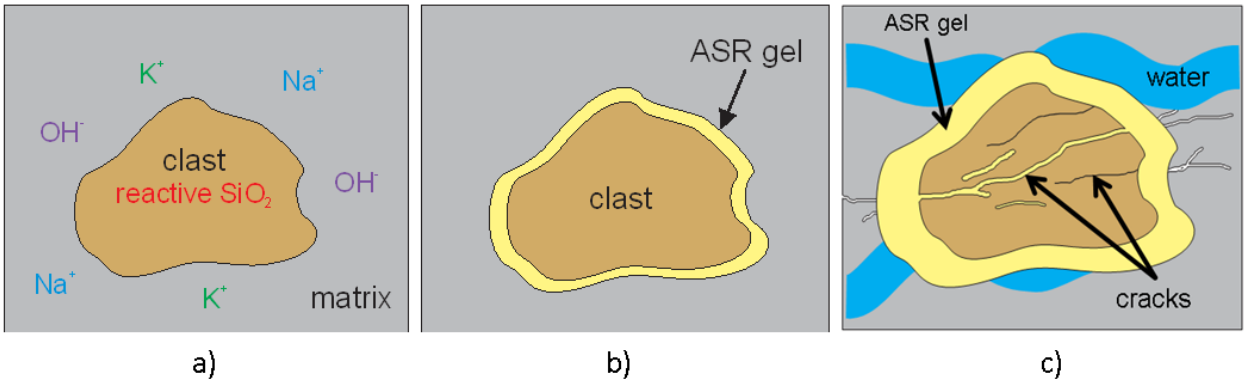

Figure. 5. Mechanism of Alkali Silica Reaction a) presence of reactive silicate and alkalis; b) formation of a hygroscopic gel; c) expansion of the ASR gel results in internal overpressure and cracking takes place. Diagram modified from Thomas et al. (2011)

Figure 6. 'Map Cracking' of concrete due to ASR (typical reaction)

Reported cases of ASR in North America are shown on Figure 6. This shows that ASR cases are not limited to a single region.

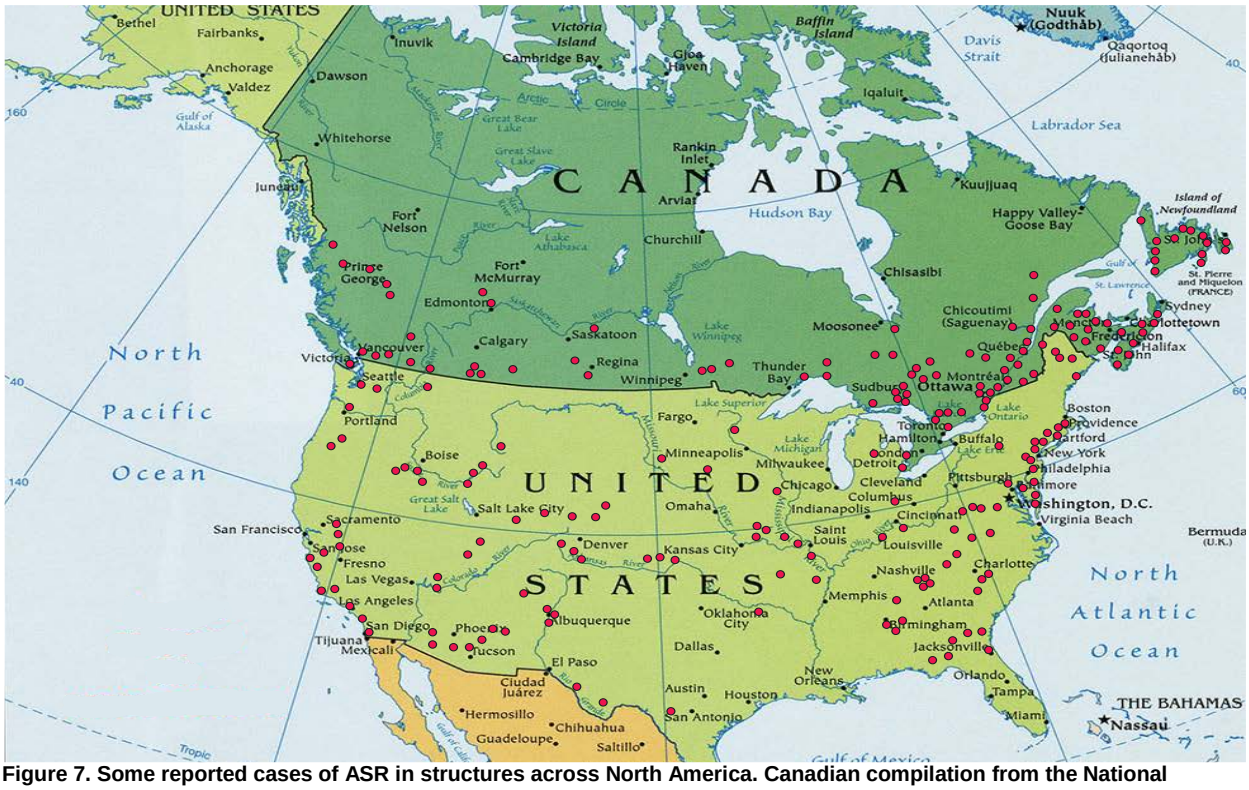

Figure 7. Some reported cases of ASR in structures across North America. Canadian compilation from the National Research Council of Canada (Grattan-Bellew and Mitchell 2002)**. The US occurrences are from the Federal Highway Administration** (Folliard et al. 2003)**.**

5.0 Assessing the alkali silica reactivity of aggregates

Ideally, consultation of historic field records is performed prior to use of an aggregate in concrete. Alternatively, if historic field records are unavailable, concrete or mortar specimens made from the unproven material should be tested. Several accelerated test methods have been developed for testing the ASR susceptibility of aggregate. Most of these methods involve exposing the specimens to simulated extreme environmental conditions to accelerate the deterioration**.**

The standard tests, guides and practices for assessing the alkali silica reactivity of aggregates from the ASTM International are listed in Table 1.

Table 1. ASTM Standard Test Methods, Practices and Guides for Assessing Alkali-silica Reactivity of Aggregates

ASTM C289	Standard Test Method for Potential of Alkali-Silica Reactivity of Aggregates (Chemical Method)
ASTM C295	Standard Guide for Petrographic Examination of Aggregates for Concrete
ASTM C227	Standard Test Method for Potential Alkali-Reactivity of Cement-Aggregate Combinations (Mortar-Bar Method)
ASTM C441	Standard Test Method for Effectiveness of Pozzolans or GBFS in Preventing Excessive Expansion of Concrete Due to Alkali-Silica Reaction (Mortar Bar Method)
ASTM C1293	Standard Test Method for Concrete Aggregates by Determination of Length of Change of Concrete Due to Alkali-Silica Reaction
ASTM C1260	Standard Test Method for Potential Alkali Reactivity of Aggregates (Mortar-Bar Method)
ASTM C1567	Standard Test Method for Potential ASR of combinations of cementitious materials and aggregates (accelerated mortar bar)
ASTM C856	Standard Practice for Petrographic Examination of Hardened Concrete
ASTM C1723	Standard Guide for Examination of Hardened Concrete Using Scanning Electron Microscopy

ASTM C289, Standard Test Method for Potential of Alkali-Silica Reactivity of Aggregates (Chemical Method), is a test method where crushed samples of aggregate are reacted with a 1N sodium hydroxide solution at 80°C for 24 hours to determine the reactivity of aggregates. The drop in alkalinity of the solution and the amount of dissolved silica is measured. While this test is rapid, it is not very reliable and if it is performed, it should be supplemented by other test methods (Farny and Kerkhoff 2007).

ASTM C295, Standard Guide for Petrographic Examination of Aggregates for Concrete is a guide for identifying and describing constituents of aggregate, including the identification and approximate quantification of reactive minerals. Petrographic analysis is recommended as an initial first step for assessing alkali-silica reactivity of an aggregate. An advantage of this analysis is that it is relatively rapid; however, an experienced petrographer is required. While this test may be used to classify an aggregate as potentially reactive, this test cannot be used for quantitatively determining an aggregate's reactivity or the appropriate levels of prevention required for its use.

ASTM C227, Standard Test Method for Potential Alkali-Reactivity of Cement-Aggregate Combinations (Mortar-Bar Method), measures the length change of mortar bars stored over water at 37.8 ºC to determine susceptibility of cement-aggregate combinations to alkali-silica reaction. The major disadvantage with this test is that it is not suitable for slowly reactive aggregates (such as those containing gneisses, quartzites, greywackes, argillites, metavolanics) (Thomas et al. 2006). Additionally, the alkali content required to produce expansion is much greater than in the concrete prism test (ASTM C1293), and there may be excessive leaching of alkalis from the specimens (Kosmatka et al. 2011) (Farny and Kerkhoff 2007).

ASTM C277 is not recommended. This test was used to evaluate the locally quarried aggregate used in the construction of the Mactaquac generating station in New Brunswick, Canada (Figures 8 and 9). The aggregate consisted primarily of greywacke and also contained slate (Hayman et al. 2010). Results of the test incorrectly indicated that the aggregate was non-reactive, and it was subsequently used for the construction of the dam. The Mactaquac generating station was constructed in the mid-1960s and within 10 years of construction, signs of ASR were already apparent. Reconstruction will need to be completed by 2030; nearly 40 years earlier than expected (Hayman et al. 2010). Even more interesting, is that since there is no local source of non-reactive aggregate for the new project, using local greywacke from the excavation is being considered. This would require use of the aggregate in combination with preventative measures such as fly ash. Hayman et al. (2010) evaluates different aggregate combinations using ASTM C1260 (to test mixes without SCMs), ASTM C1567 (for mixes with SCMs), and ASTM C1293 for 2 years (for mixes with SCMs).

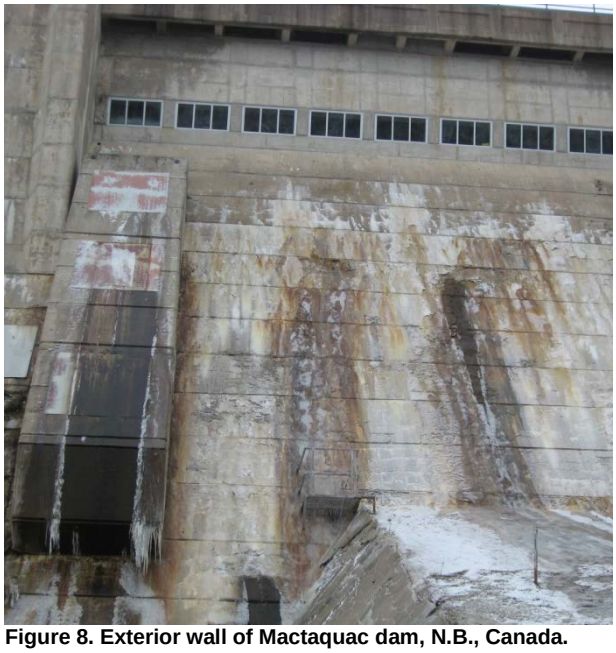

Figure 8. Exterior wall of Mactaquac dam, N.B., Canada.

Figure 9. Water flowing through crack of dam wall

ASTM C441, Standard Test Method for Effectiveness of Pozzolans or Ground Blast-Furnace Slag in Preventing Excessive Expansion of Concrete Due to the Alkali-Silica Reaction, measures the length change in mortar bars using Pyrex glass as the reactive aggregate. This test method is for determining the dosage of supplementary cementitious materials that should be used. It is a modification of ASTM C227 and is not recommended since it does not test the actual aggregate used.

ASTM C1293, Standard Test Method for Concrete Aggregates by Determination of Length of Change of Concrete Due to Alkali Silica Reaction, is used to determine the susceptibility of cement-aggregate combinations to ASR. It is a year-long test, in which concrete prisms (75 x 75 x 285 mm) cast using the aggregate in question are stored over water at 38°C (100°F). Measurements of the expansion are performed regularly during this period. If the total expansion of the prism exceeds 0.04% after one year, then the aggregate is considered to be reactive.

ASTM C1293 can also be used to investigate combinations of hydraulic cement and pozzolan or ground blast-furnace slag, but in this case, the test must be lengthened to 2 years. There have been documented cases of leaching (where condensation on the prism surfaces leads to an outward diffusion of alkalis) from the concrete (Lindgård et al. 2012); however, of the tests that were researched, this one is still considered to be the most reliable, and is the most representative of field conditions (Kosmatka et al. 2011).

Figure 10. Length comparator used to determine the expansion of the mortar bar (ASTM C1260)

ASTM C1260, Standard Test Method for Potential Alkali-Reactivity of Aggregates (Mortar-Bar Method), is a 16 day screening test in which mortar bars (25 x 25 x 285mm) made using the unproven aggregate are immersed in an alkaline solution at 80 °C (176 °F). This test is similar to ASTM C1293. It measures the expansion of the mortar bar, to determine the susceptibility of its aggregates to ASR. The aggregate is considered reactive if expansion is more than 0.20%, and is considered to be non-reactive if expansion is less than 0.10%. ASTM C1260 is described as an aggressive test because the environment is severe (temperature is high, and the samples are submerged in a 1N NaOH solution to increase the concentration of alkalis) (Folliard, Thomas and Kurtis 2003). Several aggregates that have good field performance fail this test. Similarly some aggregates fail this test, but pass the concrete prism test (Kosmatka et al. 2011). The major concern with this test is that the testing conditions are too extreme and are not representative of field conditions. Additionally, excessive alkali boosting (i.e. the 1 M NaOH solution) may have other effects on the expansion, such as accelerating the release of alkalis from certain aggregates, and changing the K/Na ratio (Lindgård et al. 2012). For these reasons, it is recommended that the results of this test be verified by petrographic analysis and by performing another test(s) (preferably ASTM C1293); particularly if results from ASTM C1260 indicate that the aggregate is reactive. The major advantage of this test is that it is rapid.

ASTM C1567, Standard Test Method for Determining the Potential Alkali-Silica Reactivity of Combinations of Cementitious Materials and Aggregate. This test method is a variation of ASTM C1260, used for evaluating combinations of cementitious material and aggregate. It shares the same advantages and disadvantages as ASTM C1260. Tests for assessing the combination of aggregates and preventative measures (this test, as well as ASTM C1293 for 2 years) are particularly useful when the aggregate is already known to be reactive or potentially reactive,

and using a non-reactive aggregate is not a feasible and/or practical option. These methods can be used to determine the dosage of preventative measure required to control the expansion due to ASR.

Petrographic and/or SEM examination of concrete samples (described by ASTM C856 and ASTM C1723) should succeed any of the mortar and concrete prism tests described above to verify that ASR gel is present in the samples at the end of testing and that the expansion of the specimens was in fact due to ASR. First, areas in the specimen with alkali silica gel must be identified. This can be done by using a technique described in ASTM C856 A1. It involves treating the specimen surface with uranyl-acetate and exposing it to short-wave UV. The alkali silica gel will fluoresce bright greenish-yellow. The areas of interest can then be analyzed more closely with the SEM, and EDX analysis can be performed to confirm its presence (the gel will always contain silicon, and varying quantities of calcium, potassium, and sodium). The aggregates in the concrete/mortar will also be examined for cracks (particularly those that appear to be tensile; narrow from center toward the outside of particle).

6.0 Conclusion and Recommendations

Without proper testing and further research, alkali-silica reaction will become a significant problem as sources of non-reactive aggregate are depleted and new un-proven and/or “reactive” sources are used instead.

- Petrographic analysis (ASTM C295) in addition to ASTM C1260 and/or ASTM C1293 is recommended for testing alkali-silica reactivity of the aggregate.
- ASTM C1293 is preferred over ASTM C1260 (time permitting).
- If testing an aggregate with a preventative measure (ex. Fly Ash) use ASTM C1293 for 2 years (time-permitting); otherwise, use ASTM C1567.
- Following mortar bar/concrete prism tests, petrographic/SEM examination of the samples (ASTM C856 and ASTM C1723) should be used to verify that ASR gel is present, and that the expansion of the specimens was in fact due to ASR.

Acknowledgements

Figures 8 and 9, photos of the Mactaquac generating station are courtesy of Jeff Bowman from Kryton Corporation Canada.

References

Bennett, S. 2015. Sand and gravel (construction): U.S. Geological Survey, Mineral Commodity Summaries, pp. 136-137.

de Brito, J., and Saikia, N. 2012. Recycled Aggregate in Concrete; Use of Industrial, Construction and Demolition Waste: Springer Science & Business Media.

Du, C. 2010. Dealing with Alkali-Aggregate Reaction in Hydraulic Structures. [Online] Available at: http://www.hydroworld.com/articles/print/volume-18/issue-3/articles/civil-works/dealing-with-alkali-aggregate.html [Accessed 20 12 2015].

Folliard, K., Thomas, M., and Kurtis, K. 2003. Report No. FHWA-RD-03-047; Guidelines for the Use of Lithium to Mitigate or Prevent ASR: Georgetown Pike, Federal Highway Administration, U.S. Department of Transportation.

Farny, J. and Kerkhoff, B. 2007. Diagnosis and Control of Alkali-Aggregate Reactions: Skokie, Portland Cement Association.

Fournier, B. and Bérubé, M. 2000. Alkali-aggregate reaction in concrete; a review of basic concepts and engineering implications: Canadian Journal of Civil Engineering, Volume 27, pp. 167-191.

Grattan-Bellew, P.E. & Mitchell, L. 2002. Preventing Concrete Deterioration Due to Alkali-Aggregate Reaction: Construction Technology Update 52, National Research Council of Canada (Construction Technology).

Hayman, S., Thomas, M., Beaman, N. & Gilks, P. 2010. Selection of an effective ASR-prevention strategy for use with a highly reactive aggregate for the reconstruction of concrete structures at the Mactaquac generating station: Cement and Concrete Research, Volume 40, pp. 605-610.

Kosmatka, S., Kerkhoff, B., Hooton, R. & McGrath, R. 2011. Design and Control of Concrete Mixtures: Ottawa, Cement Association of Canada.

Kurihara, T. and Katawaki, K. 1989. Effects of moisture control and inhibition on alkali silica reaction: Kyoto, 8th ICAAR, International Conference on Alkali Aggregate Reactions, pp. 629-634

Lindgård, J., Andiç-Çakır, Ö., Fernandes, I., Ronning, T., & Thomas, M. 2012. Alkali–silica reactions (ASR): Literature review on parameters influencing laboratory performance testing: Cement and Concrete Research, Volume 42.

Mehta, P., and Monteiro, P. 2006. Concrete: Microstructure, Properties and Materials. McGraw-Hill. pp. 4

Multon, S. and Toutlemonde, F. 2010. Effect of moisture conditions and transfers on alkali silica reaction damaged structures: Cement and Concrete Research, Volume 40, pp. 924-934.

Olafsson, H. 1986. The effect of relative humidity and temperature on alkali expansion of mortar bars. Ottawa

Portland Cement Association. nd. How Concrete is Made [Online]. http://www.cement.org/cement-concrete-basics/how-concrete-is-made [Accessed 20 12 2015].
Thomas, M., Fournier, B., Folliard, K., Ideker, J., & Shehata, M. 2006. Test methods for evaluating preventative measures for controlling expansion due to alkali-silica reaction in concrete: Cement and Concrete Research, pp. 1842-1856.
Thomas, M., Fournier, B., Folliard K., and Resendez, Y. 2011. Report No. FHWA-HIF-12-022; Alkali-silica Reactivity Field Identification Handbook: U.S. Department of Transportation. Federal Highway Administration.
World Business Council for Sustainable Development. 2009. The Cement Sustainability Initiative - Recycling Concrete: Geneva, Atar Roto Press SA.

ALLEGHANIAN MAGMATISM IN THE SOUTHERN APPALACHIANS: GEOCHRONOLOGY OF THE MULTI-PHASE DANBURG-SANDY HILL INTRUSION & COEVAL MAFIC ENCLAVES

First Author: [1]Cody M. Strack, straccm@gmail.com
Co-Authors: [1]Dr. Craig Grimes, [2]Dr. Paul Mueller, [2]Dr. David Foster, [2]Qianying Lin, [3]Matthew A. Coble
[1]Department of Geological Sciences, Ohio University
[2]Department of Geological Sciences, University of Florida
[3]School of Earth Sciences, Stanford University

ABSTRACT

Emplacement of numerous late syn- to post-tectonic Alleghanian granitoids in the Southern Appalachian Orogen (SAO) are interpreted to mark final assembly of Pangea, though a comprehensive understanding of emplacement ages and formation mechanisms remains enigmatic. We obtained SHRIMP-RG $^{206}Pb/^{238}U$ ages of zircons from 7 intrusions in Georgia, USA, and are conducting a detailed study of the Danburg pluton (NE GA) to better understand the mechanisms leading to granite formation in the SAO. Magmatic $^{206}Pb/^{238}U$ zircon ages indicate a bimodal distribution of ages from ~342-321 in the Inner Piedmont and ~306-300 Ma in accreted Gondwanan terranes to the east, which is consistent with a growing database of U-Pb zircon ages. Ages of zircon xenocrysts, zircon $\delta^{18}O$ values, and rare mafic enclaves support interpretations that these plutons derived from anatexis of older continental crust, with minor contributions from less-evolved (mantle?) magmas.

The Danburg Pluton and spatially-associated Sandy Hill 'border facies' intrude the Carolina terrane, and contain mafic enclaves that may represent a mantle contribution, if shown to be coeval. The Danburg (coarsely porphyritic, undeformed) is an I-type, magnesian, alkalic-calcic, metaluminous monzogranite ~70.0 wt. % SiO_2. The Sandy Hill (equigranular, undeformed) Sandy Hill pluton is an I-type, magnesian to ferroan, alkalic-calcic, peraluminous granite with ~73.8 wt. % SiO_2. Whole rock samples from both intrusions show linearly-correlated major element trends, consistent with the two being related through crystal fractionation. The Danburg and Sandy Hill plutons yield indistinguishable $^{206}Pb/^{238}U$ zircon ages at the 2σ level (307.0±4.7 Ma and 304.7±3.0 Ma, respectively) with few xenocrysts. They contain limited inheritance, though premagmatic zircons with ages up to 331±5 Ma are inferred on the basis of age and zircon trace element chemistry. $^{206}Pb/^{238}U$ ages of titanite from three enclaves in the Danburg yield ages of 302.6±3.7 Ma, 311.7±6.1 Ma, and 312±11 Ma. Thus, all overlap the Danburg age (zircon) within 2σ uncertainty. Accessory mineral thermobarometry of 771±27°C and 6.5±1.7 kilobars for the Danburg granite and 765±50°C and 5.1±1.4 kilobars for the enclaves supports the interpretation of crystallization under similar conditions. (average±1 st.dev.). The age, temperatures, and textural evidence are interpreted to reflect quenching of mafic melt (enclaves) upon mixing with the coexisting felsic melt.

1. INTRODUCTION

Granitic plutonism marks the culmination of the assembly of the Pangean supercontinent, but identification of the intrusive rocks emplaced during this time is not always apparent from field observations alone. Numerous tectonic and magmatic events at the present-day, southeastern margin of Laurentia produced variable overprinting fabrics and the juxtaposition of rock units by faults that are not always visible in outcrop, but may be better understood through the acquisition of well-constrained, high-precision age and whole rock geochemical data. The multi-phase Danburg and Sandy Hill granitoids located in northeast Georgia were emplaced in the Charlotte belt, which is one of the peri-Gondwanan terranes that were accreted onto the Laurentian margin as part of the Appalachian orogen. These spatially related plutons have been previously interpreted as part of a suite of felsic intrusives emplaced during the Alleghanian orogeny, reflecting the final Laurentian mountain-building event in the amalgamation of Pangea (Dvoracek, 2003).

Previous whole rock Rb/Sr Alleghanian ages have been reported for the Danburg, enclaves and Sandy Hill bodies (Dvoracek, 2003). Application of new U-Pb geochronology allows confirmation of these ages; Pb/U in single, refractory crystals (i.e., zircon) often provides a more robust age than whole rock Rb/Sr, which is more susceptible to open system chemical exchange. The connection between the Danburg and included mafic enclaves is an additional question that is addressed in this study. Age constraints and textural evidence allow interpretation of the relationship between the two lithologies, which in turn, has implications for the petrogenesis of the Danburg as well as other nearby Alleghanian plutons reported to contain mafic enclaves (e.g., Appling, Siloam, Sparta) (Dvoracek and Roden, 2005). Determining the characteristics of these plutons will add to the growing compendium of information regarding the formation of southern Appalachians and assist in constraining the geodynamic setting. This study characterizes these undeformed plutons using a combination of petrology, geochemistry, and geochronology to provide conclusive, robust interpretations of the nature of the relationship between these rocks and their petrogenesis.

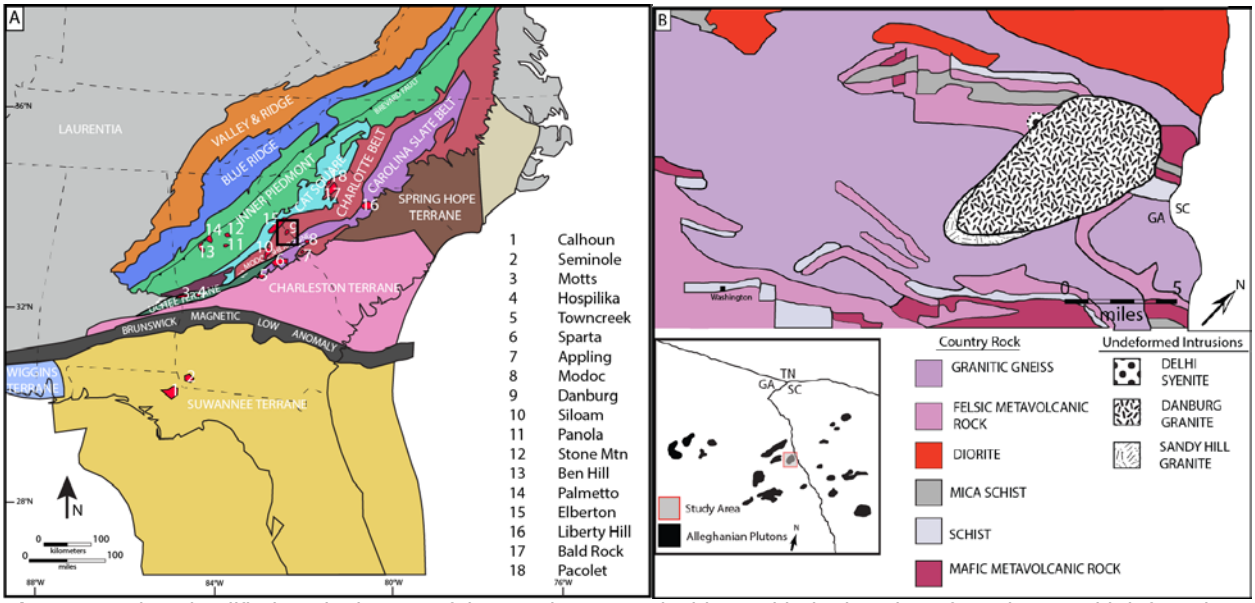

Figure 1: 1A) A simplified geologic map of the Southern Appalachians with the location of 16 plutons with inferred Alleghanian-ages. The black box surrounds the study area. 1B) A revised geologic map of the study area, after Allard and Whitney (1994). The Sandy Hill granite has only been identified along the southeastern margin of the Danburg pluton.

2. METHODS

Eight samples were identified for focused petrographic and geochemical characterization. These comprise three representative rocks from the Sandy Hill intrusion, one representative sample from the Danburg pluton, and four enclaves representative of the textural diversity observed in the field. Samples of the Danburg pluton were collected on site in northeast Georgia (Lincoln and Wilkes counties) from a currently inactive quarry. Representative samples of both the granite and mafic enclaves were selected from fresh blocks that had been mined from the quarry face. Samples of the Sandy Hill intrusion were collected from outcrops near the Danburg quarry. The rock samples were prepared for thin section analysis and subjected to point counts to classify according to the ternary QAP system (Streckeisen, 1975). Geochemical techniques include whole rock geochemistry and accessory mineral U-Pb geochronology. In preparation for whole rock geochemistry, samples were progressively crushed to gravel sized chips and then pulverized for 3 minutes using a tungsten-carbide mill. The resulting powders were fused into glass discs (32 mm diameter). Analyses were conducted on the Rigaku Supermini200 at Ohio University and using the Fundamental Parameters (FP) method and calibrated against 12 USGS rock standards. To obtain robust age data on the plutons and enclaves, zircon and titanite grains were concentrated by heavy mineral separation processes using methylene iodide (MI; density = 3.32 g/cm^3). Afterwards, the zircons and titanites were hand selected for purity, mounted on double-sided tape on glass slides in ~1 x ~6 mm rows, cast in a 25 mm diameter by 4 mm thick epoxy disc, ground, and polished to a 1 micron finish. All grains were imaged with transmitted light and reflected light on a petrographic microscope, with the addition of scanning electron microscopy on a JEOL 5600 SEM at Stanford University to identify internal structure, inclusions, possible identification of cores, and physical defects. U-Pb analyses were conducted on the SHRIMP-RG (reverse geometry) ion microprobe co-operated by U.S. Geological Survey and Stanford University in the SUMAC facility at Stanford University between 5/15/2014-5/19/2014.

3. RESULTS

The Danburg monzogranite is a porphyritic granite dominated by feldspars exhibiting rapakivi texture, in which alkali feldspar crystals are rimmed with plagioclase. It is host to mafic enclaves (~2% of the pluton). The Sandy Hill monzogranite is equigranular and not as coarse as the Danburg pluton, nor does it contain any mafic enclaves. The mafic enclaves are variable in mineral content and texture. In all samples; however, they are darker and finer-grained than their host. The mafic enclaves contain hornblende unlike their host and have several interesting mineralogical features including chilled margins, skeletal textured titanites, large rapakivi feldspars, and acicular apatite.

Table 1. Sample location and summary descriptions.

Sample	Latitude	Longitude	Location	Pluton	Major Mineralogy	SiO_2 (wt.%)	Zrn	Ttn	QAP Classification
14CG-SAO-6	33.84611	82.65215	Outcrop	Sandy Hill	Qtz, Pl, Afs, Ms, Bt	75.9	yes	—	Monzogranite
14CG-SAO-7	33.84575	82.65161	Outcrop	Sandy Hill	Qtz, Afs, Pl, Ms, Bt	74.5	yes	—	Monzogranite
14CG-SAO-8	33.84729	82.65249	Outcrop	Sandy Hill	Afs, Pl, Qtz, Ms, Bt	74.5	yes	—	Monzogranite
14CG-SAO10-2	33.88533	82.64576	Quarry	Danburg	Afs, Pl, Qtz, Bt, Ms	69.2	yes	yes	Monzogranite
14CG-SAO10-1	33.88533	82.64576	Quarry	Danburg (enclave)	Pl, Bt, Qtz, Hbl, Afs, Ttn	53.6	—	yes	Quartz Monzodiorite
14CG-SAO10-5A	33.88533	82.64576	Quarry	Danburg (enclave)	Afs, Pl, Qtz, Bt, Ms, Ttn	64.2	yes	yes	Monzogranite
14CG-SAO10-5B	33.88533	82.64576	Quarry	Danburg (enclave)	Pl, Afs, Bt, Qtz, Hbl, Ttn	55.3	—	yes	Quartz Monzodiorite
14CG-SAO10-5C	33.88533	82.64576	Quarry	Danburg (enclave)	Pl, Bt, Afs, Qtz, Hbl, Ttn	58	—	yes	Quartz Mozonite

Whole rock geochemistry of the Danburg, included enclaves, and Sandy Hill samples define a compositional suite that increases in SiO_2 content from the enclaves (53.6 wt.%) to the Sandy Hill granite (75.9 wt.%) with the Danburg granite plotting in between (69.2 wt.%). When plotted against SiO_2, the major elements of the Danburg granite, included enclaves, and the Sandy Hill granite, generally define broadly linear trends. Fe_2O_3, P_2O_5, TiO_2, CaO, Al_2O_3, MnO, and MgO versus SiO_2 define trend lines with a negative slope. K_2O and Na_2O are not as well correlated. The three Sandy Hill samples exhibit similar compositions and cluster together at the high-SiO_2 end. The Danburg sample is the median value in all major elements except K_2O and Na_2O. Additionally, the geochemistry of the samples was applied to a granite classification scheme of Frost et al. (2001). Overall, the geochemistry of the suite of rocks studied is most consistent with Caledonian granites. These granites are typical of post-collisional tectonics whereby late anatexis of crust is expressed as numerous granitic plutons. Caledonian rocks are typically K-rich, as these are. Frost and Frost (2008) shows the four granitoid classifications often follow a differentiation path on a QAP diagram. The spread of rocks follow a trend of potassic evolution as reported for Caledonian granite suites. The ferroan and alkalic nature typical of the enclaves has implications regarding its possible source.

Accessory minerals zircon and titanite were used from the granites and enclaves to determine the age of the rocks. The Danburg and Sandy Hill plutons yield is statistically equal $^{206}Pb/^{238}U$ zircon ages at the 2σ level (307.0±4.7 Ma and 304.7±3.0 Ma, respectively). Limited inheritance was observed, though premagmatic zircons with ages up to 331±5 Ma are inferred on the basis of age and zircon trace element chemistry. $^{206}Pb/^{238}U$ ages of titanite from three enclaves in the Danburg yield ages of 302.6±3.7 Ma, 311.7±6.1 Ma, and 312±11 Ma. Thus, all overlap the Danburg age (zircon) within 2σ uncertainty. Accessory mineral thermobarometry of 771±27°C and 6.5±1.7 kilobars for the Danburg granite and 765±50°C and 5.1±1.4 kilobars for the enclaves supports the interpretation of crystallization under similar conditions. (average±1 st.dev.).

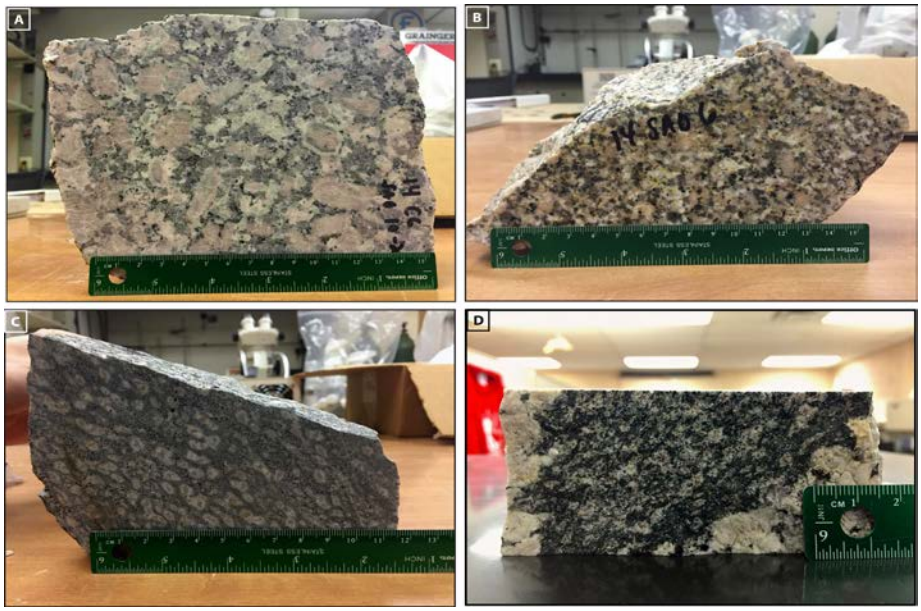

Figure 2: Representative hand samples from the rocks within this study: A) porphyritic Danburg granite, B) equigranular Sandy Hill granite, C) mafic enclave from Danburg granite, D) another mafic enclave to demonstrate enclave variability.

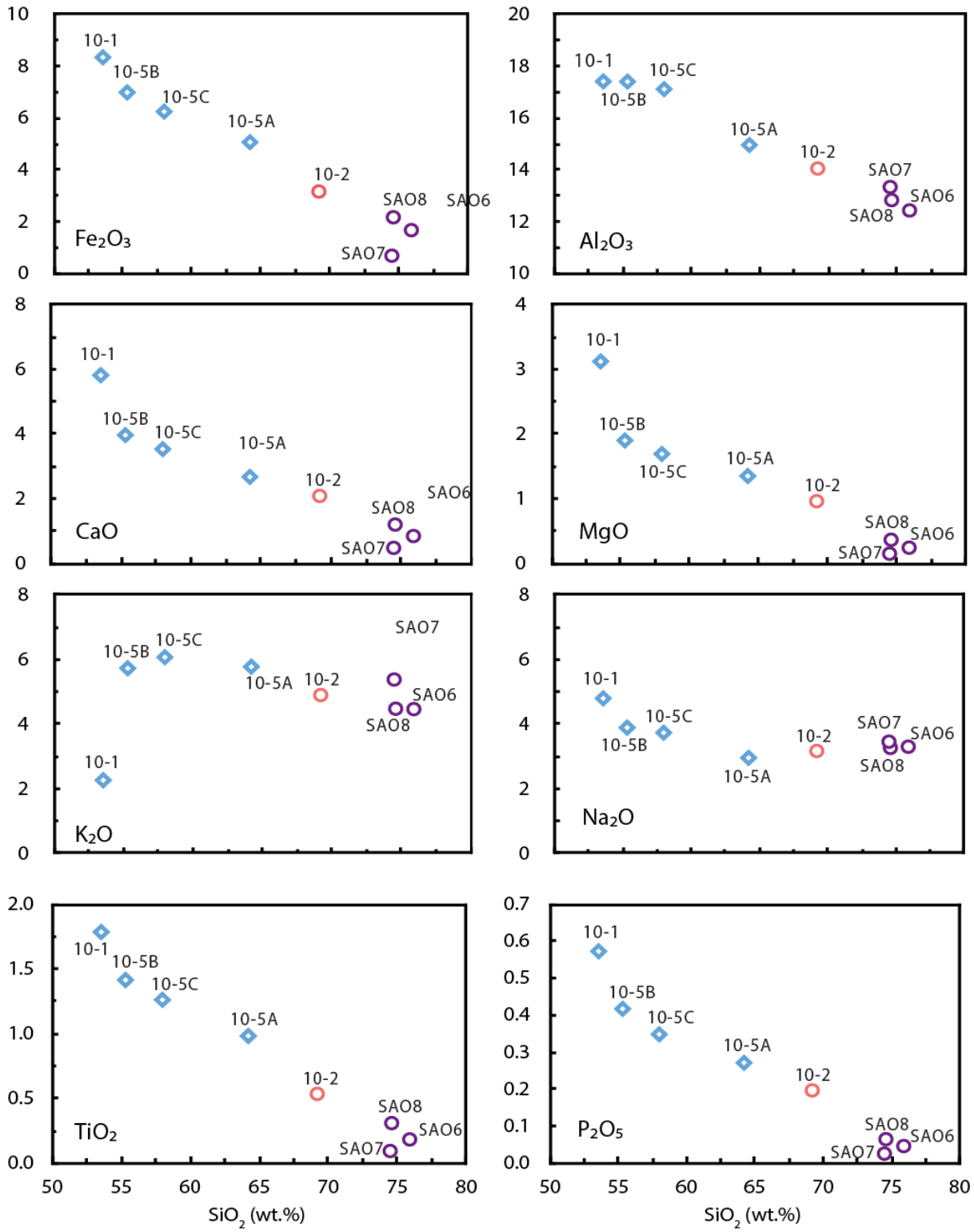

Figure 3: Harker diagrams plotting major element oxides of the Danburg granite, contained enclaves, the Sandy Hill granite, and the Delhi syenite against SiO_2 (wt.%). The plots show a cogenetic relationship between the Danburg granite, enclaves, and Sandy Hill granite. Blue diamond – mafic enclaves, red circle – Danburg granite, purple circle – Sandy Hill granite.

4. CONCLUSIONS

New SHRIMP-RG ^{207}Pb-corrected $^{206}Pb/^{238}U$ zircon and titanites yield statistically contemporaneous ages of 307±4.7Ma for the Danburg granite, 307.3±3.7Ma for the mafic enclaves, and 304.7±3.0Ma for the Sandy Hill granite confirming their connection to Alleghanian magmatism. Tectonic discrimination diagrams for whole rock data classify the Danburg-enclave-Sandy Hill suite as Caledonian granitoids forming through post-collisional magmatism; a geodynamic setting consistent with current theory on Alleghanian tectonics.

The presence of mafic enclaves within the Danburg granite presents a possible insight into its origin. A liquid origin for the enclaves is preferred due to several lines of evidence. Textural observations including chilled margins, skeletal titanites, rapakivi feldspars, and acicular apatite are consistent with mixing between mafic melts into a cooler, felsic magma chamber. Geochemistry shows well-defined linear trends between most enclaves, Danburg granite, and Sandy Hill granite, also consistent with hybridization. Both major element oxides and zirconium suggest the more juvenile melt experienced differentiation before interaction with the felsic source. Temperatures and pressures calculated through accessory mineral thermobarometry of 771±27°C and 6.5±1.7 kilobar for the Danburg granite and 765±50°C and 5.1±1.4 kilobar for the contained enclaves support crystallization under similar conditions. If correct, influx of a mafic melt indicates mantle involvement (in the form of heat and mass) in the generation of the Danburg and Sandy Hill granites, a scenario consistent with its inferred tectonic setting.

REFERENCES

Dvoracek, D.K., Geochemical and geochronological study of the Danburg and Sandy Hill granitoids and associated mafic enclaves, Northeast Georgia [dissertation]. [Georgia]: University of Georgia; 2003, 260 p.

Dvoracek, D. and Roden, M. 2005. The Danburg (GA) granite, Carolina terrane: An Alleghanian pluton showing evidence for mixing with relatively alkaline magma. Georgia Geological Society Guidebook, v. 25, p. 81-94.

Frost, B.R., Barnes C.G., Collins, W.J., Arculus, R.J., Ellis, D.J., and Frost, C.D., 2001. A geochemical classification for granitic rocks. Journal of Petrology, v.42, n.11, p. 2033-2048.

Frost, R.B., and Frost, C.D., 2008. A geochemical classification for feldspathic igneous rocks. Journal of Petrology, v.49, n.11, p.1955-1969.

Streckeisen, A., 1975. To each plutonic rock its proper name. Earth-Science Reviews, v.12, p.1-33.